"Collision-induced absorption in the rototranslational band of H_2–H_2 and in the fundamental band and first and second overtone of H_2 in dense hydrogen gas"

by

Martin Andreas Abel

THESIS

Presented to the Faculty of the Graduate School of

The University of Texas at Austin

in Partial Fulfillment

of the Requirements

for the Degree of

MASTER OF ARTS

THE UNIVERSITY OF TEXAS AT AUSTIN

August 2009

The Thesis committee for Martin Andreas Abel Certifies that this is the approved version of the following thesis:

"Collision-induced absorption in the rototranslational band of H_2–H_2 and in the fundamental band and first and second overtone of H_2 in dense hydrogen gas"

APPROVED BY

SUPERVISING COMMITTEE:

Lothar Frommhold, Supervisor

Manfred Fink

Dedicated to my family.

Acknowledgments

First of all I wish to thank my supervisor, Dr. Lothar Frommhold, for his kind support and encouragement throughout the whole year I worked together with him. Without him this work would not have been possible. It was a true pleasure to work with you and I could learn a lot from you. Your experience is an invaluable merit. Discussions with you gave me a much deeper insight into the subject I would never have obtained from written sources.

Next I would like to thank Dr. Manfred Fink who was very engaged to make this exchange program possible for me. Furthermore, he has kindly let me occupy space in his laboratory. This gave me the opportunity to get to know some of the collaborators and doctoral students of his group through daily interaction.

Finally, thanks to my family who has suported me during the complete exchange program, always giving valuable advice.

The financial support of this work from the National Science Foundation is gratefully acknowledged.

Martin Andreas Abel

The University of Texas at Austin

August 2009

"Collision-induced absorption in the rototranslational band of H_2–H_2 and in the fundamental band and first and second overtone of H_2 in dense hydrogen gas"

Martin Andreas Abel, M.A.
The University of Texas at Austin, 2009

Supervisor: Lothar Frommhold

The absorption due to pairs of H_2 molecules is an important opacity source in the atmospheres of various types of planets and cool stars, such as late stars, low-mass stars, brown dwarfs, certain white dwarfs, etc., and therefore of special astronomical interest [13]. The emission spectra of cool white dwarf stars differ significantly from the expected blackbody spectra of the cores, due to collision-induced absorption by collisional complexes of hydrogen and helium in the stellar atmospheres. In order to model the radiative processes in these atmospheres, which have temperatures of several thousand kelvin, one needs accurate knowledge of the induced dipole and potential energy surfaces of collisional complexes such as H_2–H_2. These come from quantum-chemical calculations with the H_2 bonds stretched or compressed far from equilibrium length. Since no measurements of the collision-induced absorption for these high temperatures exist, one has to undertake *ab initio* calculations which

take into account the high vibrational excitations of the hydrogen molecules. However, before one attempts to proceed to higher temperatures where no laboratory measurements exist it is good to know that the formalism is correct and reproduces the results at temperatures where measurements exist. Therefore, in order to make sure that the calculations are reliable one compares the results of the calculations with existing laboratory measurements where possible before proceeding to higher temperatures.

Molecular hydrogen has always played a special role in the collision-induced spectroscopies. The rotational transition frequencies of H_2 are widely separated so that translational, rotational and vibrational induced spectral bands can be studied separately. Moreover, the H_2 molecule has a small anisotropy of the intermolecular interactions which may often be ignored in first order approximations. In general hydrogen gas is a mixture of para- and ortho-hydrogen. Para-hydrogen at sufficiently low temperature is not rotationally excited and is therefore an isotropic system. However, the anisotropy can be turned on and off by raising and lowering the temperature, because the ratio of para- to ortho-hydrogen depends on the temperature. What is even more, roughly 90% of all the known matter in the universe is hydrogen, in the ionized, atomic or molecular states, which makes hydrogen one of the most important species in astrophysics. The hydrogen molecule is non-polar, and some of the most important spectra in the near and far infrared and microwave region are collision-induced, due to H_2–H_2 complexes.

At the temperature of 297.5K measurements of the collision-induced absorption spectra of H_2–H_2 gas are reported in the frequency range from 1900 to 2260cm^{-1} [9]. The gas densities for these measurements ranged from 51 to 610 amagat. These measurements were compared with *ab initio* calculations of the absorption. For these calculations the isotropic potential approximation was used. In contrast to previous *ab initio* calculations [9] agreement between calculations and measured spectra is now observed over the full frequency range considered. A major difference to the earlier calculations is that in this work new dipole and potential energy surfaces were used.

Furthermore, measurements exist of the fundamental band and first and second overtone of H_2 in dense hydrogen gas. They have been compared with *ab initio* calculations based on the new method. Over the full range of frequencies considered the agreement between calculations and measurements is remarkable. This work demonstrates that the new method is capable of reproducing the measured spectra where those exist with high accuracy, and predicts reliable opacities where no laboratory measurements exist.

Table of Contents

List of Figures

Chapter 1

Introduction

1.1 Historical overview

1.1.1 Discovery

Historically, collision-induced absorption was discovered in the fundamental band of oxygen and nitrogen [35]. It was discovered and explained by Welch in 1949 [13]. Afterwards, in 1954, Maryot et al. discovered CIA in the microwave region, and in 1964 Trafton found it in the infrared range in the outer planets. Most notably, Herzberg pointed out for the first time that sizable H_2 concentrations exist in the atmospheres of Uranus and Neptun [24]. In general, nonpolar species such as H_2 and He are difficult to detect remotely in such cool environments. Supramolecular signatures have been very important to reveal such gases. The early observations of absorption bands in compressed air and oxygen are now understood to be of supramolecular nature. From then on this process has had great importance and the understanding of interaction-induced absorption spectra in the atmospheres of the planets and their big moons was systematically expanded.

1.1.2 Present significance

More recently astrophysicists believe that a new, independent estimate of the age of the universe is possible, based on this field. For this, accurate knowledge of the absorption of supermolecular pairs such as H_2–H_2 and H_2–He at temperatures up to 7000K and frequencies from 0 to 20000cm^{-1} is needed [33]. Although this effect is of special importance in astronomy it is generally observed in virtually all dense matter. The earth' s atmosphere is similarly affected by interaction-induced spectral signatures in all spectral bands.

It has been well known for a few decades that dense gases of nonpolar molecules, such as H_2, absorb infrared radiation. This absorption is continuous and ranges from the microwave and far infrared regions of the spectrum to the near infrared and visible, covering all frequencies in between. The reason for these absorption continua are collissionally interacting pairs of hydrogen molecules, which in contrast to the non-interacting molecules in general possess transient electric dipole moments ([65], [13]). Planetary scientists immediately understood the significance of collision-induced absorption (CIA) for the modeling of the atmospheres of planets ([53], [54]). However, only recently it was observed that the emission spectra of cool white dwarf stars are significantly different from the expected blackbody spectrum of their cores. The atmospheres are so dense that the CIA in hydrogen and helium suppresses the infrared emissions strongly ([45], [46], [22], [51], [47], [2]). Up to now detailed modeling of cool stars with proper accounting for the collision-induced opacities has been impossible because of the highly incomplete or non-existent experimental as well as theoretical data on such opacities at temperatures of thousands of kelvin, but it is nevertheless desirable to have this information available.

In the past quantum-chemical calculations of the induced dipole surfaces of H_2–H_2 and other supermolecular complexes have been very successful ([41], [63], [60], [62]). Molecular scattering calculations, based on such data and accounting for the interactions of the molecular complexes with photons have been undertaken. Close agreement between those calculations and existing laboratory measurements at low temperatures, $T < 300K$, has been observed [13]. However, at higher temperatures virtually no laboratory measurements of such opacities exist. Since those data are needed for current astrophysical applications our group decided to extend the quantum-chemical calculations of the induced dipole (ID) and potential energy surfaces (PES) of H_2–H_2 complexes to higher temperatures. At the temperatures of concern the hydrogen molecules are highly rotovibrationally excited, which has to be taken into account properly in the calculations [33].

1.1.3 General motivation

Since molecular hydrogen is the most abundant species of the universe in order to get a deeper understanding of the universe as a whole it is important to study the properties of hydrogen. Collision-induced radiative effects play a major role in the heat transfer because H_2 is infrared-inactive. In this work the main focus is on the low absorption by collisional hydrogen complexes in the frequency range of 1900 to 2260cm^{-1}. This frequency region is of great importance for the determination of the presence and abundance of minor constituents in the atmosphere of Jupiter, based on their contributions to the observed absorption. For this the interaction-induced weak absorption of H_2–H_2 collisional complexes must be known as well as possible in order to separate the unknown contributions from the contributions due to hydrogen. Knowledge of the collision-induced H_2 pair spectra is of utmost astrophysical interest [9]. Furthermore, this work was undertaken to test the new methods developed for the high temperatures envisioned and to demonstrate their validity at temperatures where laboratory measurements exist. Calculations were undertaken for the rototranslational band of H_2–H_2 and the fundamental band and first and second overtone of H_2 at the temperature of 300K. Close agreement between measured and calculated spectra is observed.

1.1.4 Difficulties one encounters in laboratory measurements

Studies of collision-induced pair spectra consist of laboratory absorption measurements in compressed gases and gas mixtures at different frequencies, densities and temperatures. There exist numerous accurate *ab initio* calculations of H_2 pair spectra which are generally in close agreement with the laboratory measurements [13]. However, in the frequency region considered in this work one encounters several difficulties.

First of all laboratory measurements in this frequency domain are difficult to obtain accurately because of the weak collision-induced absorption of hydrogen in the 5μm band. Thus, one has to work with high gas densities, which may introduce ternary and higher order contributions that are likely to affect these measurements. In principle it is possible to separate these higher order contributions from the purely binary contributions by virial expansion techniques - described in detail below - but often with substantial associated uncertainties which renders the thus obtained binary absorption spectrum inaccurate [9]. This is purely a problem of laboratory measurements because for astrophysical applications higher order contributions in the frequency range considered here are insignificant, due to the low gas densities encountered there. Nevertheless, due to the long absorption paths collision-induced absorption intensities have considerable values in planetary atmospheres. Whereas laboratory path lengths seldom exceed a few meters planetary path lengths are in the order of kilometers. In general the absorption spectra obtained in the laboratory may be affected by ternary and higher order contributions, to an unknown extent.

Another difficulty one faces is that *ab initio* calculations of the collision-induced absorption spectra require as input the H_2–H_2 interaction potential and the interaction-induced dipole surfaces. For both surfaces remarkably accurate *ab initio* calculations exist, supported by extensive empirical data [13]. The dipole surfaces may be represented as a series of overlap-induced, quadrupole-induced, hexadecapole-induced, ... components, each of which have different significance [13]. However, whereas the stronger components may be determined with an uncertainty of a few percent by *ab initio* calculations, the weaker ones are necessarily much less well known [40]. In regions of large absorption the weaker components have often negligible contributions to the absorption but in the far wings some of the weaker, less well known dipole components have significant influence. This introduces uncertainties in such absorption calculations which are often large, even in the best theoretical calculations.

1.1.5 Content of this work

This work compares a recent, very careful measurement of the infrared absorption in the 5μm band with *ab initio* calculations of the binary absorption in dense hydrogen gas. It was undertaken in the hope to improve our understanding of this important absorption region and to demonstrate that the new methods developed for high temperature *ab initio* calculations are capable to reproduce laboratory measurements at temperatures where measurements exist. Furthermore, *ab initio* calculations were undertaken for the rototranslational band of H_2–H_2 and the fundamental band and first and second overtone of H_2 at the temperature of 300K. Close agreement between measured and calculated spectra is observed. Opacities at frequencies and temperatures where no laboratory measurements exist are predicted.

Chapter 2

Electromagnetic spectra and spectroscopy - experimental background

2.1 Experimental background

2.1.1 General background of emission and absorption of electromagnetic radiation

When physical systems change their energetic state they can emit or absorb electromagnetic radiation. This can happen in different ways: One distinguishes Line-, Band- and continuous spectra.

2.1.2 Line spectra

A Line spectrum is a spectrum that consists of separated, discrete parts of higher intensity, so called lines. Every material, since consisting of atoms and molecules, has characteristic, discrete levels of energy, that can be occupied by electrons. When electrons change between two states the energy difference between the two levels is swapped through the absorption or emission of a photon of frequency ν with energy $\mathrm{E} = \mathrm{h}\times\nu$: the difference in the energy levels equals the energy of the photon, energy conservation. Here, h denotes Plancks constant. The width of these lines is only broadened due to the finite lifetime in the order of 10^{-8}s of the excited energy levels according to

Heisenberg' s uncertainty relation,

$$\Delta E \times \Delta t \gtrsim \frac{\hbar}{2}. \tag{2.1.1}$$

These line spectra have offered important information and were essential for the development of quantum mechanics. In astronomy line spectra are an important source of information about the universe. Since they are characteristic for the atoms or molecules which are involved in the transitions one can determine the elements that exist in other planets and stars. However, the number of energy levels in a given material is often very high, but in most cases there exist a few pairs of energy levels which are more likely to absorb or emit, in other words the transition probability between these levels is higher than between other levels, so that there are lines with a much higher intensity than others.

2.1.3 Band spectra

An absorption band is a wavelength interval in which the electromagnetic radiation of a radiation source is selectively absorbed by chemical substances on its way to the detector. Originally continuous spectra of a radiation source arrive at the detector with dark breaches, so called absorption bands. Certain intervals of the whole spectrum emitted from the radiation source are now missing. The so derived picture of the spectrum is called a band spectrum as well as the corresponding emission spectrum. An absorption spectrum consists of a greater number of apart closely neighboring absorption lines which arise from the coupling of electrical oscillations and rotational excitation in molecules, so that no separated energy differences are absorbed but a whole spectrum of energy values, related to the excitation of the molecules. In certain materials and states it is possible to separate the absorption band in apart absorption lines by high enough resolution. This is called fine structure of the absorption band. Here the different molecules only absorb in a specific wavelength interval.

In atoms there exist several possible transitions. Moreover, in molecules the number of possible transitions is even more increased due to more degrees of freedom: in molecules there are besides the electronic transitions in an energy range in the order of eV furthermore vibrational transitions corresponding to an energy range in the order of meV and rotational transitions corresponding to energies of μeV. At low excitation energies usually only a few lower energy levels are occupied due to the Boltzmann distribution. With increasing excitation energies the probability for occupation of higher energy levels increases. Some of these levels correspond to a rotational state which is defined by a quantum number L. Since rotational states are degenerate by a factor of L$\times$(L+1) with increasing L this degeneration takes more and more influence on the probability distribution of occupied states. Furthermore, the number of possible transitions is increased to a large amount. But not all possible transitions are (dipole-) allowed. There exist selection rules and the light intensity corresponding to transitions that do not follow these rules is much lower than for the allowed ones. Therefore, one usually needs high resolution spectroscopy to detect them. The spectra corresponding to these molecular transitions are called band spectra since there are several lines in nearly the same energy range and with low resolution they appear as bands because the different lines cannot be resolved. This makes it even harder to detect certain transitions.

2.1.4 Continuous spectra

If one mixes several gases there also occur broadening mechanisms such as Doppler broadening and pressure broadening, so that the lines become much more diffuse and some of them even overlap. Unresolved lines appear as continuous spectra. A continuous spectrum consists at least in a certain frequency domain of photons of every frequency within that domain.

Furthermore, if one mixes several different atoms and molecules at a given temperature T, for example in the sun, one can also observe continuous spectra. According to [21], under equilibrium conditions, at temperatures of several thousand kelvin, the degree of ionization, α, of rare gases is typically small, $\alpha \ll 0.01$. Thus emission of light comes mainly from neutral-neutral collisions. However, at higher temperatures, when the degree of single ionization is still significantly smaller than unity, electron-neutral and electron-ion bremsstrahlung are among the principal sources of radiation. As is well explained by classical electrodynamics this bremsstrahlung is continuous radiation.

The continuous spectrum emitted by the sun is mainly due to bremsstrahlung.

In addition free-to-free radiative transitions of electron-ion pairs and free-to-bound radiative transitions are also continuous [21].

Continuous spectra may furthermore be due to collision-induced emission, which will be discussed further below. It generates continuous spectra in completely neutral environments [21].

According to [21] negative ions, such as H^- ([55], [18], [34], [15]) and O^- ([66], [31], [32]), absorb light very efficiently. The inverse reaction, radiative attachment, is therefore an important contributor to the continuous emission spectra whenever negative ions may be formed ([3], [4]).

2.2 Supermolecular spectra

So far we have only considered single atomic and molecular transitions. But as has been unknown for a very long time there also exist supermolecular spectra. They have their origin in transitions that occur during the interaction of several atoms or molecules. Since these transitions take place on very short time scales, i.e. for the duration of a collision, which usually is in the order of Δt$\approx 10^{-13}$s, the "lines" corresponding to this kind of spectra are very diffuse, according to Heisenberg' s uncertainty relation,

$$\Delta t \times \Delta\omega \gtrsim \frac{\hbar}{2}. \tag{2.2.1}$$

Whereas these transitions are usually not observed at standard conditions, i.e. at room temperature and pressures of a few amagat, when there are other possible transitions which correspond to much higher intensities, this kind of absorption plays a major role in dense gases when there are no other possible transitions due to non polar or symmetric molecules. This is one of the reasons why it took so long until collision-induced spectroscopy was discovered, in contrast to the common spectroscopy. For example, in cool white dwarfs, certain stars out in the universe, or in the earth' s atmosphere this kind of absorption plays a major role concerning the absorption of electromagnetic radiation, since other mechanisms nearly do not occur. Furthermore, this kind of spectra is of great importance in condensed matter physics.

Atomic and molecular systems can exist in a great variety of states. Spectroscopic lines arise from transitions between such states. However, not all possible transitions are allowed for emission or absorption of a photon. There exist selection rules which determine which of the transitions are optically allowed. However, forbidden transitions may take place without absorption or emission of a photon, for example in collisional interactions.

At high enough gas densities, corresponding roughly to atmospheric pressure or slightly higher, absorption by complexes of two or more interacting molecules takes place, called collision-induced absorption, according to [13]. This field is of great significance and continues to attract numerous scientists from various disciplines. Collision-induced absorption is a basic science that deals with the interaction of light with supramolecular systems. It should be remarked that the word supramolecular indicates that these systems possess further properties in addition to the properties of the single constituents.

Besides the many applications in atmospheric sciences it has great importance in many other fields. It generally occurs in all molecular fluids and mixtures of gases.

In virtually any gas a certain, usually small fraction of the atoms or molecules (monomers) exists as van der Waals molecules. These are systems of two or more monomers, bound together by the weak van der Waals intermolecular forces. This work is mainly concerned with complexes of two unbound monomers which exist only for the very short duration of a fly-by encounter. Free and bound van der Waals systems have many properties in common. However, only the latter possess the relative stability of a molecule. Properties of bound and free van der Waals systems are referred to as supramolecular properties.

While high-frequency spectra arise from electronic transitions that are of lesser interest in this work, the low-frequency spectra that occur in the microwave, infrared and visible region of the electromagnetic spectrum typically arise from internal rotation and vibration and from molecular encounters. Since in virtually all spectra rotation and vibration are coupled, they are refered to as rotovibrational induced spectra.

A quantitative knowledge of the absorption of light by the earth' s atmosphere is essential to scientists. Especially, it is important for astronomers who need to correct their observational data for such absorption as much as possible.

Because collisional complexes in molecular gases have much more degrees of freedom than those of monatomic gases much richer collision-induced spectra are observed in a number of spectral bands. Any collisional pair possesses the degrees of freedom of the translational motion and an associated kinetic energy of relative motion. Furthermore, if molecular collisions are considered there are additional degrees of freedom and energies associated with the rotational and vibrational motion of one or more molecules of the complex. Correspondingly, photons may be absorbed over a much greater range of frequencies, in the vicinity of the various rotovibrational bands of the molecules, and at sums and differences of such rotovibrational frequencies, if two or more molecules interact.

It should be remarked here that the spectroscopic notation X_n(j) has the following meaning: j = 0, 1, 2, ... corresponds to the rotational quantum number of the initial state. The subscript n = ν'-ν is the difference of the vibrational quantum numbers of initial (ν) and final (ν') vibrational state. Finally, X stands for one of the letters O, P, Q, R, S, ..., each specifying a different rotational transition: j$'$ - j = ..., -2, -1, 0, 1, 2, ..., respectively. In literature, the subscript n is often omitted if it is clear what vibrational band is referred to.

According to Albert Einstein, for every photon absorption process there exists an inverse process, called stimulated emission. This stimulated emission needs to be taken into account if the population of states of sufficiently high energy is significant. As an example one may consider the far infrared, where photon energies are comparable to the mean free thermal energy of collisional pairs of molecules. Stimulated emission forces the emission to zero as frequencies approach zero.

Atomic and molecular spectroscopy provides fascinating possibilities for a deeper understanding of the fundamental properties of matter and its interaction with electromagnetic radiation. It lead to the development of quantum mechanics and its experimental verification. Furthermore, the results are very important in astrophysics, plasma and laser physics. The continuous enhancement of spectroscopic applications had considerable impact on other fields, including for instance chemistry, energy research, medicine and environmental protection.

2.3 The electromagnetic spectrum

The electromagnetic spectrum (see figure 2.1) of an object is the characteristic distribution of electromagnetic radiation from that object. This spectrum extends from below the frequencies used for radio applications of 10^{-3}Hz at the long-wavelength end through gamma radiation of 10^{24}Hz at the short-wavelength end, covering all the frequencies in between. It is nowadays believed that the short-wavelength limit is in the order of magnitude of the Planck length (about 1.6×10^{-35}m) and the long-wavelength limit is the size of the universe (about 4×10^{26}m), although in principle the spectrum is infinite. Frequencies in the order of a few Hz and below can be produced by certain stellar nebulae, whereas frequencies as high as 10^{27}Hz have been detected from

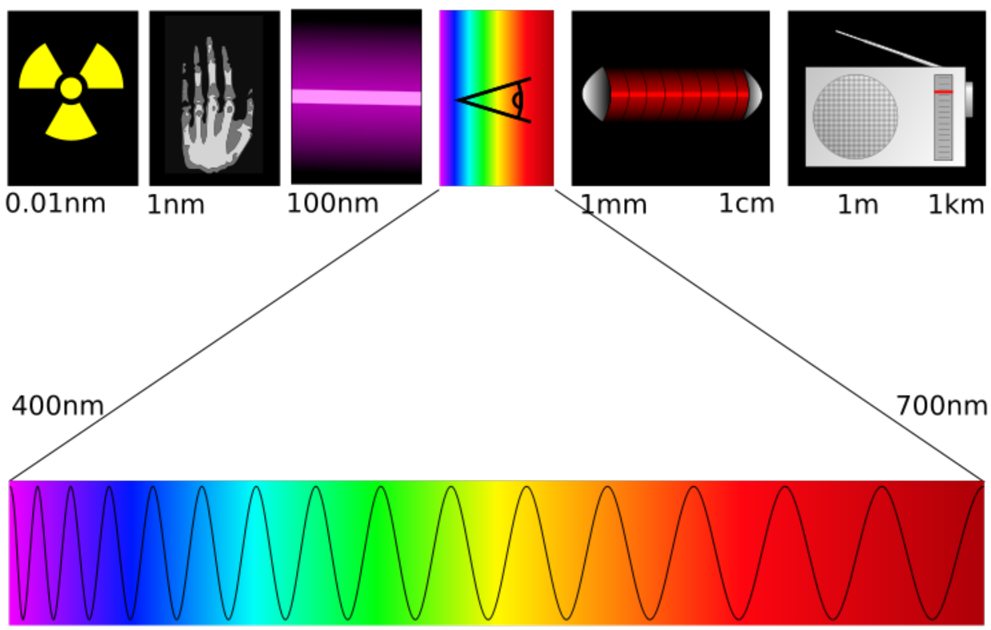

Figure 2.1: The electromagnetic spectrum

astrophysical sources. According to Albert Einstein the frequency ν of the light is related to the photon energy E by

$$E = h \times \nu = h \times \frac{c}{\lambda}. \qquad (2.3.1)$$

Here c denotes the speed of light. Therefore, high-frequency electromagnetic waves have a short wavelength λ and high energy E.

Generally, electromagnetic radiation is classified by wavelength into radio wave, microwave, infrared, the visible region we perceive as light, ultraviolet, x-rays and gamma rays. When electromagnetic radiation interacts with atoms and molecules, its behavior depends on the amount of energy per quantum it carries. Spectroscopy can detect a much wider region of the electromagnetic spectrum than the visible range of about 400nm to 800nm.

While the classification scheme is generally well defined, in reality there is often some overlap between neighboring types of electromagnetic energy. For example waves of 60Hz may be received and studied by astronomers, or may be deducted along wires as electric power. In the following a brief overview of the different frequency regions of electromagnetic radiation is given.

2.3.1 Radio frequency

Radio frequency is a frequency within the range of about 3Hz to 300GHz. This range corresponds to the frequency of alternating electrical current signals used to produce and detect radio waves. Radio waves are generally utilized by antennas of appropriate size, according to the principle of resonance, with wavelengths ranging from hundreds of meters to about one millimeter. They are used for transmission of data, via modulation. For example, television, mobile phones, wireless networking and amateur radio all use radio waves. They can be made to carry information by varying combination of amplitude, frequency and phase of the wave within a frequency band. Since most of the range of this radiation is beyond the vibration rate that most mechanical systems can respond to, radio frequency refers to oscillations in electrical circuits. When electromagnetic radiation strikes upon a conductor it couples to the conductor, travels along it and induces an electric current on the surface of that conductor by exciting the electrons of the conducting material. This effect, called skin effect, is applied in antennas. It describes the tendency that an alternating electric current distributes itself inside a conductor so that the current density near the surface of the conductor is greater than at its core. Furthermore, with increasing frequency the Poynting vector, which describes the direction and amplitude of the electromagnetic energy flux, gets crowd out of the conductor. This effect causes the effective resistance of the conductor to increase with frequency of the current and thus sets a high frequency limit for the application of antennas. Electrical currents that oscillate at radio frequency have special properties not shared by direct current signals, for instance the ease with which they can ionize air to create a conductive path through air.

2.3.2 The microwave region

Electromagnetic radiation is also able to cause certain molecules to absorb energy and thus to heat up, causing thermal effects. This is used in microwave ovens. Microwaves are capable of heating materials in less than one percent of the time conventional heating methods would take.

The super high frequency and extremely high frequency of microwaves comes next up the frequency scale. They are waves which are short enough to employ tubular metal waveguides of reasonable diameter. Wavelengths range from 1mm to 1m. Apparatus and techniques may be described qualitatively as "microwave" when the wavelengths of the signal are roughly the same as the dimensions of the equipment. As a consequence, practical microwave techniques tend to move away from the discrete resistors, capacitors and inductors used with radio waves. Instead, open wire and coaxial transmission lines give way to waveguides, and lumped-element turned circuits are replaced by cavity resonators or resonant lines. Effects of reflection, polarization, scattering, diffraction and atmospheric absorption usually associated with visible light are of practical significance in the study of microwave propagation. Microwave energy is produced in vacuum tube based devices which operate on the ballistic motion of electrons in a vacuum under the influence of controlling electric or magnetic fields. They include the magnetron, klystron, traveling wave tube and gyrotron and work in the density modulated mode rather than the current modulated mode. This means that they work on the basis of clumps of electrons flying ballistically through them, rather than using a continuous stream.

They can also be created by a Maser, which is a device similar to a laser.

Microwaves are absorbed by molecules with a dipole moment in liquids. This dipole moment does not have to be a permanent dipole moment, since the microwaves field-induce dipoles. Due to a change in direction and amplitude of the electromagnetic field they are capable of producing dipole moments even in nonpolar matter. The microwaves couple to the permanent or induced dipole moment causing forces that attempt to rotate the molecules in order to minimize the energy of the molecules in the field. However, because the direction of the microwaves changes with their period, in every half period the molecules get oriented in a different direction. This causes the molecules to oscillate around their equilibrium position, which means that their temperature is increased. It should be remarked that every kind of matter possesses a certain loss angle for microwaves, whose magnitude depends on the material under consideration and on the frequency of the microwaves. The loss angle quantifies the inherent dissipation of electromagnetic energy by the material at a certain frequency. Volumetric heating as used by microwaves transfers energy through the material electromagnetically, not as a thermal heat flux, which causes a more uniform heating and reduced heating time. Above 300GHz, the absorption of electromagnetic radiation by the earth' s atmosphere is so great that it is effectively opaque, until the atmosphere becomes transparent again in the so called infrared and optical window frequency ranges as is illustrated in figure 2.2.

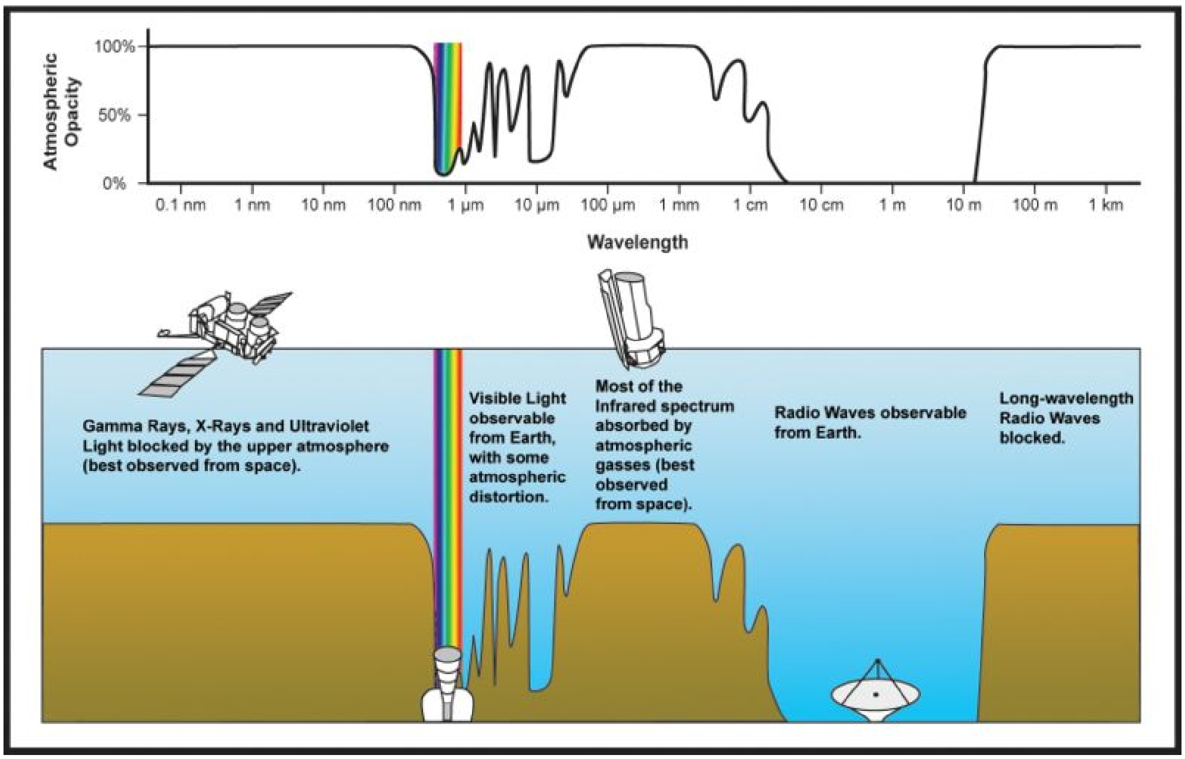

Figure 2.2: The earth' s atmospheric transmittance to various wavelengths of electromagnetic radiation (from NASA)

2.3.3 Terahertz radiation

Terahertz radiation is the region of the spectrum between the far infrared and microwaves. Until recently the range was rarely studied but applications such as imaging and communications are now appearing. It is non-ionizing submillimeter microwave radiation and shares with microwaves the capability to penetrate a wide variety of non-conducting materials. It can pass through clothing, paper, cardboard, wood, masonry, plastic and ceramics but it cannot penetrate metal or water. The earth' s atmosphere absorbs terahertz radiation very strongly, so its range is quite short. Terahertz radiation is emitted as part of the black body radiation from anything with a temperature greater than about 10K. While this thermal emission is very weak, observations at these frequencies are important for characterizing the cold 10 - 20K dust in the interstellar medium in the Milky Way galaxy, and in distant starburst galaxies. Telescopes operating in this band include the James Clerk Maxwell Telescope, the Caltech Submillimeter Observatory and the Submillimeter Array at the Mauna Kea Observatory in Hawaii. The opacity of the earth' s atmosphere to submillimeter radiation restricts these observatories to very high altitude sites, or to space. As of 2004 the only viable sources of terahertz radiation were the gyrotron, the backward wave oscillator, the far infrared laser, the quantum cascade laser, the free electron laser, synchrotron light sources, photo mixing sources and the single cycle sources used in Terahertz time domain spectroscopy.

2.3.4 Infrared radiation

The infrared part of the electromagnetic spectrum covers the range from 300GHz to 400THz and can be divided into three parts: from 300GHz to 30THz there is the far-infrared. This radiation is typically absorbed by rotational modes of molecules in the gas-phase, by molecular motions in liquids and by phonons in solids. The water in the earth' s atmosphere absorbs so strongly in this range that it renders the atmosphere effectively opaque. However, there are certain wavelength ranges within this range which allow partial transmission and can be used for astronomy. The far-infrared region may be used for rotational spectroscopy which studies the absorption and emission of electromagnetic radiation by molecules associated with a corresponding change in the rotational quantum number of the molecule. This kind of spectroscopy is only really practical in the gas phase where the rotational motion is quantized. In solids or liquids the rotational motion is usually quenched due to collisions. Rotational spectra from a molecule (to first order) require that the molecule has a dipole moment, that means a separation between two unlike charges. It is the dipole moment that enables the electric field of the light to exert a torque on the molecule causing it to rotate more quickly or slowly.

Diatomic molecules, such as dihydrogen (H_2), do not have a dipole moment and hence no purely rotational spectrum. However, electronic excitations can lead to asymmetric charge distributions and thus provide a net dipole moment to the molecule. Under such circumstances these molecules will exhibit a rotational spectrum. As the number of atoms increases the spectrum becomes more complex as lines due to different transitions start overlapping.

In quantum mechanics the free rotation of a molecule is quantized, that is, the rotational energy E_{rot} and the angular momentum L can only take certain fixed values. What these values are is simply related to the moment of inertia **I** of the molecule. Furthermore, a molecule is always in vibration. As the molecule vibrates, its moment of inertia changes, which causes the rotational energy to change. It should be remarked that in general the time for vibration is much shorter than the time required for rotation so that rotation and vibration can approximately be treated separately.

After this range there comes the mid-infrared with frequencies from 30 to 120THz. Hot objects can emit strongly in this range. It is absorbed by molecular vibrations, where the different atoms in a molecule vibrate around their equilibrium positions. This range is sometimes called the fingerprint region since the spectrum of a binding is very specific for that binding. A group of atoms in a molecule may have multiple modes of oscillation caused by the stretching and bending motions of the group as a whole.

Then follows the near-infrared with frequencies of 120 to 400THz. Physical processes that are relevant for this range are similar to those for visible light, which comes above the infrared light and is really a very small portion of the electromagnetic spectrum. Infrared radiation can be used to determine remotely the temperature of objects (if the emissivity is known), which is called thermography. The amount of radiation emitted by an object increases with temperature according to the Stefan Boltzmann law. Therefore, thermography allows one to see variations in temperature. In the range of the visible light the sun and the stars similar to it emit most of their radiation. It is typically absorbed by electrons of the constituents that change from one energy level to another.

Traditionally, microwave spectra were determined using a simple arrangement in which low pressure gas was introduced to a section of waveguides between a microwave source (of variable frequency) and a microwave detector. The spectrum was obtained by sweeping the frequency of the source while detecting the intensity of the transmitted radiation. More recently, microwave spectra have often been obtained using Fourier Transform Microwave Spectroscopy.

Microwave spectroscopy is commonly used in physical chemistry to determine the structure of small molecules with high precision. Other common techniques such as x-ray crystallography do not work very well for some of these molecules, especially the gases, and are not precise. However, microwave spectroscopy is not useful for determining the structure of large molecules such as proteins. Microwave spectroscopy is one of the principal methods by which the constituents of the universe are determined remotely from the earth.

2.3.5 Visible electromagnetic radiation - light

If radiation having a frequency in the visible region of the electromagnetic spectrum reflects off of an object and then strikes our eyes this results in our visual perception of the scene. A typical human eye will respond to wavelengths in air from about 380nm to 750nm. A light adapted eye generally has its maximum sensitivity at around 555nm, that is in the green region of the optical spectrum. The spectrum does not, however, contain all the colors the human eye and brain can distinguish. Unsaturated colors such as pink are absent, because they can only be made by a mix of multiple wavelengths. The eyes of many species perceive wavelengths different from the spectrum visible to the human eye. For example, many insects can see light in the ultraviolet, which is useful for finding nectar in flowers.

The visible spectrum can be analyzed by using a prism: when a narrow beam of visible light strikes the ace of a glass prism at an angle, some of the beam passes into and through the glass, emerging as different color bands. All light travels at the same speed in vacuum, whereas the speed of light within a material is lower than the speed of light in vacuum, and the ratio of speeds is known as the index of refraction of the material. Because the refractive index of a wave in material depends on its frequency (in accordance with a dispersion relation), light consisting of multiple frequencies - for instance "white" light - will be dispersed at the interface between the material and air or vacuum.

2.3.6 Ultraviolet radiation

Next in frequency comes ultraviolet. As this kind of radiation is very energetic it can break chemical bonds, making molecules unusually reactive or ionizing them, in general changing their mutual behavior. The sun emits a large amount of UV radiation which could quickly turn the earth into a barren desert. Fortunately, most of it is absorbed by the atmosphere' s ozone layer before reaching the surface. Most humans are aware of the effects of UV radiation through the painful condition of sunburn. The UV spectrum has many other effects, including both beneficial and damaging changes to the human health.

2.3.7 X-rays

Next come x-rays. They penetrate with little loss through some things and high loss through others, and have many applications in high energy physics and astronomy. This kind of radiation is emitted by neutron stars and accretion disks around black holes which enables us to study these objects. X-rays are capable of passing through most substances which makes them useful in medicine and industry. They are given off by stars and strongly by some types of nebulae. An x-ray machine works by firing a beam of electrons at a target. If the electrons are fired with sufficient energy, x-rays will be produced.

2.3.8 Gamma rays

After the hard x-rays there come gamma rays. They are the most energetic photons having no defined lower limit to their wavelength. They are useful to astronomers in the study of high energy objects and find use with physicists due to their penetrative ability and their production from radioisotopes. Their wavelength can be measured with high accuracy by means of compton scattering.

2.4 Electromagnetic spectroscopy

The spectroscopy of electromagnetic spectra emitted from atoms emitting quanta of electromagnetic radiation is called electromagnetic spectroscopy. It is done with the aid of appropriate spectrometers. This spectroscopy can be classified into narrower fields, although in some spectroscopic techniques several processes may be happening at the same time.

Emission spectroscopy is the study of electromagnetic radiation spectra emitted by atoms or molecules that undergo transition to a lower energy level. It determines the wavelength of the emitted photons. Since each element emits a characteristic set of discrete wavelengths according to its electronic structure, the elemental composition of a sample can be determined by observing these wavelengths. Generally, emission spectroscopy deals with visible light and shorter wavelengths, since fluorescence and phosphorescence, as these processes are called, less likely happen with longer wavelengths. However, there are many ways in which atoms can be brought to an excited state.

Absorption spectroscopy, on the other hand, is the study of electromagnetic radiation spectra absorbed by atoms or molecules that change energy levels. Often it is used as an analytical technique, since specific chemical compounds have a specific absorption spectrum that acts as a fingerprint for these compounds. Moreover, the amount of absorption is related to the amount of absorbing compound. Thus, absorption spectroscopy can be used to determine the concentration of chemical compounds in samples.

2.4.1 Supramolecular spectroscopy

Spectroscopy is concerned with the interaction of light with matter.

Generally it is observed that the spectra of dense gases differ from the spectra of the same gases at low densities. With from near zero increasing gas density first the familiar, allowed rotovibrational and electronic bands may appear in the appropriate frequency region (if there is such an allowed spectrum) [13]. Intensities of this spectrum increase linearly with increasing gas density. As the gas density is further increased, at intermediate densities generally new absorption bands occur whose intensity increases in any case nonlinearly in gas density, quadratic, cubic, ... The origin of these new bands are van der Waals complexes of two or more molecules which may be free, i.e. transient collisional complexes, or bound, i.e. weakly bound van der Waals molecules. Generally such absorption bands are found in all molecular gases, no matter wether the gases consist only of infrared-inactive molecules.

The H_2 molecule, like other diatomic molecules with inversion symmetry, is certainly infrared inactive, because this symmetry is inconsistent with the existence of a dipole moment. Thus, at low gas densities no absorption of electromagnetic radiation by hydrogen molecules occurs. Nevertheless, in solid, liquid and gaseous hydrogen at high enough densities absorption in the infrared part of the electromagnetic spectrum is observed. This absorption can be explained with the model of a supramolecular (collision-induced) process, which will be discussed further in the next chapter.

This work deals with collision-induced absorption of radiation in gases in the infrared region of the spectrum. Supramolecular spectra arise from interaction-induced dipole moments, i.e. dipole moments that do not exist in the non-interacting molecules. For any detailed treatment of interaction-induced processes the concept of a supramolecule is a most useful concept.

For a long time spectroscopists have known certain phenomena caused by collisions, such as the pressure broadening of spectral lines. However, pressure broadened lines are normally not considered to be collision-induced. Pressure broadened means that no new intensity is created but the existing line intensities are just spread over a greater frequency band. In contrast to that collision-induced means that new intensity is created that does not have its origin in single molecules but in the existence of supramolecules. The definition of interaction-induced absorption as it is used in this work implies the existence of a dipole component that arises from the interaction of two or more atoms or molecules, leading at high enough gas density to discernible spectral line intensities in excess of the sum of the absorption of the atoms/ molecules of the complex.

2.5 Dimers and larger clusters

At close range intermolecular forces are repulsive and become attractive at distant range. At intermediate gas densities most of the common gases form dimers. At high densities higher than binary complexes are expected, too.

Collision-induced absorption arises mainly from multi-polar induction.

The frequencies of interest for studies of collision-induced absorption range from microwave frequencies to the ultraviolet, depending on the systems and specific transitions considered. Collision-induced absorption is not limited to the far infrared. As is well known molecules may vibrate. In general vibrational transition frequencies are much higher than rotational transition frequencies, namely roughly a few thousand cm^{-1}.

The light sources, monochromators, detectors and pressure cells needed for such studies are more or less the same as in the conventional spectroscopies. Temperature control has been essential in much of the studies of collision-induced absorption. Temperature variation accesses different parts of the intermolecular interaction potential and redistributes the relative importance of overlap and multi-polar induction. As a note aside it should be mentioned that at low temperatures collision-induced line shapes are relatively sharp, so that induced lines may be resolved whose structures may be masked at higher temperatures.

Figure 2.3 shows the absorption spectra of gaseous, liquid and solid hydrogen. As is obvious from the figure the absorption spectra become more striking with lower temperature from the gaseous over the liquid to the solid state.

According to [13] the translational state of a pair of atoms is given by the energy, E, and the angular momentum, L^2, L_z, of relative motion. A major difference between this energy and the vibrational energy, E_ν, is that it is continuous whereas vibrational energies are discrete. The angular momentum

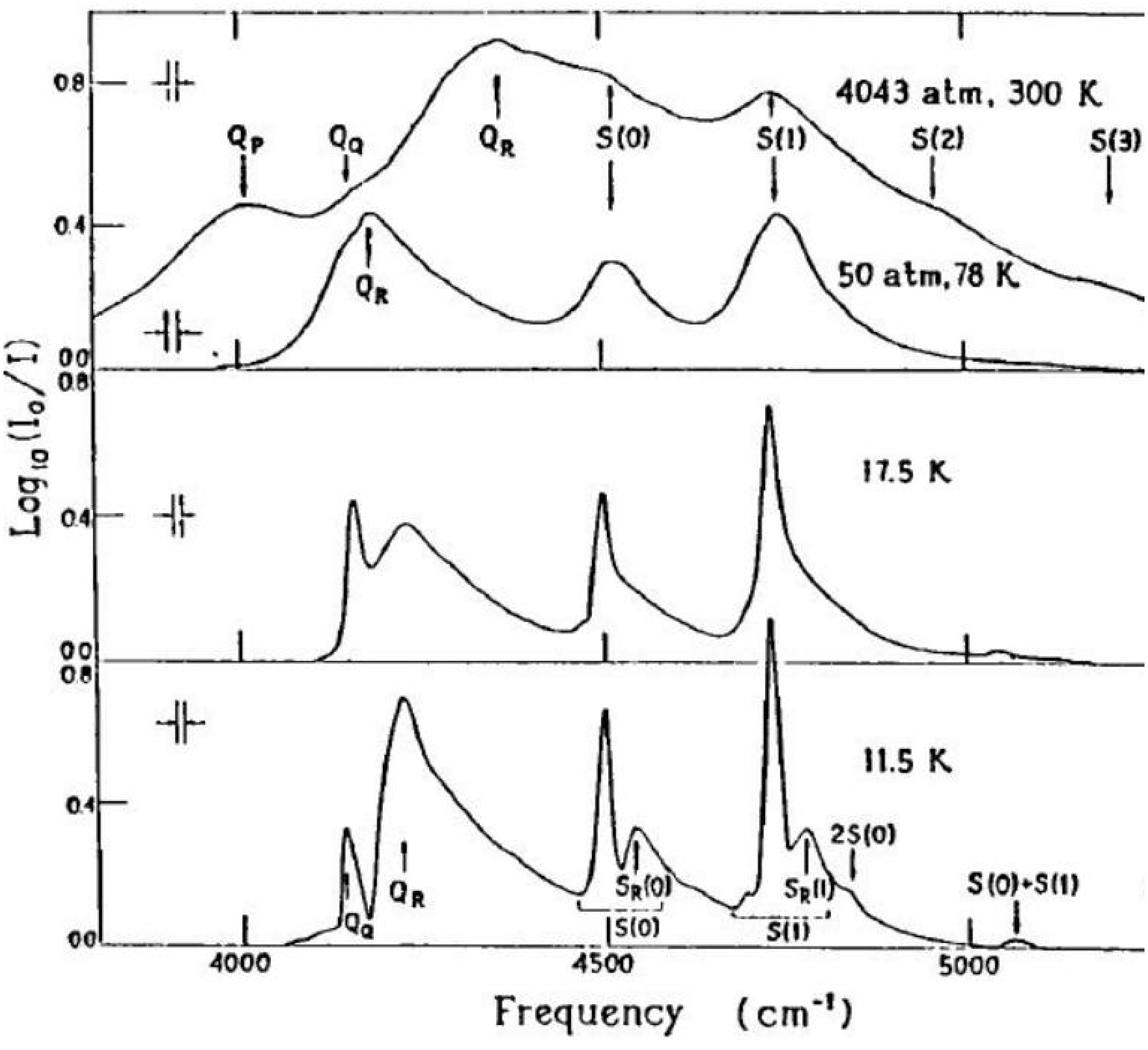

Figure 2.3: Comparison of collision-induced absorption in gaseous (upper part), liquid (middle part) and solid (lower part) hydrogen

is analogous to the rotational angular momentum, J^2, J_z.

It should be pointed out here that the translational transitions of virtually all molecules are infrared active, even if the individual molecules are not. This is true for all supramolecules, except for those which posses a symmetry, which is inconsistent with the existence of a dipole moment. Supramolecular spectra, like molecular and electronic spectra, may be of the electronic or the rotovibrational type. However, in this work only the rotovibrational type is investigated. Supramolecular electronic spectra exist, but are not as universal as the rotovibrational induced spectra. The major concern of this work is on absorption of electromagnetic radiation by binary complexes, for which numerous high quality measurements exist. These can be described theoretically quite rigorous. This makes it possible to compare the fundamental theory directly with the measured binary spectra.

2.5.1 Laboratory measurements

Since collision-induced absorption is usually very weak but gas cell dimensions are generally limited laboratory measurements of collision-induced absorption require compressed gases, i.e. higher densities than what is usually encountered in the absorbing regions of planetary and stellar atmospheres. Measurable CIA requires either long path lengths or high densities. However, the high pressure used for laboratory measurements can introduce many-body effects. These effects are undesirable if one wants to study the purely binary collision-induced absorption. Theory is capable of describing the binary collision-induced absorption. This is one of the points that distinguishes good laboratory measurements from bad ones, the amount to which they attempt to minimize many-body effects. Another point to mention is the temperature where one makes measurements. It is fair to expect laboratory measurements at room temperature to be more accurate than at other temperatures because for room temperature one does not have to deal with undesired temperature gradients. Despite the many difficulties one encounters in laboratory measurements of collision-induced absorption some excellent measurements exist.

In measuring near infrared spectra one can use photomultipliers and photo diodes. However, in the far infrared, where photon energies are much lower, one has to use thermistors and thermopiles. It is even more difficult to obtain accurate measurements of translational spectra.

Chapter 3

Theoretical Background

There exist numerous monographs, review articles and other references such as the excellent book [13] on the general theory of collision-induced absorption. In the following a short overview, based on [19] will be given. Most of the presented formulas are so general that they are valid for a great variety of gases and mixtures. Throughout this overview the Born-Oppenheimer approximation is applied, i.e. the nuclear motions are assumed to be slow compared to the electronic motions, that is, all potential energy and dipole surfaces are assumed to be independent of the velocity of the nuclei. Bound composites, so called van der Waals molecules, are formed by most pairs of atoms or molecules. At low temperatures, i.e. in the order of hundred Kelvin and less, these contribute to the CIA spectrum with sharp features. However, this work will only deal with higher temperatures and thus free-free transitions dominate the spectra. Van der Waals molecules can safely be ignored, since their effect at the temperatures considered is negligible.

In the following all formulas are presented in cgs units. However, if one prefers SI units proper factors of $4\pi\epsilon_0$ have to be inserted in all formulas that contain electromagnetic fields. The necessary physical constants can be found in the appendix.

3.0.2 Intermolecular potentials

The ideal gas law is valid for non-interacting point like particles. It is a good approximation for rarefied gases at high temperatures in that it is in close agreement with measurements of the pressure, density and temperature. However, it obviously neglects important features of gaseous matter, for instance condensation and incompressibility of liquids and solids.

Even though the true nature of intermolecular forces could only be understood after the development of quantum mechanics it is remarkable that as early as in 1873 van der Waals developed his famous equation of state [13]. This was a significant improvement over the ideal gas law for the description of real gases. It assumes a repulsion like that of hard spheres at near range and attraction at more distant range. However, the Pauli principle, developed much later, is needed to understand why at close range there occurs repulsion. When atoms or molecules approach each other closely enough so that their electronic clouds overlap, the energy increases because the Pauli principle forces electrons into higher states [13]. According to the principle of energy minimization this causes repulsion. It should be mentioned that not only the electrons but also the Coulomb forces between the nuclei contribute to the repulsion at near range.

For Gravitational forces up to now no satisfying theory exists that is compatible with the other forces but since they are roughly 30 orders in magnitude weaker than the electrical forces they can safely be ignored in most cases.

From the discovery of quantum mechanics to the late 1960s most research on intermolecular forces was based on two assumptions, first that the intermolecular potential could be represented by simple functions such as the two-parameter Lennard-Jones model, and secondly that the intermolecular energy of a molecular complex is well represented by the sum of their pair interaction energies. However, both assumptions turned out to be wrong and have obstructed significant progress in the field (Maitland et al., 1981). This changed significantly since the 1970s with the advent of new accurate measurements of various bulk properties [13]. More recently also vastly improved *ab initio* computations and direct inversions of measurements have been possible. These permit the construction of intermolecular potentials without any ad hoc assumption concerning the analytic form of the potential. Today it is well known that the repulsive branch of the intermolecular energy of rare gas pairs has an exponential form, in contrast to the R^{-12} dependence of the Lennard-Jones model.

It should be mentioned that in general, if molecules are involved, isotropic potential functions are inadequate since angular dependencies reflecting the molecular symmetries have to be taken into account. In general up to five angular variables may be needed for a complete description of the anisotropy. However, in many cases the isotropic interaction approximation (IPA) can be used with sufficient accuracy [13].

In general molecules have internal degrees of freedom. They may vibrate or rotate, which modifies their interactions with other molecules. Vibrating molecules often appear bigger and more anisotropic. However, the vibrational dependence has only been carefully modeled for a few systems, and only a few molecular interaction potentials are well known.

3.0.3 Cross sections

There are many ways how one can define a cross section of collisions, for example for elastic, inelastic, super-elastic, reactive, etc. collisions. In this work the main focus is on elastic collisions of atoms and molecules in the presence of light.

According to [13] for isotropic potentials the differential scattering cross section is given by

$$\frac{\partial Q_{12}}{\partial \Omega} = \frac{1}{2i\kappa} \sum_{l=0}^{\infty} (2l+1)\, P_l\left(\cos\left(\chi\right)\right) \left[\exp\left(2i\eta_l\right) - 1\right], \tag{3.0.1}$$

where $\mathrm{P}_l(\cos(\chi))$ are the Legendre polynomials, η_l are the scattering phase shifts and the magnitude of the wave vector κ is related to the translational kinetic energy of relative motion E_T via $\hbar\kappa = 2\mathrm{m}_{12}\mathrm{E}_T$. It should be pointed out here that the expression for the scattering cross section is consistent with all experimental facts. From equation (3.0.1) the total cross section can be calculated according to [13],

$$Q_{12} = 2\pi \int_0^{\pi} \frac{\partial Q_{12}}{\partial \Omega} \sin(\chi)\, d\chi. \tag{3.0.2}$$

In general it is a function of the relative speed v_{12} of the encounter and is large at the smallest speeds, where the intermolecular forces dominate.

3.1 Time scales

In the theory of collisions, at not too high gas densities, one distinguishes three different times associated with collisions. They turn out to be helpful for the understanding of spectral line shapes and are namely the average time between collisions, the duration of a molecular fly-by and the duration of the spectroscopic interaction.

The mean time between collisions, τ_{12}, is the reciprocal collision frequency ν_{12}, which in turn is related to the total scattering cross section Q_{12}. Further details may be found in [13]. For rough estimates, the collisional cross section may be assumed to be velocity-independent,

$$Q_{12} = Q_0 = constant \tag{3.1.1}$$

(hard sphere approximation) and the mean time between collisions can be estimated as

$$\tau_{12} = \frac{1}{\nu_{12}} = \frac{1}{\bar{v}_{12} n_2 Q_0} \tag{3.1.2}$$

with

$$\bar{v}_{12} = \sqrt{\frac{8kT}{\pi m_{12}}}. \tag{3.1.3}$$

Here, n is the particle number density and m_{12} is the reduced mass of the collisional pair,

$$m_{12} = \frac{m_1 m_2}{m_1 + m_2} \tag{3.1.4}$$

with the masses m_i of species i. The average relative speed of a collisional pair is of the order of the root-mean-square speed, which is approximately equal to the speed of sound and varies with temperature as $T^{-1/2}$. For hydrogen gas at standard temperature (273K) and pressure (1 atmosphere) the mean time between collisions amounts to roughly 0.07×10^{-9}s [13]. The mean time between collisions decreases with density as 1/n.

The duration of a fly-by encounter is according to [13] approximately given by

$$\Delta t \approx \frac{\sigma}{\bar{v}_{12}}. \tag{3.1.5}$$

$\sigma = \sigma_1 + \sigma_2$ is the sum of the diameters of the interacting atoms (hard sphere approximation) and may be approximated by the root of the intermolecular interaction potential, $V_0(\sigma) = 0$. This duration varies with temperature as $T^{-1/2}$, is density invariant and for hydrogen gas at standard temperature amounts roughly to 1.6×10^{-13}s [13].

Spectral intensities are proportional to the dipole moment squared. In optics the mean duration of optical interactions is given by

$$x\Delta t' = R_s/\bar{v}_{12}, \tag{3.1.6}$$

where R_s is the range of optical interactions. For details the reader is referred to [13]. Typically durations vary as $T^{-1/2}$, are density independent and amount to roughly 10^{-13}s at room temperature.

It should be pointed out here that near standard temperature and pressure, the time between collisions is about three orders of magnitude greater than the duration of a collision. Thus, a Maxwellian distribution of velocities is reasonable and, if the interactions have a range not greater than the size of the atoms, the concept of binary interactions appears to be a good model [13]. However, at densities approaching liquid state density, i.e. several hundred amagats, the time between collisions and the duration of a collision become comparable and each particle is interacting with several partners at a time. Under such conditions the time scales considered above become meaningless.

Even though collisional complexes exist only for very short times, i.e. times in the order of 10^{-13}s, the duration of a molecular fly-by encounter, they are a physical reality like for example van der Waals molecules. Whereas conventional spectroscopy generally emphasizes the measurement of frequency and energy levels, collision-induced spectroscopy mainly aims for the measurement of absorption intensity and line shape [13]. Collision-induced spectroscopy may be used to provide information on intermolecular interaction, e.g. multipole moments and range of exchange forces, intermolecular dynamics and optical bulk properties [14].

The kinetic energy of relative motion of a molecular pair is a continuum with width in the order of the thermal energy, $E_{free} \approx 3kT/2$ [13]. There occur radiative transitions between free states which are relatively diffuse, in reflection of the short lifetime of the supramolecule. It should be mentioned that van der Waals molecules have relatively few bound states. At not too low temperatures many more free pair states are populated than dimer states which results in smaller intensities.

In general collision-induced spectra consist of contributions arising from free-to-free, free-to-bound, bound-to-bound and bound-to-free transitions. At temperatures T much greater than the well depth ϵ of the intermolecular potential, $kT \gg \epsilon$, the observed absorption is nearly fully due to free-to-free transitions, but individual dimer lines or bands may still be quite prominent unless pressure broadening or perhaps ternary interactions have obliterated such structures. On the other hand, at low temperature, $kT \lesssim \epsilon$, spectral components involving bound dimers become most prominent [13].

3.1.1 The hydrogen molecule

In the following some relevant formulas for the hydrogen molecule will be covered. These considerations are generally valid for all diatomic molecules [19]. Since this work deals with H_2 molecules in their electronic ground state, i.e. in the $^1\Sigma_g^+$ state, only this case will be treated. Thus, it is sufficient for a description of the dynamics to consider the Hamilton operator for the nuclear motion,

$$H^{H-H}(\mathbf{r}) = -\frac{\hbar^2}{m_H}\nabla_{\mathbf{r}}^2 + V^{H-H}(\mathbf{r}). \tag{3.1.7}$$

Here, $\mathbf{r}$ is a vector of length r pointing in the direction from one proton to the other, m_H is the atomic hydrogen mass and V^{H-H} is the inter-atomic potential energy. $\hbar$ is the reduced Planck constant and $\nabla_{\mathbf{r}}$ is the nabla operator. It should be noted that in the isotropic potential approximation the potential energy only depends on the relative distance r between the two protons. In the expression for the kinetic energy operator in equation (3.1.7) the Laplace operator can be rewritten according to [19] as follows,

$$\nabla_{\mathbf{r}}^2 = \frac{1}{r}\frac{\partial^2}{\partial r^2}r - \left(\frac{\mathbf{j}}{\hbar r}\right)^2. \tag{3.1.8}$$

In this equation $\mathbf{j}$ is the dumbbell angular momentum of the diatom [19]. Like in any other central force problem the Hamilton operator in equation (3.1.7) has eigen functions of the form

$$\frac{\upsilon_{\nu j}(\mathbf{r})}{r} Y_{jm_j}(\hat{\mathbf{r}}). \tag{3.1.9}$$

These are separable in the radial and in angular coordinates [19].

$$\hat{\mathbf{r}} = (\cos(\Phi) \times \sin(\Theta), \sin(\Phi) \times \cos(\Theta), \cos(\Theta))^T \tag{3.1.10}$$

is the unit vector used to indicate the angular variables Θ and Φ and T denotes the transpose. Since

$$\mathbf{j}^2 Y_{jm_j} = \hbar^2 j\,(j+1)\,Y_{jm_j}, \tag{3.1.11}$$

the Schroedinger equation for the H_2 molecule, which in general is a second order partial differential equation,

$$(H^{H-H} - E_{\nu j} \times \mathbf{I}) \frac{\upsilon_{\nu j}(r)}{r} Y_{jm_j}(\hat{\mathbf{r}}) = 0, \tag{3.1.12}$$

where $\mathbf{I}$ is the unit operator, becomes a second order ordinary differential equation of one variable, the radial distance r,

$$\left(-\frac{\hbar^2}{m_H} \frac{d^2}{dr^2} + \frac{\hbar^2 j(j+1)}{m_H r^2} + V^{H-H}(r) - E_{\nu j} \right) \upsilon_{\nu j}(r) = 0 \tag{3.1.13}$$

for the radial wave function $\upsilon_{\nu j}$ [19]. These vibrational wave functions, $\upsilon_{\nu j}$ can be obtained by numerical integration of equation (3.1.13) using the

Numerov procedure and an *ab initio* potential V^{H-H} from [59]. Although the convention of the signs of the radial wave function is arbitrary here they have been fixed for convenience so that the matrix element

$$\langle \nu j | r | \nu' j' \rangle := \int_{-\infty}^{\infty} v_{\nu j}^{*}(r) r v_{\nu' j'}(r) \mathrm{d}r \tag{3.1.14}$$

is always positive. * denotes the complex conjugate. The eigen values $\mathrm{E}_{\nu j}^{H-H}$ can be obtained by solving equation (3.1.13) [19].

3.1.2 Identical nuclei

In quantum mechanics whenever two or more nuclei of a molecule are identical one has to take into account exchange symmetry. Then, including the nuclear spin state χ and the electronic wave function Φ rather than the wave function in equation (3.1.9) one has the following eigen state of a diatom [19],

$$\Psi(\mathbf{r}; 1, 2) = \frac{v_{\nu j}(r)}{r} Y_{j m_j}(\hat{\mathbf{r}}) \chi_{S M_S}(\mathbf{s}_1, \mathbf{s}_2) \Phi(r). \tag{3.1.15}$$

In equation (3.1.15) $\mathbf{s}_1$ and $\mathbf{s}_2$ are the two nuclear spins, and by the laws of quantum mechanics for the addition of spins $\mathbf{S} = \mathbf{s}_1 + \mathbf{s}_2$ is the total nuclear spin. The eigenvalues m_1 and m_2 of the z-components of $\mathbf{s}_1$ and $\mathbf{s}_2$, and $\chi_{S M_S}$ are according to [19] related to each other by the Clebsch-Gordan series, given by

$$\chi_{SM_S}(\mathbf{s}_1, \mathbf{s}_2) = \sum_{m_1, m_2} C(\mathbf{s}_1, \mathbf{s}_2, \mathbf{S}; m_1, m_2, M_S) |m_1 m_2\rangle. \tag{3.1.16}$$

If the two nuclei are identical, $s_1 = s_2$ and quantum statistics requires that

$$\Psi(-\mathbf{r}, \mathbf{s}_1, \mathbf{s}_2) = \pm\Psi(\mathbf{r}; \mathbf{s}_1, \mathbf{s}_2) \tag{3.1.17}$$

with the + sign for bosonic nuclei (integer spin) and the - sign for fermionic nuclei (half-integer spin). In this work only the electronic ground state is of interest. For homo-nuclear diatoms the electronic ground state is one of Σ_g^+, Σ_g^-, Σ_u^+ or Σ_u^-. The majority of the diatoms is in the state Σ_g^+. The H_2 groundstate is without exception $^1\Sigma_g^+$. The Σ_g^+ and Σ_u^- states are even under nuclear exchange, i.e. $\Phi(-\mathbf{r}) = \Phi(\mathbf{r})$, whereas the Σ_g^- and Σ_u^+ states are odd, so that $\Phi(-\mathbf{r}) = -\Phi(\mathbf{r})$. For the case of diatoms consisting of hydrogen the nuclei are two protons which have spin 1/2. Thus, the spin states χ_{SM_S} are the anti-symmetric

$$\chi_{00} = \frac{1}{\sqrt{2}}\left(|\uparrow\downarrow\rangle - |\downarrow\uparrow\rangle\right) \tag{3.1.18}$$

and the symmetric triplet states

$$\chi_{1-1} = |\downarrow\downarrow\rangle, \tag{3.1.19}$$

$$\chi_{10} = \frac{1}{\sqrt{2}} \left(| \uparrow\downarrow\rangle + | \downarrow\uparrow\rangle \right), \tag{3.1.20}$$

$$\chi_{1+1} = | \uparrow\uparrow\rangle, \tag{3.1.21}$$

where $\uparrow$ indicates m = 1/2 and $\downarrow$ indicates m = -1/2. The radial part of Ψ is unaffected by an exchange of nuclei and Φ is even. Thus, $\mathrm{Y}_{jm_j}(\hat{\mathbf{r}})$ and χ_{Sm_S} have to fulfill the requirements of equation (3.1.17). The spherical harmonics obey the relation

$$Y_{jm_j}(-\hat{\mathbf{r}}) = (-1)^j Y_{jm_j}(\hat{\mathbf{r}}). \tag{3.1.22}$$

Therefore, if j is even the nuclear spin state has to be a singlet and if j is odd it must be one of the triplet states. Correspondingly, in nature there are three times more possibilities for odd j than for even j [19]. In theory this difference in abundance is described by the nuclear spin statistical weight g_j. Values of g_j can be read of from tables of Clebsch-Gordan coefficients.

Often a hydrogen molecule in the odd j state is referred to as ortho-hydrogen, o-H_2, and if it is in the even j state it is called para-hydrogen, p-H_2. If no magnetic material is present to enhance the spin flip rate in reality nuclear spin flips are extremely rare in ordinary collisions between molecules or between the molecules and the container walls. Thus, in practice, para-hydrogen behaves as a different species than ortho-hydrogen, and computations can be carried out for one species at a time [19].

3.1.3 The radiation field

Including the electromagnetic field in the Hamilton operator requires a quantized description of the radiation, i.e. one has to treat light using the photon formalism. This is strictly speaking a quantum field theory of electromagnetism, called quantum electrodynamics (QED). In this theory the Hamilton operator of the radiation field is written in terms of creation and annihilation operators, as for example discussed in [10],

$$H_{rad} = \sum_{\mathbf{k}r} \hbar\omega_{\mathbf{k}} \left(a^{\dagger}_{\mathbf{k}r} a_{\mathbf{k}r} + \frac{1}{2} \times \mathbf{I} \right). \tag{3.1.23}$$

The summation is over all wave vectors $\mathbf{k}$ and polarizations r and the eigen frequencies are given by $\omega_{\mathbf{k}} = c|\mathbf{k}|$. $a^{\dagger}_{\mathbf{k}r}$ are creation operators and $a_{\mathbf{k}r}$ are annihilation operators. In collision-induced absorption one is concerned with photons incident from a given direction with given frequency and polarization. For n photons the radiation field in this given mode with frequency ω is given as the eigenstate $|n\rangle$ of the equation

$$H^{rad}|n\rangle = n\hbar\omega|n\rangle. \tag{3.1.24}$$

In this equation the vacuum field energy $\hbar\omega/2$ has been suppressed because it only results in a shift of the energy scale.

It should be remarked that in this case perturbation theory leads to the same results as quantum electrodynamics. However, since QED is the more general theory in this work the quantum electrodynamical treatment is presented.

3.1.4 Interaction with dipoles

In the following some results from [11] and [42], which are relevant for this work, are presented. Because the wavelength of infrared light is much larger than the size of collisional complexes, the dipole approximation is certainly not bad for the situation discussed in this work. According to [10] the energy of a dipole interacting with an electric field is given by

$$V^{rad} = -\boldsymbol{\mu} \times \boldsymbol{E}(t). \tag{3.1.25}$$

Here $\boldsymbol{\mu}$ is the dipole moment and $\boldsymbol{E}$ is the electric field vector of the light. In the quantized formalism the electric field can be written as

$$\boldsymbol{E}(t) = i \sum_{\boldsymbol{k}r} \sqrt{\frac{2\pi\hbar\omega_{\boldsymbol{k}r}}{\Phi}} c\epsilon \left(a_{\boldsymbol{k}r} \exp\left(-i\omega_{\boldsymbol{k}} t\right) - a^{\dagger}_{\boldsymbol{k}r} \exp\left(i\omega_{\boldsymbol{k}} t\right) \right), \tag{3.1.26}$$

where Φ is the radiation flux in photon number per area per time. With the assumption of linear polarization along the $\hat{z}$ axis of the eigen state $|n\rangle$ introduced above one has

$$\langle n|V^{rad}|n'\rangle = -iW \left(\exp\left(-i\omega t\right) \delta_{nn'-1} - \exp\left(i\omega t\right) \delta_{nn'+1}\right), \tag{3.1.27}$$

where

$$W = \sqrt{\frac{2\pi\hbar\omega\Phi}{c}}\boldsymbol{\mu}_z. \tag{3.1.28}$$

Thus W has the same dependence on the angular coordinates of the particles as $\boldsymbol{\mu}_z$. The $\hat{z}$ direction is chosen as the direction along which angular momenta are quantized. It should be noted that the dipole coupling in equation (3.1.27) is complex. Since the scheme is perturbative in the radiative coupling it is possible to obtain a purely real matrix element. By Fermi' s Golden rule one takes the square of the dipole coupling matrix elements in order to calculate radiative transition probabilities,

$$|\langle f|V^{rad}|i\rangle|^2. \tag{3.1.29}$$

According to equation (3.1.27) this is time independent, which implies that one can take arbitrary values for t. For the choice t = -$\pi/2\omega$ the final expression for the dipole coupling is

$$\langle n|V^{rad}|n'\rangle = W\delta_{nn'-1} + W\delta_{nn'+1} \tag{3.1.30}$$

3.1.5 Electric dipole moment induced by interactions

From elaborate quantum-chemical calculations accurate interaction-induced dipole surfaces can be obtained [40]. For several binary systems in literature *ab initio* dipoles and empirical ones are available. Even though the subject of this work is not to compute collision-induced dipole surfaces in the following physical mechanisms will be discussed that cause an induced dipole moment.

This work is concerned with binary complexes of H_2. Since these pairs have inversion symmetry no dipole moment can be produced. This is clear in all cases of two identical atoms, but also in the case of two identical molecules with all quantum numbers equal. As an example one may consider two hydrogen molecules, both with the configuration $|\nu j\rangle = |00\rangle$. Since j being zero also implies that m_j is zero they do not possess a collision-induced dipole moment [19].

One can divide the van der Waals force of two nonpolar particles according to [17] into two components. There is a short range exchange term which has its origin in the Pauli exclusion principle and prohibits extensive overlap of the electronic distributions and secondly there is a long range dispersion term which has its origin in fluctuations of the charge causing dipole-dipole interaction. The one mechanism for the induction of a dipole moment is the same as the one producing the force between the particles. To good approximation this dipole moment is proportional to that force. It has a short range term [13],

$$\mu_e \approx \exp\left(-R/R_0\right), \tag{3.1.31}$$

and a long range dispersion term [13], which to lowest order behaves as

$$\mu_e \approx -\frac{1}{R^7}. \tag{3.1.32}$$

In the case when at least one particle is a molecule another mechanism, called multipole-induction, appears. The hydrogen molecule naturally carries a permanent quadrupole moment. If another particle, for example an atom is in its proximity, this particle will be polarized in the quadrupole field of the hydrogen molecule. This mechanism is apparently more long range than the van der Waals interaction. According to [52] for large distances R it has approximately the form

$$A_{23}(r,R) \approx \frac{\sqrt{3}\alpha_0}{R^4} Q_2(r). \tag{3.1.33}$$

Here $Q_2(r)$ is the quadrupole moment of the hydrogen molecule and α_0 is the polarizability of the other particle. The indices 23 will be described further below and have to do with the orientational dependence. It should be remarked that equation (3.1.33) is exact outside the molecule.

If molecular gases are considered infrared spectra are richer than those in the rare gases. Even if the molecules are non-polar, besides the translational spectra various rotational and rotovibrational spectral components may be expected. Furthermore, other than overlap other induction mechanisms become important. Dipole components may be thought of as being modulated by the vibration and rotation of the interacting molecules so that induced supramolecular bands appear at the rotovibrational frequencies. Lines at sums and diferences of these frequencies also occur and are common in the fundamental and overtone bands [13].

The electronic charge distribution of H_2 is inversion symmetric and thus the H_2 molecule is necessarily non-polar. H_2–H_2 pairs, just like pairs of virtually all other molecules possess an induced dipole moment (except for certain molecular orientations of high symmetry). However, the H_2 molecule differs from most neutral molecules by its large rotational constant, $B_0 = 59\text{cm}^{-1}$, compared for instance to rotational constants of N_2 and O_2 of just a few wavenumbers [13]. Thus, collision-induced spectra of systems containing H_2 generally show well separated H_2 rotational lines, unless temperatures are so high that lines begin to merge. The lowest order multipole consistent with the symmetry of H_2 is the electric quadrupole. The H_2 S_0 lines arise basically from quadrupolar induction, a small overlap component is nearly negligible [41].

A rotation of the H_2 molecule through 180 degrees creates an identical electric field. This means that for every full rotation of a H_2 molecule the dipole induced in the collisional partner oscillates twice through the full cycle. Thus, quadrupole induced lines occur at twice the classical rotation frequencies, or with selction rules $J \rightarrow J\pm2$ like rotational Raman lines of linear molecules. Orientational transitions (J = constant, ΔM not equal to zero) occur at zero frequency and make up the translational line [13]. For H_2–H_2, molecule 1 induces a dipole in 2 and vice versa, thereby doubling intensities.

In the center of mass fixed frame six independent coordinates are sufficient to describe the positions of three particles. In quantum-chemical calculations the Cartesian components of the dipole moment are obtained, $\boldsymbol{\mu}_x$, $\boldsymbol{\mu}_y$ and $\boldsymbol{\mu}_z$. For example, one may take a look at table 1 in [37]. Because of the induction of the dipole in scattering calculations it is convenient to perform the transformation into spherical components, according to [49] one has

$$\boldsymbol{\mu}_0 = \boldsymbol{\mu}_z, \tag{3.1.34}$$

$$\boldsymbol{\mu}_\pm = \frac{1}{\sqrt{2}}(\pm\boldsymbol{\mu}_x - i\boldsymbol{\mu}_y). \tag{3.1.35}$$

According to [48] one can obtain from these the tensor coefficients, $A_{\lambda L}$ (r,R), via the series expansion

$$\mu_\nu(\mathbf{r},\mathbf{R}) = \frac{4\pi}{\sqrt{3}}\sum_{\lambda L} A_{\lambda L}(r,R)Y^{1\nu}_{\lambda L}(\hat{\mathbf{r}},\hat{\mathbf{R}}), \tag{3.1.36}$$

where the vector coupling function $Y^{1\nu}_{\lambda L}(\hat{\boldsymbol{r}})$ is defined in equation (3.1.22). Since the H_2 molecule is symmetric with respect to inversion the coefficients $A_{\lambda L}$ are non-zero only if λ is an even number [19], because the dipole is invariant under the parity operation $\hat{\mathbf{r}}_1 \to -\hat{\mathbf{r}}_1$, $\hat{\mathbf{r}}_2 \to -\hat{\mathbf{r}}_2$, $\hat{\mathbf{R}} \to -\hat{\mathbf{R}}$. Here $\hat{\mathbf{R}}$ denotes the vector from the center of mass of the molecule to one of the hydrogen atoms, $\hat{\mathbf{r}}_1$ is the vector from the center of mass of hydrogen atom 1 to its electron and similarly $\hat{\mathbf{r}}_2$ is the vector from the center of mass of hydrogen atom 2 to its electron. Furthermore, the dipole operator is a rank one tensor, which implies the triangular condition $|\lambda - L| \leq 1$ and also that $\lambda + L$ is odd, so that $\boldsymbol{\mu}$ does not change under reflection in a plane through the origin.

According to [13] in order to calculate the collision-induced absorption spectra one needs the vibrational matrix elements of the tensor components $A_{\lambda L}$,

$$B_{\lambda L}^{\nu j \nu' j'}(R) = \langle \nu j | A_{\lambda L} | \nu' j' \rangle \tag{3.1.37}$$

for the lines arising from the transition $\nu j \rightarrow \nu' j'$.

The energy levels for a rotovibrational state corresponding to the vibrational and rotational quantum numbers ν and j are labeled $E_{\nu j}$. They are considered to be unperturbed during collisions, which is another way to express the assumption that the colliding partners have strong internal interaction while they interact weakly with each other.

The Hamilton operator describing the interaction between two hydrogen molecules with rotating and vibrating degrees of freedom in the presence of a radiation field is according to [19] given by

$$H(\mathbf{r}, \mathbf{R}) = H^{H-H}(\mathbf{r}) - \frac{\hbar^2}{2m} \nabla_{\mathbf{R}}^2 + V(\mathbf{r}, \mathbf{R}) + V^{rad}(\mathbf{r}, \mathbf{R}) + H^{rad}, \tag{3.1.38}$$

where V is the intermolecular potential of the H_2–H_2 complex and m is the reduced mass. In equation (3.1.7) the Hamilton operator for the isolated

H_2 molecule, H^{H-H}, is given. The inter-atomic potential is included in H^{H-H} and not in V. The reduced mass is the two particle mass,

$$m = \frac{m_1 + m_2}{m_1 \times m_2}. \tag{3.1.39}$$

The radiative coupling V^{rad} and the Hamilton operator for the isolated photon field H^{rad} are the ones discussed above. The total wave function can be factorized as the product of the scattering wave function and the photon state [19],

$$\Psi_\alpha(\boldsymbol{r}, \boldsymbol{R}; E) \otimes |n\rangle = \sum_{\alpha' n'} \frac{\upsilon_{\nu' j'}(r)}{r} \frac{1}{R} F^{n'n}_{\alpha'\alpha}(R; E) Y^{J'M'}_{j'l'}(\hat{\boldsymbol{r}}, \hat{\boldsymbol{R}}) \otimes |n'\rangle, \tag{3.1.40}$$

where $\alpha = (\nu, j, l, J, M)^T$ and $Y^{J'M'}_{j'l'}(\hat{\boldsymbol{r}},\ \hat{\boldsymbol{R}})$ is the vector coupling function, corresponding to $\mathbf{J} = \mathbf{j} + \mathbf{l}$, i.e. the total angular momentum is the sum of rotational and translational angular momentum. Now the Schroedinger equation reads

$$\left(H - E \times \boldsymbol{I}\right) \Psi_\alpha \otimes |n\rangle = 0. \tag{3.1.41}$$

Operating from the left with

$$\langle n''| \otimes \int r v^\star_{\nu'' j''}(r)\, dr \int Y^{J''M''\star}_{j''l''}(\hat{\boldsymbol{r}}, \hat{\boldsymbol{R}})\, d\hat{\boldsymbol{r}}\, d\hat{\boldsymbol{R}} \tag{3.1.42}$$

integrates out five of the six spatial variables [19], where the integral $\int d\hat{\boldsymbol{r}}\, d\hat{\mathbf{R}}$ denotes the integral over the solid angles of the vectors $\mathbf{r}$ and $\mathbf{R}$, respectively. Evaluation yields the radial equation

$$\begin{aligned}\left(E_{\nu''j''} - \frac{\hbar^2}{2m}\frac{d^2}{dR^2} + \frac{\hbar^2 l''\left(l''+1\right)}{2mR^2}s + n''\hbar\omega - E\right) F_{\alpha''\alpha}^{n''n}\left(R;E\right) & \\ + \sum_{\alpha' n'}\left[V_{\alpha''\alpha'}\left(R\right)\delta_{n''n'} + W_{\alpha''\alpha'}\left(R\right)\delta_{n''\pm 1,n'}\right] F_{\alpha''\alpha}^{n''n}\left(R;E\right) & = 0,\end{aligned} \tag{3.1.43}$$

which is a coupled differential equation in the intermolecular spacing R.

3.1.6 The absorption coefficient

As shown in [30] the binary collision-induced absorption coefficient of a gas at temperature T can be calculated from the S-matrix. In the following i and f designate the initial and final channels, respectively, i.e. channels with one or no photon. For temperatures up to a few hundred kelvin only the vibrational ground state of H_2 is populated [19]. Thus, for the rototranslational band $\nu_f = 0$ and for the fundamental band $\nu_f = 1$, and the absorption coefficient is according to [13] given by

$$\alpha\left(\omega, T\right) = \rho^2\lambda_0^3\frac{1-\exp\left(-\beta\hbar\omega\right)}{\Phi\hbar}\sum_i P_{0j_i}\left(T\right)\int_0^\infty \exp\left(-\beta E_i\right)\sum_f \left|S_{fi}\left(E_i\right)\right|^2 d\mathrm{E_i}, \tag{3.1.44}$$

where f $= \left(j_f, l_f, J_f\right)^T$ and i $= \left(j_i, l_i, J_i\right)^T$. Φ is the radiation flux in photon number per unit area and time and $\beta = 1/\mathrm{k}_B\mathrm{T}$. Since the matrix elements are both proportional to $\delta_{MM'}$ there is no summation over the quantum number M in equation (3.1.44). The thermal de Broglie wavelength is defined by

$$\lambda_0^2 = \frac{\beta\hbar^2}{2\pi m}. \tag{3.1.45}$$

$$P_{\nu j}\left(T\right) = \frac{g_{j_i}\exp(-\beta E_{\nu j})}{\sum_{\nu j} g_j\left(2j+1\right)\exp\left(-\beta E_{\nu j}\right)} \tag{3.1.46}$$

is the rotovibrational occupancy function of H_2 [13]. For low temperature, roughly T$\leq$1000K, the summation in the denominator, the rotovibrational partition function, only runs over j values and ν can be fixed to zero. The factor g_j is the nuclear spin statistical weight for the hydrogen molecule. The initial kinetic energy is defined as

$$E_i = E - \hbar\omega - E_{0j_i}. \tag{3.1.47}$$

Equation (3.1.44) decouples according to [19] which makes the calculations of the absorption coefficient less time consuming. First, there are no couplings between channels with odd and even j, since without magnetic field spin flips are very rare. Thus the calculations for ortho- and para-hydrogen can be carried out separately. While in radiative transitions parity must change it is conserved within the initial and final channels. Thus, the calculations with odd l_i and even l_f can be separated from the ones with even l_i and odd l_f.

3.1.7 Theoretical importance

Interaction-induced absorption of electromagnetic radiation is important in any cool and dense environment. From the time of the discovery of collision-induced absorption on many absorption bands by binary complexes of molecules have been investigated both experimentally and theoretically. Rotovibrational and electronic bands are found even in regions which are forbidden in the non-interacting molecules and there also occur new bands at sums and differences of rotovibrational frequencies. Supramolecular absorption and Raman spectra are due to interaction-induced dipole moments and polarizability invariants, respectively, of two or more interacting molecules [14]. The absorption intensity I shows a strong dependence on the density ρ of the considered species and via a virial expansion, binary, ternary, etc. contributions are distinguishable. In the vicinity of the low-pressure limit induced spectra may be described by a virial expansion [13],

$$I = A \times \rho + B \times \rho^2 + C \times \rho^3 + ... \qquad (3.1.48)$$

with coefficients representing the dipole-allowed contributions, A, and the induced binary, B, ternary, C, ..., spectral components. For ordinary atoms or molecules, the intensity I varies linearly with density ρ, whereas intensities of collision-induced spectra vary with the second and higher powers of density, in any case non-linearly. The virial expansion of the absorption coefficient in dense mono-molecular gases is according to [13] given by

$$\alpha(\omega) = \alpha_1(\omega) \times \rho + \alpha_2(\omega) \times \rho^2 + \alpha_3(\omega) \times \rho^3 + ..., \tag{3.1.49}$$

where ρ denotes the number density, $\alpha_1(\omega)$ is the allowed spectrum (if one exists at frequencies ω of interest), and $\alpha_j(\omega)$ (j > 1) describes the binary, ternary, ..., collision-induced absorption. For infrared inactive gases the coefficient $\alpha_0(\omega)$ vanishes. At fixed frequency ω and temperature T, a virial expansion of the absorption coefficient $\alpha(\omega,\text{T})$ is often possible. The higher order coefficients with j > 1 are often separable in actual measurements. At low densities the second and higher spectral virial terms are insignificant. However, at sufficiently high density they become significant. At densities approaching liquid state density, many-body interactions may be expected to dominate the optical properties. Under such conditions virial expansions are meaningless. One has to use other theories in these cases.

The most familiar virial expansion is probably that of the equation of state, which relates pressure, volume and temperature of a real gas, as opposed to an ideal gas. There are similar virial expansions related to supramolecular properties known such as the Clausius-Mossotti equation for the dielectric constant ϵ and the Lorentz-Lorenz equation for the refractive index n and some others [36]. Via measurements at different densities allowed spectral contributions can be separated from the induced binary, ternary, ... ones.

Due to virial expansions at intermediate gas densities one need not consider the complex many-body system consisting of all molecules of the collisional complex. Instead, the supramolecules may be described by a series of relatively simple two-, three, ... body Hamilton operators [13]. At sufficiently small gas densities this series may be truncated after the first few leading terms to model the spectroscopic properties of the whole system accurately.

The effects on pressure of binary interactions are summarized in the second virial coefficient, and in general, N-body interactions are described by the nth virial coefficient, in similar ways [39]. It should be pointed out here that while the virial expansion of pressure has a significant one-body term, for infrared inactive gases and mixtures the leading term of collision-induced absorption will be a two-body term.

Absorption in hydrogen proceeds mainly via quadrupole induction which is coupled to the rotation of the molecule [13]. Rotational S_0 lines are therefore observed at the appropriate frequencies. The ortho-H_2 molecules are in one of the orientational sublevels, $M_J = 0, \pm 1$, of the J = 1 rotational state which is optically anisotropic, and induced magnetic transitions ($\Delta M_J = \pm 1$) at zero frequency occur.

While in this work only binary complexes of molecules will be considered it should be mentioned that a few semi-quantitative data exist at present towards an understanding of ternary spectra which are much more complicated to treat theoretically. Nevertheless, there is experimental evidence of important N-body spectral contributions, with $N > 2$, even at densities that are much lower than condensed matter densities [36]. Supramolecular spectra may be considered collision-induced spectra, or pressure-induced spectra, or even more general interaction-induced spectra. Other than the supramolecular absorption bands just mentioned there furthermore exists a Raman process which results from polarizability increments, induced by molecular interactions. This process is also called collision-induced light scattering (CILS).

The molecular complexes from which these CIA spectra arise are called supramolecules. They are free pairs, triples, ... of ordinary molecules that interact via the weak van der Waals forces, so that collisionally interacting pairs, triples, ... arise. A complex of two or more molecules may be considered another molecule, with new properties and spectra, besides those of its constituents. Their origin causes the supramolecules to have new interaction-induced and interaction-modified properties besides the sum of the properties of the unperturbed, i. e. non-interacting or well separated, constituent molecules. Such a complex is called a supramolecule, even if its lifetime is rather short. The term molecule will be reserved for the constituents that make up a supramolecule. Changed properties include multipole moments and polarizabilities, and the associated rotovibrational, electronic and Raman spectra, especially in (dipole) forbidden molecular bands [14]. Furthermore, via single photon emission/ absorption there can occur simultaneous double, triple, ... transitions, at sums and differences of molecular transition frequencies and these transitions can even take place at (dipole-) forbidden frequencies of the single constituents.

3.1.8 Comparison between rotovibrational and collision-induced spectra

If one compares rotovibrational molecular and collision-induced supramolecular spectra one notes a number of differences. Spectral intensities are proportional to the square of the dipole moment from which they arise. It is thus logical that a (dipole-) allowed rotational line of a polar molecule may be stronger than an induced one by several orders of magnitude. However, at intermediate gas densities many more pairs or triplets, ... exist than monomers, and for dense systems induced spectra may actually be strong because of large numbers of molecules. Because of the generally great differences of intensity in the presence of dipole-allowed lines or bands the induced components are rarely discernible without ambiguity. In general the dipole strengths of supramolecules are several orders of magnitude weaker than that of the constituents, who usually possess a dipole moment in the order of 1 debye. Accordingly, line intensities of supramolecular spectra are typically insignificant at low densities, but they may be quite striking as gas densities are increased. Moreover, interaction-induced lines usually possess dimer features near the line centers. It should also be mentioned that supramolecular dipole strengths fall of rapidly with increasing separation. This is one of the reasons why it took so long until supramolecular spectra were discovered. Nevertheless, at high density supramolecular spectra may be quite intense.

Observable intensities, when integrated over a line or spectral band, are proportional to the number of molecules, i.e. to the density, if the spectra of polar molecules are considered [13]. Supramolecular dipoles cause absorption in certain regions of the electromagnetic spectrum. These dipoles are responsible for the second, third, ... virial coefficients. Another point to mention is that molecular absorption spectra vary linearly with density whereas supramolecular absorption spectra of infrared-inactive constituents vary nonlinearly with density, at low densities the dependence is to good approximation quadratic. Rotovibrational bands of van der Waals dimers may be detected near all rotovibrational transition frequencies of the individual molecules. However, these are usually very weak and strongly pressure broadened. Usually the number of collisional pairs is much greater than the number of bound dimers so that the integrated dimer intensities are generally much weaker than the collision-induced contributions. The latter appear as strong background of the bound dimer signatures. Whereas molecular absorption profiles are usually sharply peaked supramolecular spectra consist of diffuse lines. This can easy be understood by consideration of the Heisenberg uncertainty relation, $\Delta \mathrm{t} \times \Delta\omega \geq 0.5$ and the generally short lifetime Δt of the supramolecular complexes in the order of $10^{-13}s$ whereas molecules in most cases can be considered to be stable [13]. This short duration of collisions in most cases renders rotational bands quasi-continuous.

If monochromatic laser light is incident on a molecule, the electric field will polarize the molecule. This so-called field-induced dipole will emit or scatter radiation of the frequency of the incident light. Furthermore, it will emit at other frequencies that are shifted relative to the laser frequency by certain rotovibrational transition frequencies, provided the molecule is Raman-active, in other words, if the invariants of the polarizability tensor are nonzero for certain rotational and/ or vibrational transitions of the molecule [14]. Even if the individual molecules are Raman-inactive, the compressed gases of these molecules generally show a variety of additional Raman bands. As an example, one may consider rarefied monatomic gases: here the scattered light will be strictly at the laser frequency and no shifted Raman lines or bands exist. However, if the rare gas is compressed, Raman continua occur which are due to collisional and, to some extent, to bound van der Waals pairs (and at higher densities even of triples, ...) of the interacting atoms.

3.1.9 Collision-induced dipoles

Usually, when absorption or emission of electromagnetic radiation occurs, one can identify an electric dipole moment being responsible for such spectroscopic processes [13]. If in a molecule the centers of positive and negative charge do not coincide these molecules have a permanent dipole moment. These dipole moments can also be induced by external fields (polarization) or momentarily by collisional interactions. Absorption and emission of rotating or vibrating electric dipoles generally occur at the frequencies of rotation and vibration. In contrast to that translationally accelerated charges (dipoles) emit continuous radiation, as is well explained by classical electrodynamics. Even if no permanent dipole moment exists, molecules can emit in transitions between electronic states, but these transitions typically require more

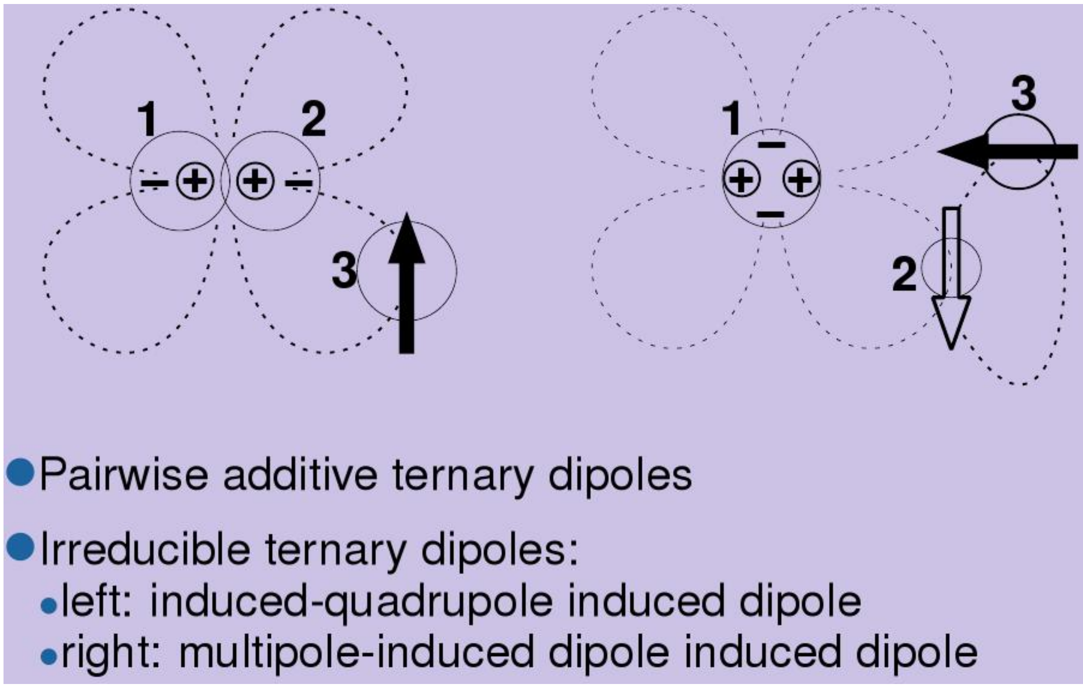

Figure 3.1: The different types of ternary dipoles

energy than the rotovibrational ones, a higher photon energy for absorption and a higher excitation energy, such as provided by higher temperature, for emission. Common homo-nuclear diatomic gases, such as hydrogen and nitrogen, do not undergo electronic transitions at frequencies in the infrared at room temperature. Because the inversion symmetry is inconsistent with the existence of a dipole moment no absorption is observed. In contrast to that, supramolecular systems usually possess a transient dipole moment during their short existence.

As a note aside it should be mentioned that so far collision-induced absorption by pure monatomic gases has never been observed. This is easy to understand, since collisional pairs of like atoms cannot develop a collision-induced dipole due to their inversion symmetry which is inconsistent with the existence of a dipole moment [13]. Nevertheless, theoretically triatomic (see figure 3.1) and higher order complexes of like atoms could absorb infrared radiation, but the fact that no absorption has been observed suggests that these absorption coefficients are so small that they are within the error bars of the measurements not detectable [36]. Only a very small upper limit of the infrared absorption coefficient could be established for a few rare gases in liquefied form. Pure monatomic gases are probably the only gases that do not show significant collision-induced absorption at any frequency well below x-ray frequencies.

However, mixtures of monatomic gases of dissimilar pairs such as He–Ar generally support a dipole moment, since they lack the inversion symmetry. Even if gas densities are well below liquid state densities absorption by dissimilar pairs is well known.

Forces that can generate dipole moments in supramolecules

Induced dipole moments (see figure 3.2) are generated by the same processes which cause intermolecular repulsion at near range and attraction at long range. Dispersion and exchange forces are both quantum mechanical in nature. The former may be described in semi-classical terms of fluctuating dipole-induced dipole interactions and the latter arise from the exchange symmetry of the electronic wavefunctions imposed by the Pauli principle [13]. If

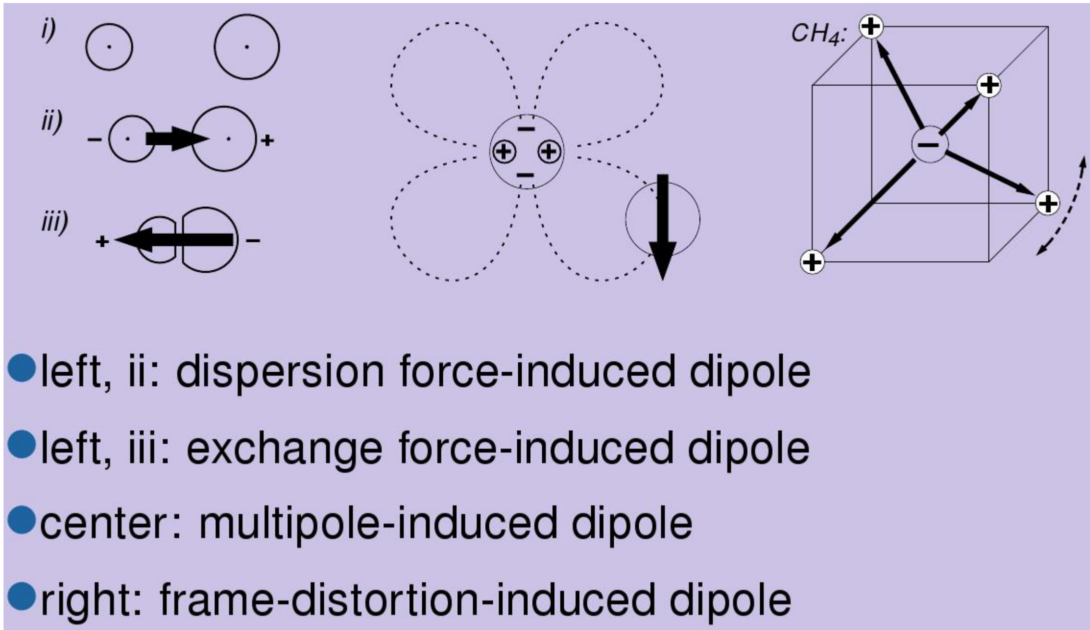

Figure 3.2: The mechanisms that can generate a dipole moment

at least one of the interacting particles is a molecule further induction mechanisms arise.

On a scale of the order of atomic size, molecular multipole fields vary strongly with orientation and separation. Thus, there can generally be found induced dipole components arising from field gradients of first and higher order which interact with the so-called dipole-multipole polarizability tensor components, such as the **A** and **E** tensors [14].

Not all of these induced dipole types exist in any given system. The components that exist generally couple in different ways to the translational, rotational, vibrational, etc. states of the complex and usually are associated with different selection rules, thus generating different parts of the collision-induced spectra.

Supramolecules usually possess an electric dipole moment even if its individual constituent molecules are nonpolar. Up to now from the studies of intermolecular forces there are four different universal mechanisms known that can generate these dipoles in supramolecules, which are familiar from the studies of the intermolecular forces [14]:

(1) Dispersion force-induced dipoles

Dispersion forces control the attractive part of the intermolecular interactions. The electronic charge clouds of the constituent molecules may be slightly displaced by intermolecular dispersion forces during intermolecular interactions, generating an electric dipole moment of the supramolecule. Over moderately wide separations, atoms or molecules interact through dispersion forces that arise from electronic intercorrelation. For dissimilar pairs, these are associated with a dipole moment whose asymptotic strength is to leading order in the expansion in terms of 1/R proportional to the inverse seventh power of the intermolecular separation R [14]. The dispersion force-induced dipole is usually weaker than multipole-induced and overlap-induced dipoles, but generally discernible in discriminating analyses.

(2) Exchange force-induced dipoles

In a collision at near range, when the electronic charge clouds of the collisional partners overlap, according to the Pauli exclusion principle a momentary redistribution of electric charge occurs that is caused by electron exchange. A slight displacement of the electronic charge clouds relative to their nuclei may be caused by intermolecular exchange forces. In general, this will generate a net dipole moment in the supramolecule [14]. Exchange forces control the repulsive part of the intermolecular interactions. Because dispersion forces are attractive and caused by an enhancement of electronic charge in the space between the molecules the polarity of that induced dipole is the opposite of the dispersion force-induced dipole. On the other hand, exchange forces are repulsive and cause a depletion of electric charge in the region between the interacting constituent molecules. This mechanism is usually the dominant one when dissimilar particles collide. It should be remarked that exchange force-induced dipoles in molecules can also have a certain anisotropy of quadrupolar or higher symmetry.

(3) Multipole-induced dipoles

In general molecules are surrounded by an electric field which may be described, as is well known from classical electrodynamics, by a multipole expansion, i. e. by a superposition of dipole, quadrupole, octopole, ... fields. While molecules are electrically neutral, the electric field surrounding each molecule is set up by the internal electronic and nuclear structure of the molecule. In the fields of the permanent multipoles the interacting atoms or molecules will be polarized [14]. For all neutral homo-nuclear diatomic molecules the monopole and dipole terms are zero, so that the lowest order multipole is a quadrupole. When two such molecules interact, the collisional partners are polarized and thus for the duration of the collision possess dipole moments that interact with electromagnetic radiation.

For the case of pure compressed hydrogen gas quadrupolar induction is responsible for nearly 90 percent of the total induced absorption [14]. Because the quadrupole field rotates with the molecule, the collision-induced rotational S lines are quite prominent in the spectra of compressed hydrogen.

(4) Collisional frame distortion-induced dipoles

Many molecules of a high degree of geometric symmetry posses strong internal dipoles which are arranged that way that the net dipole moment is zero in the unperturbed frame. For example, the H–C-branches in the CH_4 molecule possess four very strong dipole moments. Owing to the tetrahedral symmetry these add up to zero in the unperturbed CH_4 molecule. However, during a collision a proton may temporarily be displaced and thus a transient, sizable supramolecular dipole moment may be generated [14].

The strength and separation dependence of the different dipole components can be seen in figure 3.3. As is obvious from the plot the $\lambda_1\lambda_2\Lambda\mathrm{L} =$ 0223/2023 and 2233 dipole components are more long-range than the other dipole components, which fall off rapidly.

At large separations, a collisional complex such as He–Ar will be non-polar. However, at intermediate separations dispersion forces may induce a dipole moment in any dissimilar pair and at near range exchange forces induce a dipole moment of opposite polarity.

It should be pointed out that in general some or all of the mechanisms

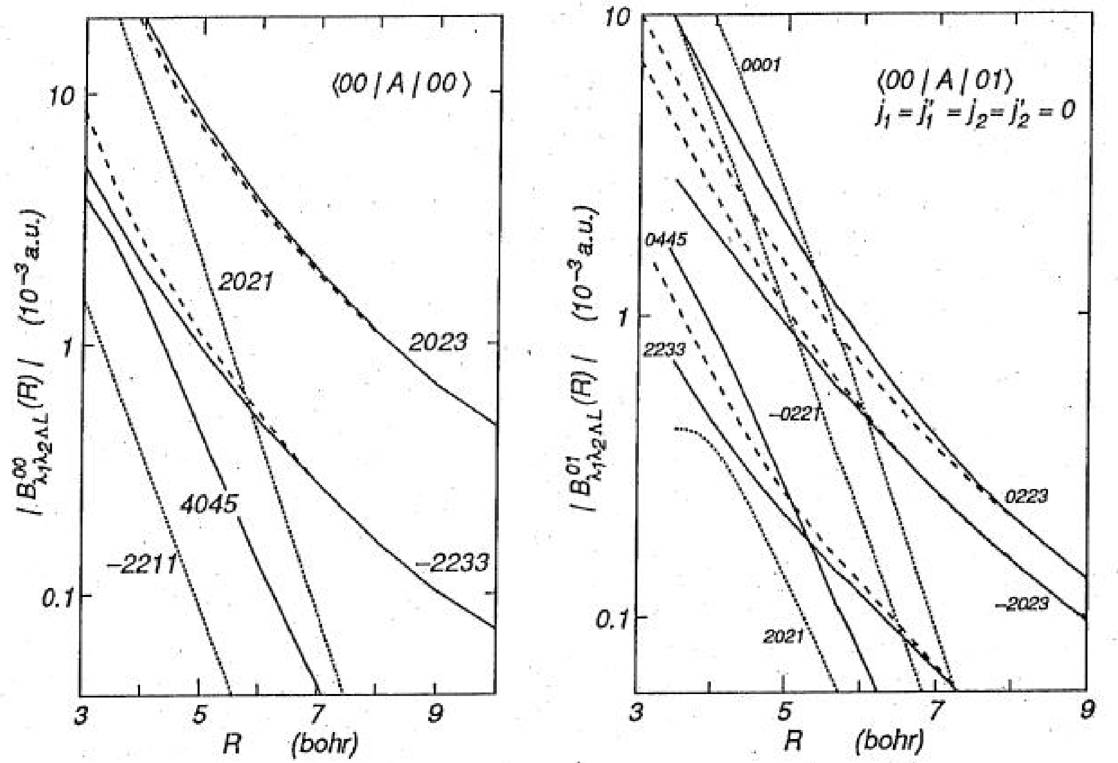

Figure 3.3: The separation dependence of the principal dipole components of H_2–H_2. In the left-hand plot the ground state vibrational averages are shown. Dots represent overlap-induced terms, the solid line corresponds to multipole-induced ones. The classical approximation is dashed. The right-hand side shows the same, but for the vibrational transition elements, $\nu = 0 \rightarrow \nu' = 1$ [13]

mentioned above will induce electric dipole moments whenever molecules or dissimilar atoms interact, no matter what kind of particles is considered or how many particles actually interact at any given time, or wether the particles are bound (van der Waals molecules) or free (in collisional interaction). They cause collision-induced absorption, as well as the absorption of bound van der Waals systems. Like intermolecular forces, supramolecular dipoles are omnipresent.

Generally, the word interaction-induced spectra is used to describe spectra arising from interacting pairs, triples, ... of molecules that exceed the simple sum of the spectra of the non-interacting, individual molecules. They are observed in absorption, emission and light scattering (Raman scattering) [36]. Such spectra can be computed on the basis of reliable intermolecular potential and induced dipole or polarizability surfaces. In the past close agreement between laboratory measurements and these computed spectra has been observed [13]. However, in some cases those surfaces are not available from the fundamental theory. In these cases reasonable induced dipole surfaces can be obtained from laboratory measurements which often makes reliable temperature interpolation and in some cases even extrapolation for applications possible.

Supramolecular emission and absorption are generally observed in high density environments and of great importance if no allowed spectra are present. Although usually studied in the infrared and microwave regions supramolecular spectra also exist in the visible and ultraviolet [13]. Up to now many laboratory measurements of the most common gases have been carried out at a variety of temperatures, and successfully analyzed in terms of multipole-induced dipoles and simplified molecular scattering considerations. Recently, *ab initio* quantum-chemical calculations of the induced dipole surfaces of binary van der Waals complexes have been undertaken and combined with molecular quantum scattering calculations for low temperatures.

At not too high gas densities, i. e. gas densities in the order of 10 amagat, a large part of the induced rotovibrational spectra is demonstrably of binary origin [13], ignoring small regions around the intercollisional dip which will be described further below. In the vibrational band of pure, i. e. unmixed hydrogen, two major induction processes occur, namely overlap- and quadrupole-induction shape the spectra. Consequently, two types of spectral profiles are expected. The isotropic overlap induction generates most of the Q line intensity and quadrupole induction shapes the S lines, and also a small component of the Q branch related to the orientational magnetic transitions is discernible [13]. Thus, the Q branch is a superposition of at least two different profiles. A total of eleven components must be expected for the fundamental band of hydrogen [13]. Specifically, the eleven profiles include the obvious single transitions, i.e. the rotovibrational transitions in just one of the two colliding H_2 molecules. These are the $S_1(0)$, $S_1(1)$ and $Q_1(1)$ transitions in one of the two interacting molecules. There also take place double transitions in both collisional partners, such as the simultaneous transitions $Q_1(1)+S_0(0)$, which occur near the $S_1(0)$ transition frequency and $Q_1(1)+S_0(1)$ near $S_1(1)$.

With their superposition the measurements can be reproduced closely [13]. The different transitions of a pair of H_2 molecules are shown in figure 3.4.

When densities are increased to about 100 amagats or more, additional three body contributions are readily discernible in most gases but they may well be present even at much lower densities [13]. To illustrate the effects of pressure on the collision-induced spectra figure 3.5 shows the collision-induced absorption spectrum of hydrogen in the region of the fundamental band for various pressures at the temperature of 298K. As can be seen in the figure the absorption intensity shows a strong dependence on the gas density. It should also be noted that the positions of the maxima of the absorption are strongly dependent on the density. With increasing density the absorption intensity gets larger. However, no general dependence of the position of the absorption maxima can be observed from the figure. The first absorption peak is shifted to lower frequencies with increasing density whereas the second and third ones are shifted to higher frequencies.

The spectra of liquids and solids cannot be studied here in any detail. The interested reader can find more information about them in other works, such as the two volumes by Gray and Gubbins, and the review articles by Guillot and Birnbaum (1989).

3.1.10 Ternary systems

Spectroscopic signatures arising from more than just two interacting atoms or molecules have also been discovered in the studies of collision-induced

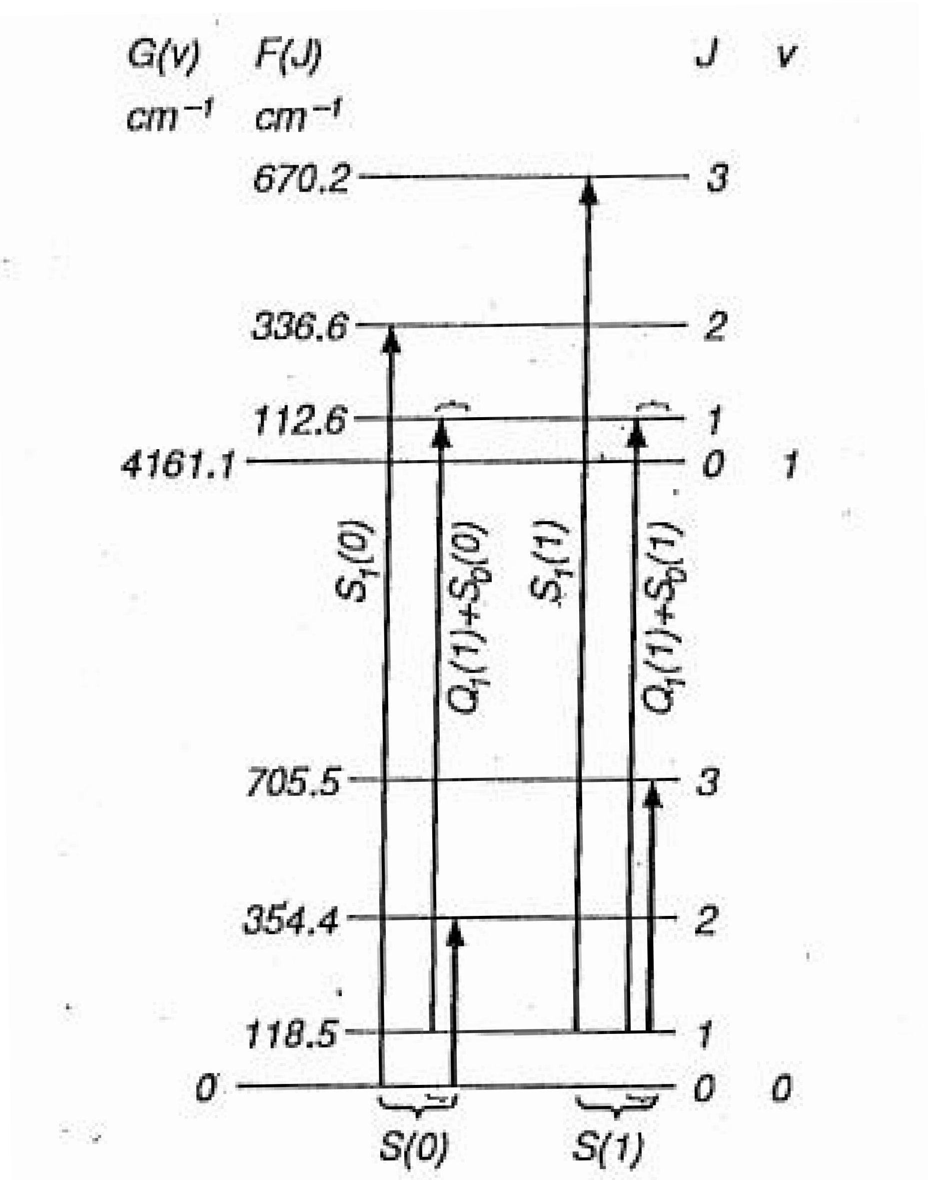

Figure 3.4: The rotovibrational term scheme of H_2 showing single and double transitions of pairs [13]

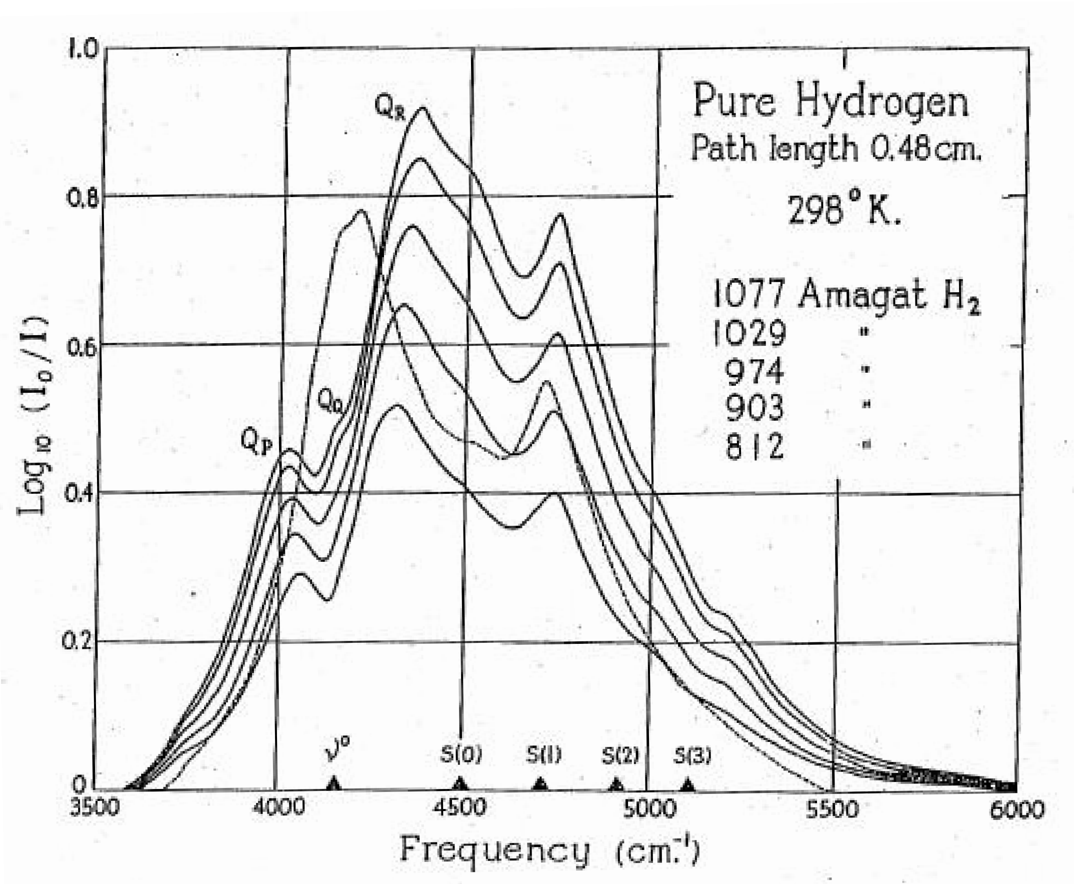

Figure 3.5: The fundamental collision-induced absorption band of H_2 at various pressures in the range of 2006 to 4003 atm. The dotted line corresponds to the lower pressure contour extrapolated by the square law to a density of 1077 amagat [23]

absorption [36]. These involve a variation with pressure of the normalized profiles, $\alpha(\omega)/\rho^2$, which are pressure invariant only in the low-pressure limit.

In early years after the discovery of ternary dipoles in supramolecular systems models were proposed that treat the ternary dipoles in terms of pairwise-additive dipole components [13]. However, these attempts were not very successful. More recently, evidence, experimental as well as theoretical, has emerged that substantial irreducible ternary dipole components exist [13], at least for some systems. For all systems for which reliable pair dipoles are known, pairwise-additive ternary dipole components were reported. Significant shortfall of the calculated spectral moments compared with measurements of the ternary spectral moments of the absorption spectra of numerous gases and mixtures has been observed. This has been interpreted as an indicator that irreducible ternary dipole components exist in most - if not all - systems considered, certainly in unbound systems consisting of three H_2 molecules.

It was observed that with increasing temperature the significance of the irreducible dipole contribution increases rapidly [13]. This suggests that the ternary dipole components result from close encounters, i.e. from triple collisions with more or less overlapping electron clouds. Generally, the interaction-induced dipoles resulting from three interacting molecules consist of the vector sum of the pairwise additive dipole components, in addition to an irreducible ternary surface. Several studies suggest that the principal irreducible dipole component is of the exchange quadrupole-induced dipole (EQID) type, but more work is needed for a better understanding of the irreducible ternary dipole surfaces [13]. Momentarily, during a binary collision, at near range exchange forces displace the electronic molecular clouds relative to the nuclei to the far sides of the binary complex. This generates momentarily a strong quadrupole moment. In the electric field of the exchange force-induced quadrupole the third molecule is then polarized.

EQID is a quantal mechanism. In early years it was proposed that the irreducible dipole could be the classical permanent quadrupole-induced dipole-induced dipole. It was found, however, that this dipole was not nearly as strong as EQID in the three interacting H_2 molecules [13].

In dense systems such as in liquids and solids, the three-body and probably higher order cancellations due to destructive interference are very important. One distinguishes two components of translational spectra, one due to the diffusive and the other due to the oscillatory ("rattling") motions of the molecules in a liquid. The latter is analog to the intercollisional spectrum and consists of a dip to very low intensities near zero frequency. In contrast to the good understanding of translational spectra of mono-atomic liquids, very little is known about those of molecular liquids. The understanding of ternary spectra is in its beginnings, but much more work is needed.

3.1.11 Intercollisional dips

Virial expansions of supramolecular absorption have been known for a long time. In a number of cases ternary and sometimes even higher-order contributions have been isolated. Theoretical studies of the intercollisional dip [13] of rare gas mixtures have shown that without the assumption of an irreducible ternary dipole component in rare gas triples the experimentally observed spectra could not be reproduced theoretically. Furthermore, in 1995 Reddy and associates found a spectral feature in the interaction-induced second overtone of H_2 that corresponds to a simultaneous transition of three molecules, three H_2 molecules in collisional interaction, underwent a simultaneous vibrational transition in the presence of a single photon. These simultaneous triple transitions with absorption of one photon have long been predicted by theorists [14]. They are believed to be due to irreducible dipole components.

It should be remarked here that a single, semi-quantitative dipole model explains the three independent observations (third virial coefficient, intercollisional dip, triple transitions) which suggest the existence of irreducible dipole components. In contrast to early suggestions of the nature of ternary irreducible dipole components it seems now that the exchange quadrupole-induced dipole (EQID) component is a principal contributor to the irreducible dipole (at least in the case of compressed hydrogen gas).

Correlations of interaction-induced dipoles can lead to destructive interference in subsequent collisions. This is one possible reason for the experimentally observed quite striking absorption dips of isotropic induced dipole components, typically at zero frequency shifts, e. g. Q-branches. These so called intercollisional absorption dips may be considered many body effects. When the time t between two collisions is much larger than the mean duration Δt of a collision these dips are sharp features. At such frequencies virial expansions of the line shapes are not possible, in other words it is impossible to separate contributions at frequencies where absorption dips occur. If one considers small enough frequency shifts the absorption dips may be considered true many-body effects [13]. In the past the shapes of absorption dips have been modeled by inverted Lorentzian profiles [13].

3.1.12 Electronic collision-induced spectra

All spectra we were concerned with thus far arise from supramolecular transitions that leave the electronic states of the collisional partners unchanged. If photon energies are sufficiently small, the possibility of changing electronic states is finite. Typically collision-induced electronic spectra occur at higher photon energies than those considered so far [13]. However, some of the common molecules possess electronic states with excitation energies so low that electronic collision-induced spectra in the infrared, visible and near ultraviolet region can occur. As an example one may consider the O_2–N_2 and O_2–O_2 spectra in the visible [13].

According to [21] absorption of a photon of energy E by an interacting molecular pair A+B can be written

$$A + B + E + \Delta E \rightarrow A' + B' + \hbar\omega, \tag{3.1.50}$$

where ΔE corresponds to a change of the energy of the pair and primes indicate a possible change of the internal states. $\hbar\omega$ stands for a photon emitted in the process. Furthermore, there exist associative processes ('half collisions') [21], such as

$$A + B + \Delta E \rightarrow A'B' + \hbar\omega. \tag{3.1.51}$$

Here A and B may be neutral atoms or molecules, possibly in an excited rotovibrational or electronic state. In weakly ionized environments, A may be an electron or ion interacting with a neutral particle or ion B. It should be remarked that the two sides in the equations (3.1.50) and (3.1.51) of the photon and the change of energy may be arbitrarily interchanged, depending on the specific process one wants to describe. One may distinguish two different supramolecular collision-induced absorption processes: the one only affects the rotovibrational energies of A, B, while the other involves electronic transitions. Typically electronic collision-induced absorption requires visible and ultraviolet photons, whereas rotovibrational collision-induced absorption normally occurs in the microwave and infrared regions of the spectrum. These boundaries are not strict and depend on the specific properties of the systems considered.

3.1.13 Collision-induced polarizabilities

An electric field $\mathbf{E}$ of strength E polarizes all molecules. This means that the electric field pulls the electrons slightly off to one side and the nuclei to the other so that a field-induced dipole moment $\mathbf{p}$ results,

$$\mathbf{p} = \mathbf{P} \times \mathbf{E}. \tag{3.1.52}$$

If an alternating field is used, the field-induced dipole moment oscillates and thus radiates at the same frequency as the incident light, which is called Rayleigh scattering. Furthermore, the scattered light is modulated by certain molecular rotation and vibration frequencies. The polarizability $\mathbf{P}$ is a 3×3 tensor with two invariants, trace and anisotropy [13]. It depends on the molecular orientation and the nuclear structure of the molecule [14]. Supramolecular Raman spectra have their origin in the excess of the polarizability invariants of the interacting complex over the sum of the corresponding invariants of the non-interacting members of the supramolecular complex. As a simple example one may consider the atoms of monatomic gases, which are completely isotropic. Thus, the field-induced dipole will always be exactly parallel to the applied field, so that the anisotropy, which would rotate the dipole relative to the field, is zero, as long as the atoms are sufficiently spaced apart, as is the case in rarefied gases. However, at higher densities, one cannot ignore the likelihood of another atom B close enough so that the local field of the external field and the electric field at the position of atom A are perturbed. It is now the vector sum of the external field and the electric field set up by the dipole induced in atom B that represents the total electric field.

3.1.14 Van der Waals molecules

Compared to chemical forces that bind the common molecules van der Waals forces are weak, so weak that most dimer-monomer collisions will dissociate the dimer. Typically, this destruction is balanced out by a certain rate of formation, so that the bound dimer concentrations are kept at a low level [13]. In many cases the average lifetime of bound dimers corresponds to a free mean time between monomer collisions, which is roughly in the order of 10^{-9}s in air at standard temperature and pressure, and decreases correspondingly with increasing density and temperature [36]. For comparison, a collisional complex may be thought to exist for the time of the duration of a fly-by encounter which is three orders of magnitude shorter. Van der Waals dimer bands are known to be highly susceptible to pressure broadening, which is one reason why it took so long to actually record dimer bands. Moreover, for spectroscopical resolution of dimer bands high spectral resolution has to be employed.

3.1.15 Collision-induced emission

While this work mainly deals with collision-induced absorption it should be remarked that any gas that absorbs electromagnetic radiation will also emit. Supramolecular absorption and emission are inseparable [14]. However, cold gases emit in the infrared, which often goes unnoticed. Striking supramolecular emission occurs in hot and dense environments, such as in shock waves and cold stars.

3.1.16 Pair polarizability increments

In an external electromagnetic field molecules are polarized. This field-induced dipole oscillates with the frequency of the incident radiation, but it may also be modulated with the rotovibrational molecular frequencies [14]. These dipoles are the reason for Rayleigh and Raman scattering of light.

In general the polarizability invariants, trace and anisotropy, of the supramolecules differ from the simple sums of these quantities of the non-interacting individual constituents of the supramolecules [14]. This has two reasons:

(1) Due to the presence of the field-induced dipoles of molecules nearby the local fields of each molecule differ from the external radiation field. This local field distortion has lead to the classical dipole-induced dipole (DID) expression of the supramolecular polarizability invariants.

(2) Due to the intermolecular exchange and dispersion forces the molecular electronic clouds are slightly rearranged. For a few binary systems, such as He–He, quantum-chemical calculations of the pair polarizability increments exist.

For the more highly polarizable molecular gases the DID model is more reasonable successful.

It should be pointed out that the study of the Kerr and the dielectric second virial coefficients also provide valuable information concerning interaction-induced polarizability invariants.

Collision-induced absorption is generally observed in gases, liquids, solids and even in plasmas [13]. However, since it is usually very weak, for experimental measurements high collision rates are necessary. This may lead to the assumption that the denser the medium the stronger the absorption. This suggests that liquids and solids should be better suited for measurements than dilute gases. However, due to the inversion symmetry a perfectly isotropic liquid prohibits any interaction-induced dipole moments. In real liquids there are particle fluctuations around the isotropic configuration, so that nevertheless interaction-induced dipoles come about, but the CIA is generally weaker in liquids than expected from their high particle density.

Most accessible and theoretically easy to understand are binary systems, from which the so-called pair spectra arise. However, experimentally it turns out to be difficult to distinguish binary contributions from those due to systems of three or more interacting molecules, which generally possess irreducible dipole components in addition to the pairwise additive components. Although some attempts exist to model ternary systems, exact quantum treatments of collision-induced spectra are presently only known for binary systems. In moderately dense media this binary contribution dominates the spectra.

3.2 The absorption coefficient

The absorption coefficient $\alpha(\nu)$ is not only a function of frequency but also of temperature, density and, of course, the nature, composition, and state of matter (gaseous, liquid, solid) of the sample.

For any detailed discussion of collision-induced spectra it is advantageous to study the shape of the spectral function g(ν) [13] which is related to the absorption coefficient $\alpha(\nu)$ via

$$\alpha\left(\nu\right)=\frac{\left(2\pi\right)^{3}N_{a}^{2}}{3\hbar}\rho_{1}\rho_{2}\nu\left[1-\exp\left(-\frac{hc\nu}{k_{B}T}\right)\right]Vg\left(\nu\right), \tag{3.2.1}$$

where N_a is the number of particles per cubic centimeter of the gas under consideration, ρ_1 and ρ_2 are the relevant gas densities, $\hbar$ is Planck' s constant h divided by 2π, c is the vacuum speed of light, k_B is the Boltzmann constant and V is the volume of the sample. It should be mentioned that the spectral function g(ν) is proportional to the reciprocal volume so that the product Vg(ν) does not depend on the volume of the sample. Essentially the absorption coefficient $\alpha(\nu)$ and the spectral function g(ν) differ by the frequency dependent factor $\nu\left[1-\exp\left(-\frac{hc\nu}{k_BT}\right)\right]$. This factor causes the absorption to fall off to zero as ν^2 as ν tends to zero. Stimulated emission is responsible for the Boltzmann term.

One can consider the translational spectral function g(ν) a (very diffuse) spectral line centered at zero frequency which arises from transitions between the states of relative motion of the interacting pair [13]. It is the free-state analog of the familiar vibrational and rotational transitions of bound systems, with the major difference that the motion here is aperiodic since there is no restoring force. Near the line centers, the spectral functions have often been approximated by a Lorentzian [13]. On the other hand, the far wings may be better modeled by exponential functions [13]. However, there are better model profiles [13]. At constant temperature the observed widths of the spectral functions decrease with increasing mass of the collisional system, which is a simple consequence of the fact that the translational energy $\frac{1}{2}m_{12}v^2 = \frac{3}{2}\mathrm{k}_B\mathrm{T}$ is the same for all pairs [13]. However, the interaction time is roughly proportional to the reciprocal root mean square speed, and thus to the square root of the reduced mass.

For like molecular pairs inversion symmetry does in general not exist because of the anisotropic structure and vibrational excitations of the individual molecules.

According to Lambert' s law (if absorption occurs) the intensity of light falls of exponentially with increasing path length L,

$$I\left(L\right) = I_0 \times \exp\left[-\alpha \times L\right]. \tag{3.2.2}$$

Thus, measurements of the initial intensity I_0 and the intensity I after transmission through a path of length L determine the absorption coefficient α as a function of frequency, temperature, and, provided one deals with binary complexes, as a function of the densities ρ_1 and ρ_2 of the two species. Usually the absorption spectrum α is presented by the normalized absorption coefficient, $\alpha/\rho_1\rho_2$, which is invariant under changes of densities, as long as no three body or higher order interactions interfere with the measurements, that is, at intermediate gas densities, that are well below the liquid state densities.

3.2.1 Spectral moments

For a detailed study of collision-induced spectra and the comparison of measurements with theory, certain integrals of the spectra, the spectral moments, are of interest. One may define the nth spectral moment as an integral of the line profile according to [13] as

$$M_n = \int_{-\infty}^{\infty} \nu^n V g(\nu)\, d\nu, \tag{3.2.3}$$

where g(ν) is the spectral density function and the order number n is a non-negative integer. These integrals converge due to the nearly exponential fall-off of typical spectral functions. Rather than reflecting the specific shape of the absorption profile the zeroth order moment represents the total intensity and is related by theory to familiar sum formula. The first order moment corresponds to the mean width. For nearly classical systems, that means massive pairs at high temperature and not too high frequencies, the first moment is relatively small and drops to zero in the classical limit. The ratio of second and zeroth moment defines some average frequency squared that may be considered a mean spectral width squared.

Theoretically, a complete set of spectral moments may be considered equivalent to the knowledge of the spectral line shape [13]. However, practically speaking, moments higher than the second have rarely been determined, presumably because of experimental difficulties related to the exponential intensity fall-off of the profiles. Nevertheless, knowledge of only the lowest three moments, and a good choice of a model profile are sufficient to obtain surprisingly good representations of many spectra of practical significance [13]. Up to now only the zeroth, first and second spectral moments have been computed with semi-classical expressions. For higher order moments one has to take into account quantum mechanics. For the spectral moments also virial expansions exist.

Chapter 4

The Approach

4.1 *Ab initio* calculations of interaction-induced spectra

The theory of collision-induced absorption developed by van Kranendonk and coworkers [56] and other authors ([5],[7], [6], [43], [44]) has emphasized spectral moments (sum formulas) of low order. These are given in closed form by relatively simple expressions and can be obtained from spectroscopic measurements by integration over the profile as discussed in the last chapter. The spectral moments characterize spectral profiles in important ways. However, it is clear that some information is lost if a spectroscopic measurement is reduced to just one or two numbers. Furthermore, even if large parts of the spectra are known accurately, for the determination of experimental spectral moments substantial extrapolations of the measured spectra to low and high frequencies are usually necessary [13]. Thus, for detailed analyses of measured spectra line shape computations are indispensible, especially where the complete absorption spectra cannot be measured. Moments are integrals, i. e. averages, of the spectral function and are thus generally less discriminating than line shape calculations to the subtle differences of dipole model and interaction potential, if only a small number of moments is known.

Highly developed quantum-chemical methods exist to compute with an ever increasing precission molecular and supramolecular properties from first principles.

Early attempts to calculate the induced dipole moments of H_2–H_2 from first principles are described in [61]. Only recently substantial problems of those computations could be controlled and precise data be generated by SCF and CI calculations, so that the basis set superposition errors were small and the CI excitation level adequate for the long-range effects. Details of these computations can be found in [61] and [63]. The SCF-CI quantum chemical methods are clearly the methods of choice for the computation of induced dipole surfaces where practicable. However, the computational requirements are high and approximations with much less stringent demand are of considerable interest.

Sometimes applications require supramolecular absorption spectra at temperatures, for which no laboratory measurements exist or when laboratory measurements had to be taken at much higher densities than atmospheric densities. In these cases calculations of spectral profiles and intensities of supramolecular spectra are necessary [13]. Given that one has reliable intermolecular potential and induced dipole functions available using a quantum formalism the spectra of interacting pairs of molecules may be modeled. Since for many applications the anisotropy of the interaction potential may be neglected the isotropic potential approximation can be used [13]. This simplifies the computational procedures enormous and makes it possible to do complete line shape calculations on personal computers within a few days. As a first step such calculations involve the determination of the rotovibrational energies of the bound dimer. It is already possible to compute reliable free-to-free, free-to-bound, bound-to-free and bound-to-bound transition dipole matrix elements so that complete spectra can be composed for comparison with measurements and for various applications in planetary and earth science. In the past close agreement between these calculated spectra and the measured ones has been observed [13].

However, calculations accounting for the anisotropy of the intermolecular potential may be done but are very computation intensive [9]. They may be marginally feasible for the massive molecular systems one is concerned with in studies of the earth' s atmosphere. Thus, it is interesting to compare the results of these calculations that take into account the anisotropy of the intermolecular potential with simplified quantum calculations that can be done in minutes even on personal computers, whereas close coupled computations may take months of computer time.

It should be mentioned that due to the smallness of interaction-induced dipoles measurements of supramolecular absorption spectra are quite demanding [13]. To make up for that deficiency in laboratory measurements one may be tempted to use high gas densities. However, one has to be careful to avoid ternary and higher-order contributions that may not be present, to such an extent, in atmospheric research, where gas densities are generally lower. Furthermore, measurements of the so-called enhancement spectra of gas mixtures usually possess a somewhat greater uncertainty than measurements of pure gases [14]. This is a result of the fact that in gas mixtures such as of helium and hydrogen one has to subtract the H_2–H_2 contributions from the sum of absorptions due to the H_2–H_2 and H_2–He pairs. Since the spectra are fairly similar subtraction of comparable intensities renders the end result more uncertain.

Some calculations exist that account for the anisotropy of the intermolecular interactions, based on the close coupled (CC) scheme ([9], [19]). Their computational procedures are substantially more complicated and such calculations are very time consuming.

Rotovibrational combination lines are usually very diffuse and overlap, so much that individual lines cannot be resolved. However, in the isotropic potential approximation their contribution to the opacity must be calculated individually and afterwards summed over all dipole-allowed and significant lines.

4.2 Line shape calculations

As mentioned above measurements of collision-induced absorption spectra and absolute intensities are difficult and only a limited number of accurate measurements for certain species and temperatures exist so far. However, for astrophysical applications, in particular for the modeling of planetary and stellar atmospheres, one needs absorption spectra at arbitrary temperatures. For this, extrapolations of the measured absorption coefficients to temperatures and frequencies of interest are needed, but these are often inaccurate. Alternatively, one can rely on accurate computed absorption profiles. These profiles can be computed with high precission and made available for applications for arbitrary temperatures.

For computation of the binary collision-induced absorption the intermolecular potential, or potential energy surface is needed, in order to determine the dynamics of the collision [13]. In addition, one needs the interaction-induced dipole surface to obtain the radiative transition probabilities [9]. For the interaction-induced dipole surfaces the best data are almost exclusively obtained from quantum-chemical *ab initio* calculations. However, the best values for the potential of the weakly interacting van der Waals complexes are typically semi-empirical [13]. It is generally possible with *ab initio* calculations to obtain the long-range attractive part and the short range repulsive part with good precision, but for the intermediate region, better results are obtained from measurements of scattering cross sections [13].

Given these intermolecular potentials and interaction-induced dipoles one can compute CIA line shapes to provide astrophysicists and other specialists with the data they need. Since its discovery the understanding of collision-induced absorption by binary systems has made huge progress and quantum calculations of CIA line shapes are in good agreement with laboratory measurements [36]. For the calculation of collision-induced absorption spectra for this work Fortran program codes and the Intel Fortran compiler were used.

4.2.1 Opacity calculations

For comparisons of measured spectra of diatomic molecules with quantum calculations the isotropic potential approximation (IPA) [13] has been applied. In this approximation one neglects the dependence of the intermolecular potential on the orientation of the diatomic molecule, which simplifies the calculations enormously (and makes extended calculations possible at the elevated temperatures envisioned).

4.2.2 About collision-induced spectral "lines"

The collision-induced absorption (CIA) pair spectra consist of a great number of spectral "lines" at the rotovibrational transition frequencies,

$$\hbar\omega_{\nu_1 j_1 \nu_1' j_1' \nu_2 j_2 \nu_2' j_2'} = E(\nu_1' j_1') - E(\nu_1 j_1) + E(\nu_2' j_2') - E(\nu_2 j_2) \,, \tag{4.2.1}$$

which are their center frequencies. The E($\nu_i j_i$) are the well-known rotovibrational levels of the H_2 molecule. ν and j are vibrational and rotational quantum numbers, respectively. i labels the molecule (i = 1 or 2). Unprimed quantum numbers represent the initial rotovibrational state and a prime indicates the final such state of the two interacting molecules considered. It should be remarked that ternary and higher-order collisional complexes require different treatment [13] and are not considered in this work. The rotovibrational combination "lines" are actually quasi-continuous, i. e. they are very broad (a spectroscopist would say "diffuse") and usually overlap, so much that individual lines cannot be resolved. Typical atomic lines in the visible have a natural width in the order of about 10^{-3} cm^{-1}, independent of temperature. CIA "lines," on the other hand, are roughly 100,000 times broader, amounting in dense hydrogen gas to about 100 cm^{-1} at 300K, because of the short duration of a (binary) collision: $\Delta t \approx 10^{-13}$ s, compared to the lifetime of atomic states in the order of 10^{-8}s: $\Delta t \times \Delta\omega \geq \frac{1}{2}$, Heisenberg's uncertainty relation. Nevertheless, in the IPA, their contribution to the opacity has to be calculated individually and must be summed over all significant (dipole-) allowed lines in the end.

The angular frequency $\omega = 2\pi f = 2\pi ck$ in equation (4.2.1), and the associated frequencies f and k, are "absolute" frequencies and always non negative. These are to be distinguished from the frequency shifts, relative to the line centers,

$$\omega_{\text{sh}} = \omega - \omega_{\nu_1 j_1 \nu_1' j_1' \nu_2 j_2 \nu_2' j_2'} \ . \tag{4.2.2}$$

Frequency shifts are considered when the wings of the individual lines are concerned. They may be positive or negative and will be distinguished by a subscript, ω_{sh}, f_{sh}, and k_{sh}, respectively.

4.2.3 About the ID and PE surfaces

The CIA spectra are quasi-continua in the infrared and extend at high enough temperatures into the visible part of the electromagnetic spectrum [13]. The absorption profiles and -intensities can be calculated if

i) the induced dipole (ID) and

ii) the intermolecular potential energy (PE) surfaces

are known (IDS, PES). These must come from quantum-chemical computations that are refined to the point where the weak (!) van-der-Waals interactions are accounted for with sufficient accuracy. K. L. C. Hunt and X. Li at Michigan State University [33] have provided such data for pairs of highly rotovibrating hydrogen molecules. These have been cast in spherical tensor form, i. e. the direct results of the quantum-chemical calculations, which are obtained in cartesian tensor form, $\boldsymbol{B}(\boldsymbol{r}_1, \boldsymbol{r}_2, \boldsymbol{R})$ with $\boldsymbol{B} = (B_x, B_y, B_z)^T$, and $V(\boldsymbol{r}_1, \boldsymbol{r}_2, \boldsymbol{R})$ are converted to spherical tensor form $B_{\lambda_1\lambda_2\Lambda L}(\boldsymbol{r}_1, \boldsymbol{r}_2, \boldsymbol{R})$ and $V_{\lambda_1\lambda_2 L}(\boldsymbol{r}_1, \boldsymbol{r}_2, \boldsymbol{R})$, of which only the leading component $\mathrm{V}_{000}(\mathrm{r}_1, \mathrm{r}_2, \mathrm{R})$ is used in the isotropic potential approximation [13]. $\boldsymbol{r}_1$ and $\boldsymbol{r}_2$ are the separation vectors of the nuclei of each molecule, and $\boldsymbol{R}$ is the center-to-center separation of the molecules, also in vector form. The λ_1, λ_2, Λ, and L are the expansion parameters [13]. The dipole $\boldsymbol{B}$ is a rank 1 tensor and the potential energy V is of rank 0. The spherical tensor components of the IDS and PES of H_2–H_2 complexes were made available in table form.

4.3 Calculation of collision-induced absorption spectra from first principles

The collision-induced absorption spectra are functions of angular frequency ω and temperature T and are calculated according to equation (3.2.1),

$$\alpha(\omega,T) = \frac{2\pi}{3\hbar c}\,\frac{1}{2} N_a^2 \rho^2\, \omega \left(1 - \exp\left[-\frac{\hbar\omega}{k_B T}\right]\right)\; V g(\omega,T), \tag{4.3.1}$$

where N_a is Avogadro's number, ρ is the number density of the gas in amagat units, k_B is Boltzmann's constant, V is the volume, and $g(\omega, T)$ is the spectral function [13],

$$V g(\omega,T) = \sum_{s,s'} P_s \sum_{t,t'} V P_t \frac{1}{4\pi\epsilon_0} \left|\langle t\,| \boldsymbol{B}_{s,s'}(R) |\, t'\rangle\right|^2 \;\delta(\omega_{s,s'} + \omega_{t,t'} - \omega)\;. \tag{4.3.2}$$

Here, s = $\{\nu_1 j_1 \nu_2 j_2\}$ labels the initial rotovibrational states of molecules 1 and 2. A prime indicates the final state. P_s and P_t are the (temperature-dependent) population probabilities of the molecular and the translational states [13]. t = $\{E_t \ell\}$ labels the translational state of the collisional pair. Dirac's δ distribution conserves energy, with $\omega_{s,s'}$ given by equation (4.2.1), and the dipole transition element will be discussed below. The spectral function may be rewritten according to [13], as

$$\begin{aligned} &g(\omega,T) \qquad\qquad\qquad\qquad\qquad\qquad\qquad\qquad\qquad\qquad\qquad (4.3.3)\\ &= \sum_{\lambda_1\lambda_2\Lambda L} \sum_{s,s'} (2j_1+1) P_1\, C(j_1\lambda_1 j_1';000)^2\,(2j_2+1) P_2\, C(j_2\lambda_2 j_2';000)^2 \\ &\qquad\qquad\qquad\qquad\qquad\qquad G_{\lambda_1\lambda_2\Lambda L}(\omega - \omega_{s,s'}, T). \end{aligned}$$

The G functions are the individual "line profiles", [13],

$$G_{\lambda_1\lambda_2\Lambda L}(\omega_{\rm sh},T) = \lambda_0^3\hbar\sum_{\ell,\ell'}(2\ell+1)\,C(\ell L\ell';000)^2\,w(\ell\ell' j_1 j_1' j_2 j_2') \int_0^\infty \exp\left[-\frac{E_t}{kT}\right]\mathrm{d}E_t\,\left|\left\langle t\left|B^{s,s'}_{\lambda_1\lambda_2\Lambda L}\right|t'\right\rangle\right|^2 \quad (4.3.4)$$

and $\omega_{\rm sh} = \omega - \omega_{s,s'}$ is the frequency shift relative to the line center. Energy conservation may be written as

$$E(\nu_1 j_1) + E(\nu_2 j_2) + \hbar\omega + E_t = E(\nu_1' j_1') + E(\nu_2' j_2') + E_{t'}\ , \quad (4.3.5)$$

or simply $\hbar\omega_{\rm sh} = E_{t'} - E_t$.

4.3.1 Supermolecular ID and PE matrix elements

The induced dipole and potential energy surfaces of a pair of hydrogen molecules were obtained by Hunt and Li by highly refined quantum-chemical methods, which account for the weak van-der-Waals interactions of collisional pairs of molecules. Induced dipoles and intermolecular interaction potentials depend on the rotovibrational states of the two molecules involved, which at the temperatures of interest is of quite significant importance. These quantities were obtained for a set of separations ($4 \leq R \leq 10$ bohr) and bond distances ($0.942 \leq r_1, r_2 \leq 2.801$ bohr) [33]. The cartesian tensor components of rank 1 and 0 were then converted to spherical tensor components, $B_{\lambda_1\lambda_2\Lambda L}(r_1, r_2, R)$ and $V_{000}(r_1, r_2, R)$, the anisotropic components $V_{\lambda_1\lambda_2\Lambda}(r_1, r_2, R)$ are ignored in the isotropic potential approximation. Up to 26 dipole components with different labels $\lambda_1\lambda_2\Lambda L$ are known, but only about half of them are significant for opacity calculations. These B and V_{000} coefficients were made available in the form of numerical tables, in atomic units.

The in equation (4.3.4) required supermolecular dipole transition elements are calculated from these tables, according to

$$B^{s,s'}_{\lambda_1\lambda_2\Lambda L}(R) = \langle \nu_1 j_1 \nu_2 j_2 \,| B_{\lambda_1\lambda_2\Lambda L}(x_1, x_2, R) |\, \nu'_1 j'_1 \nu'_2 j'_2 \rangle \,. \tag{4.3.6}$$

The $B_{\lambda_1\lambda_2\Lambda L}(x_1, x_2, R)$ are analytical functions, obtained by a *least-mean-squares* fit of each complete table by two-dimensional polynomials of 3rd order, with $x_i = r_i - \langle r \rangle$ for i = 1, 2, with $\langle r \rangle = 1.449$ bohr. It should be remarked here that the preferrable product ansatz of two polynomials, e.g. $P_1(x_1) \times P_2(x_2)$, did not give the desired accuracy at the more highly excited rotovibrational states and was abandoned. The $|\nu_1 j_1 \nu_2 j_2\rangle$ are the *radial* rotovibrational matrix elements of the molecular pair, ignoring at this point the translational state of relative motion of the pair. The matrix elements $B^{s,s'}_{\lambda_1\lambda_2\Lambda L}(R)$ are made available in the so-called *b*- or β-functions, for example b0223.for, b0445.for, etc., etc., where the four numerals stand for λ_1, λ_2, Λ, L, and the ending .for is the typical Fortran extension. These twentysix β functions are labeled with the expansion parameters just mentioned, but will implicitly reflect the molecular states s, s' as well: Prior to any call to these β functions, there must be a call to betacom, an entry used but once in these Fortran functions, which prepares these functions for the various molecular states as required. It should be noted that the Clebsch-Gordan coefficients in equation (4.3.3) eliminate all but a few of the final rotational states:

$$j_1 - \lambda_1 \leq j_1' \leq j_1 + \lambda_1 \quad \text{and} \quad j_2 - \lambda_2 \leq j_2' \leq j_2 + \lambda_2 \tag{4.3.7}$$

corresponding to the selection rules from the triangular inequalities of the Clebsch-Gordan coefficients, with $\mathrm{j}_1 \geq 0$ and $\mathrm{j}_2 \geq 0$. For a given set of initial rotovibrational quantum numbers s, all other j' values give zero contributions to the opacity. However, no selection rules exist for the vibrational molecular states ν_1, ν_2. In other words, many overtones and combination overtones exist in the CIA profiles.

4.3.2 Translational ID matrix elements

The in equation (4.3.4) required radial translational dipole matrix elements are obtained from equation (4.3.6) by calculating the translational wave functions of relative motion of the pair $|t\rangle = |E_t, \ell\rangle$ by integrating the radial Schroedinger equation (3.1.13). Since a great variety of initial and final states is required, the intermolecular potential energy surface — the state-sensitive intermolecular potential — must be set up such that initial and final states are appropriately reflected. This is done by calling the entry vacumon once prior to calling the V000rvib.for function, with the appropriate bimolecular states s and s'. This is done automatically when running cirme.for. (This is similar to running betacom in order to set up the β functions, also done automatically when starting cirme.for.)

The fortran program cirme.for computes the translational dipole matrix elements,

$$\left\langle E_t \ell \left| B^{s,s'}_{\lambda_1 \lambda_2 \Lambda L}(R) \right| E_{t'} \ell' \right\rangle , \tag{4.3.8}$$

required in the individual line profiles, equation (4.3.4). Cirme stands for "collision-induced radial matrix elements." The program requires carefully selected input ("cirme.in") and produces many MB of output ("_X.RME") to store the significant 10^6 or so matrix elements and labels, equation (4.3.8). A follow-up fortran program aline.for (for "absorption line") then computes the individual line profile, the integral in equation (4.3.4), and outputs files of these profiles on a frequency and temperature grid. These must be then summed over all significant line profiles, for use by the astronomers.

4.4 The Fortran programs

4.4.1 The LINES code

First of all one has to choose a certain mean temperature $\langle \mathrm{T} \rangle$, a frequency range one is interested in and a cut-off value for the population probabilities one wants to account for in the calculations. This is input for the program lines.for. This Fortran program gets furthermore as input the potential energy levels of the atomic species under consideration. While running lines.for an output file, lines.out, is produced, which lists the quantum numbers of the transitions that have a higher probability than the previously described probability cut-off and are important for the temperature and frequency range chosen. These quantum numbers become input for the Fortran program cirme.for, to be discussed in the next section.

4.4.2 The CIRME code

The collision-induced translational radial dipole matrix elements, equation (4.3.8), are computed by running CIRME.FOR for the many "lines" that contribute to the absorption at the frequencies of concern. cirme.for must be compiled and linked with a beta function, the appropriate intermolecular potential function (V000rvib.for or vaoo.for), and several mathematical subroutines as needed. After that, a suitable input file cirme.in must be written. Reasonable choices must be made for a number of very important quantities, such as:

- a suitable range of partial waves with quantum numbers $0 \leq \ell \leq \ell_{\max}$
- one of many "lines" of interest must be chosen: $\nu_1 j_1 \nu_2 j_2 \to \nu_1' j_1' \nu_2' j_2'$, depending on the frequency range considered, and corresponding to the lines output
- an array (called a range) of frequency shifts ω_{sh} must be chosen, units are cm^{-1}
- an array (called again a range) of free-state kinetic energies, E_{CI}, of relative motion must be chosen, for the chosen "mean temperature", units are also cm^{-1}
- a few other choices may be made to shorten the extensive calculations.

There are plenty of choices one has to make and many of them can go wrong, but no internal warnings are issued — one just gets bad numbers. It is therefore of the utmost significance to check the calculations carefully every step along the way: convergence of sum over partial waves, suitably dense range of frequency shifts and kinetic energies, sum formulas, etc.. (Most of these checks can be made only after running aline.for, to be discussed in the next section). If anyone of the checks does not look 100% solid, it is often possible to obtain a clue as to the likely cause of the inaccuracy, unless there were too many bad choices.

Before one can compute the translational dipole matrix elements, equation (4.3.8), one needs the operator $B^{s,s'}_{\lambda_1\lambda_2\Lambda L}(R)$ of these matrix elements. This is done automatically: prior to every call of the beta function, the ENTRY BETACOM is called where for the given "line" the necessary operations are done. Similarly, for each new "line" a different intermolecular potential function is needed, which is set up automatically by calling VACOM prior to any call to VA. It should be mentioned that the results of executing cirme.for are stored in the file _X.RME, which usually has a size between 10 and 50 MB. Since there will in the end be very many of these, it is best to immediately run aline.for after cirme.for and let the file _X.RME be overwritten by executing another cirme.for run. However, the results of aline.for are to be archived carefully — which is all that is needed for the calculations of opacities, and their names are carefully designed so that overwriting does not happen (except the aline.out files will go away, which is o.k. once all the checks were made).

When choosing a "line", selection rules must be obeyed. First λ_1 and λ_2 are selected by choosing a b$\lambda_1\lambda_2\Lambda L$.for function, and then j_1 and j_2, to obtain the possible upper rotational states (regardless of the ν_1, ν_2 values),

$$\begin{aligned} j_1 - \lambda_1 \leq j_1' \leq j_1 + \lambda_1, \\ j_2 - \lambda_2 \leq j_2' \leq j_2 + \lambda_2, \end{aligned} \tag{4.4.1}$$

with the additional requirements, j ≥ 0 and "even j $\rightarrow$ even j" and "odd j $\rightarrow$ odd j" for each H_2 molecule.

The chosen "mean temperature" $\langle T \rangle$ or "mean energy" $\langle E_{\mathrm{ci}} \rangle = \langle k_B T \rangle$ defines a meaningful range of kinetic energies, E_{ci}, of relative motion. In previous work in the group, it was found nesessary to choose a range of free state energies from roughly $\frac{1}{20}\langle k_B T \rangle$ to $20\langle k_B T \rangle$; a geometric progression is desirable, which, however, limits the increments to approximately k_BT or less for the lowest temperatures of about $\frac{1}{2}\langle k_B T \rangle$ anticipated. It should be remarked that such a choice of a mean temperature permits usually opacity calculations for temperatures T from $\frac{1}{2}\langle T \rangle$ to $2\langle T \rangle$, if the E_{ci} array is properly chosen.

The array of frequency shifts ω_{sh} must go from large negative values to large positive values, so that the lowest wing intensities are small enough for the range of opacities anticipated. For instance, if the peak of the opacity is, for example, 10^{-5} cm^{-1} amagat^{-2}, and one wants the smallest meaningful opacities to be around 1/1000 or 1/10000 of the peak, for each line opacities must be computed down to well below that desired value. The red wing falls off faster than the blue wing and requires smaller negative shifts than the blue wing. At shifts near the line center a dense grid is desirable (to get the spectral integrals with good accuracy), but the nearly exponential fall-off of the far wings usually permits much larger shifts (and permits reasonable inter- and even extrapolations).

4.4.3 The ALINE code

To run aline.for, it must be compiled and linked with several mathematical functions as usual. The input, aline.in, is straight-forward; a range of temperatures should be specified such that its output can directly be included in the opacity tables to be discussed in the next subsection. The name of the output tape is a series of twelve one-digit numbers,

$$\lambda_1\lambda_2\Lambda L\nu_1 j_1\nu_2 j_2\nu_1' j_1'\nu_2' j_2'. \tag{4.4.2}$$

For example, the file with the name 022301010103 presents one of the main quadrupole-induced components of the important (collision-induced) rotational $S_0(1)$ line of H_2: specifically molecule 1 remains in the groundstate and molecule 2 undergoes the $S_0(1)$ transition (which is (dipole-) forbidden in non-interacting H_2 molecules). Each number has just one digit - the name is 4+8 single digit numbers long. Since rotational quantum numbers greater than 9 will eventually arise, A is used for 10, B for 11,$\cdots$, Z for 36. It should be repeated here once more that these files (4.4.2) must be carefully archived, if one does not want to repeat the corresponding line calculations over and over. Aline.out is not needed once all the necessary testing is done, described in the previous subsection - which must precede the archiving of the above files.

It should be mentioned here that many lines have an identical twin. Whenever $\lambda_1 \neq \lambda_2$,

$$\lambda_1\lambda_2\Lambda L\nu_1 j_1\nu_2 j_2\nu_1' j_1'\nu_2' j_2' \quad \text{and} \quad \lambda_2\lambda_1\Lambda L\nu_2 j_2\nu_1 j_1\nu_2' j_2'\nu_1' j_1' \tag{4.4.3}$$

are identical (exchange of molecules!). If one wants to save computer time one should not compute identical results (although it would be perfectly alright): lengthy cirme calculations need not be duplicated. Rather, one must set up a procedure that generates identical files.

4.4.4 The OPACITY code

Finally, after the contributions from all significant lines have been computed in the way described above the absorption intensities from the different dipole components and lines have to be sumed up. This is done by running the Fortran program opacity.for. This program gets as input a selected temperature within the range of $\frac{1}{20}\langle k_B T\rangle$ to 20 $\langle k_B T\rangle$ and the lines that were computed with lines.for. It produces as output a table that lists the absorption coefficient α as a function of frequency ω, in the form of a table, in increments of 20cm^{-1}.

4.4.5 Opacity tables

The astronomers, who have great need for the opacity data, want the results in the form of a big (!) table.

- Temperatures from 1000 to 7000 K as a minimum, in steps of 250 K. (For brown dwarfs, temperatures down to 50K are of interest)

- Opacities at absolute frequencies from 667 through 20,000 cm^{-1} are needed, in steps of 20 cm^{-1}.

Such tables will be readily compiled by summing the various tapes directly — a trivial task. However, it is of great importance that these tapes are good.

4.5 The calculations

For all calculations in this work the isotropic potential approximation (IPA) was used, which simplified the calculations enormously. An example of an anisotropic potential CIA calculation can be found in [9]. It is easy to generate some numbers with a computer, but the important part of the work was to make sure that these numbers are correct and meaningful. To ensure the reliability of the generated numbers several checks were performed:

4.5.1 Convergence of partial wave expansion

The expansion of partial waves is in general infinte. However, since one has only finite computer time available and the higher order waves have less and less contribution, one has to truncate the partial wave expansion at a certain cut-off angular momentum. However, one has to make sure that one does not truncate the partial wave expansion too soon and takes into account all physically relevant features. The programs were run with different numbers of included partial waves and the results of these runs were compared with each other to ensure convergence. It should be noted that the higher the highest energy E_{ci} and temperature, the more partial waves are needed. Here as above

E_{ci} denotes the initial kinetic energy of relative motion of the colliding pair of molecules. It should further more be pointed out that exchange force-induced dipole components may require more partial waves than multipole-induced ones so that it was necessary to compare the complete spectra for each number of partial waves. Nevertheless, agreement between all calculations for different numbers of included partial waves to better than 0.2 % was observed.

4.5.2 Properly selected array of frequency shifts ω_{sh}

Since the collision-induced lines are very asymmetric with respect to their line centers, negative frequency shifts as well as positive ones have to be considered. It should be pointed out that the blue wing is much wider than the red wing so that much larger positive frequency shifts (the blue wing) had to be chosen than negative ones. In general, a very dense spacing was chosen near zero frequency shifts to ensure that the zeroth moments along with the strongest contributions of the lines were obtained accurately. Farther out into the wings, where nearly exponential fall-off sets in, monotonically increasing larger spacings were used, in order to ensure that spline interpolation was still accurate. The lowest and highest frequency shifts were chosen generous.

Again to ensure numerical accuracy the programs were run with a chosen array of frequency shifts ω_{sh} and afterwards the same calculations were repeated with an array of frequency shifts with the double step size. The two results were compared and a relative deviation of a maximum of 0.5% was observed. It was furthermore ensured that the line wings were computed down to small enough opacities, both in the red and in the blue wing. For the strongest lines, the ratio between line center intensity to wing intensities was larger than 10^7. For the weak lines, the calculated extreme wing intensities where comparable to the cut-off values chosen for the strong lines. If this were not the case, it would be possible to find steps in the final opacity spectrum, which of course would be an undesirable artifact. In this work the focus is on single-photon absorption processes and the broad free-free features of collision-induced spectra. These allow for a rather sparse frequency grid, so that the computer times were accepable.

4.5.3 Properly selected array of free state energies $\mathbf{E}_{ci}$

The initial kinetic energies of the relative motion of the colliding pair of molecules, E_{ci}, depend on the temperatures considered. The calculated radial matrix elements have to be averaged over the free state energies of the Maxwell distribution of velocities. The processes relevant for collision-induced absorption take place in an energy intervall from roughly $\frac{1}{20}k_BT$ to $20k_BT$. For the averaging procedure spline integration was chosen, based on an energy grid E_{ci}, properly chosen for the temperature under consideration. Similar to the array of frequency shifts the calculations were performed with a selected array of free state energies E_{ci} and afterwards the same computation was repeated with an array of free state energies with the double step size. Again the two results were compared and the relative deviation was seen to be less than 0.5%.

4.5.4 Accounting for all relevant lines

After a certain frequency range was chosen as input for lines.for and the calculations were performed a wider frequency range was chosen to make sure that all contributing transitions are included in the calculation. The results of the two computations were compared and agreement was observed. Afterwards the population probability cut-off was changed from 0.01 to 0.005 and the calculations were repeated. Here a significant difference between the two calculations was observed. Nevertheless, it should be mentioned that according to the selection rules (arising from the triangular inequality of the Clebsch Gordan coefficients) many of the included lines are weak or have zero intensity. Thus, lower population probability cut-offs were not further investigated.

Since there were many choices to be made repeated calculations were performed in order to ensure that the produced numbers are reliable. For each change of data set a new calculation was run. As a further test of these line shape calculations, the zeroth, first and second spectral moments have been computed in two different independent ways: by integration of the spectral functions with respect to frequency and also from the well known quantum sum formulas. The two results were compared and agreement to better than 1.5% was observed.

Collision-induced (CIA) pair spectra in general consist of a great number of spectral lines at the rotovibrational combination frequencies $\omega_{\nu_1 j_1 \nu_1' j_1' \nu_2 j_2 \nu_2' j_2'}$. However, in the IPA all these lines have to be calculated separately and afterwards sumed up. It should be remarked that ternary and higher order collisional complexes require different treatment and were not considered in this work.

As input for the calculation of absorption profiles and -intensities the induced dipole (ID) and the intermolecular potential energy (PE) surfaces have to be known. As mentioned above these come from quantum-chemical computations which are refined to the point where the weak van der Waals interaction is accounted for with sufficient accuracy. Such data of highly rotovibrating hydrogen molecules were provided for this work from K. L. C. Hunt and X. Li at Michigan State University [33]. The direct results of the quantum-chemical calculations which have been obtained in cartesian tensor form were cast in spherical tensor form. For the isotropic potential approximation only the leading component is used. The isotropic interaction potential [38] supports just one vibrational dimer level, the ground state n = 0. For the computation of the collision-induced spectra the Schroedinger equation (3.1.13) was integrated numerically. For supramolecules with a limited number of electrons, such as H_2–H_2, H_2–He, ..., very accurate quantum-chemical calculations of the dipole surfaces exist. Such *ab initio* results show clearly the various dipole components: exchange force-induced dipoles show an exponential decrease with increasing separation R between the interacting molecules. Dispersion force-induced dipoles fall of to leading order in the expansion in terms of 1/R as R^{-7}, and multipole-induced dipoles have their characteristic long-range behavior of exactly R^{-N}, with N = 3 for dipolar induction, N =

4 for quadrupolar induction, etc. It is important to mention that quantum-chemical studies of this kind can provide some guidance for the development of empirical models for bigger systems that cannot be treated by the demanding quantum-chemical methods.

For binary multi-electron supramolecules, such as the ones found in the Earth' s atmosphere (N_2–N_2, N_2–O_2, ...) or the H_2–H_2 supramolecules considered in this work, the dipole surfaces may often be represented by the (semi-) classical multipole-induced dipole approximation, which neglects or else models empirically the quantum effects of the exchange forces. Generally applicable expressions have been given by Poll and Tipping.

The multipole-induced dipole components are typically much stronger than the overlap and exchange contributions if one or both of the interacting molecules are highly polarizable [13]. Thus, the former may be neglected or perhaps represented by small and relatively inexact, empirical corrections. Then the induced dipole components may be computed by use of classical electrodynamics from the knowledge of molecular multipole strengths and polarizabilities. Tensor calculations by Hunt and collaborators also account for the non-uniformity of the local electric field, the gradient of the field, the dispersion dipole and the hyperpolarizabilities. It should be mentioned that the electronic supramolecular spectra arise similarly by multipolar induction, but in this case the electronic multipoles are due to electronic configurations.

4.5.5 Symmetry considerations

The two interacting hydrogen molecules can be considered to be chemically distinguishable at the kinetic energies considered in this work [19]. Thus, exchange of one proton belonging to molecule 1 with one of molecule 2 and similar with 1 and 2 interchanged does not have to be considered. This proton exchange only has to be taken into account when the two interacting molecules have the same total nuclear spin. Therefore, p-H_2 and o-H_2 are distinguishable from one another, whereas two p-H_2 molecules as well as two o-H_2 molecules have to be considered identical particles and their wave functions must be symmetrized correctly. Since for ground state hydrogen both electrons are in s orbitals the electronic wave functions are unaffected from this operation.

p-H_2 has zero nuclear spin so that the weights for symmetric, ω^+, and antisymmetric, ω^-, respectively, are [9]

$$w_{pp}^{+} = 1 \tag{4.5.1}$$

and

$$w_{pp}^{-} = 0. \tag{4.5.2}$$

Therefore, the only allowed solutions for the coupled equations involving p-H_2 are symmetric. In the case of o-H_2 molecules (nuclear spin one), the normalized nuclear weights are

$$w_{oo}^{+} = 2/3 \tag{4.5.3}$$

and

$$w_{oo}^{-} = 1/3. \tag{4.5.4}$$

As long as no magnetic material is present in reality the probability for spin flips is extremely small. Thus, in the present model no interaction is involved that can flip spin, so that the $\pm$ symmetry is conserved in the calculations.

4.5.6 The measurements

A measurement of the collision-induced rototranslational spectrum of dense hydrogen gas at the temperature of 297.5K has been reported [9]. For the recording of the infrared spectrum a Bruker IFS 66V Fourier-transform spectrometer with a resolution of 0.5cm^{-1} was used. The calibration was done by comparison with lines in the fundamental band of CO. For each interferogram an averaging procedure over 512 scans was employed with a four-term Blackmann-Harris apodization. The path length of the high pressure absorption cell was 214.4cm. The cell was equipped with thick CaF_2 optical windows. The hydrogen gas which was purchased from Air Liquide had an ultrahigh purity grade (99.9999%). It had an ortho/para ratio of 3:1 (normal hydrogen). At the temperature of 297.5K the collision-induced absorption spectra of hydrogen have been recorded at frequencies from 1900 to 2260cm^{-1} at gas densities ranging from 51 to 204 amagats.

From the measured intensities I the absorption coefficient $\alpha(\nu)$ may be obtained via

$$\alpha(\nu) = -Log[I(\nu)/I_0(\nu)]/L, \tag{4.5.5}$$

where I denotes the transmitted intensity and I_0 is the incident intensity, either measured, when the cell is evacuated or filled with helium gas. The optical path length is denoted by L. The absorption coefficient is generally a function of frequency ν, temperature T and gas density ρ. The binary absorption coefficient is defined according to

$$\alpha_0(\nu) = \alpha(\nu)/\rho^2. \tag{4.5.6}$$

It gives, to good approximation, the total absorption due to supramolecules, if ternary and higher order contributions are negligible. In this formula ρ denotes the gas density. Since even in the best measurements ternary and possibly higher order contributions to the absorption may be present, the binary absorption coefficient was obtained via extrapolation to the limit of zero density of the values $\alpha_0(\nu)$, at fixed frequencies ν spaced evenly 10cm^{-1} apart from one another. For each frequency ν with increasing density ρ 12 intensities $\alpha(\nu)$ were recorded. This set of 12 data points was fitted by an unconstrained least squares fit to a low-order polynomial in the gas density ρ. It was estimated that the absolute uncertainty of the thus defined binary absorption coefficient is equal to the statistical error, defined as three times the standard deviation (3σ) of the least squares fit. Compared to the uncertainty in the baseline (I_0) location the experimental errors due to the measurement of temperature, pressure and the purity of the gas, the determination of the gas density and the optical path length or the treatment of the interferograms are believed to be small. In order to evaluate the uncertainty of $\alpha_0(\nu)$ statistical methods were applied to several spectra with baselines varying within the believed uncertainty. The thus obtained uncertainties were found to be within the range of 3 to 8%.

Chapter 5

Results and analysis

Translational spectra involve transitions between states of relative motion of the collisional pair, without changing the rotovibrational or electronic states of the interacting molecules themselves. They occur at zero frequency but due to their considerable widths, their wings generally extend well into the microwave and far infrared regions of the electromagnetic spectrum.

As mentioned above it is very important to compare *ab initio* calculations of collision-induced absorption spectra with existing measurements before one proceeds to temperatures where no measurements exist. Accurate knowledge of the collision-induced absorption spectrum of molecular hydrogen in the 5μm region is necessary for detailed analyses of the atmospheres of the outer planets. However, since the absorption is weak laboratory measurements must be carried out at much higher densities than those encountered in planetary atmospheres. Thus the laboratory measurements might be affected by ternary and possibly higher order contributions that do not significantly exist in the atmospheres.

Previously [9] a comparison of a measurement of the collision-induced absorption by hydrogen in the rototranslational band with calculations of binary collision-induced absorption was undertaken to test the binary nature of the measurement, but certain inconsistencies were observed in the blue wing of the spectrum. At that time no definite conclusion could be drawn wether the measurement was deficient or the calculation [9]. For example, theory could have truncated the expansion of the spherical tensor components of the induced dipole surface to soon, when including more dipole components was no option at that time. On the other hand, measurements of the far wing of the translational spectrum are difficult because of the weak absorption, so that fairly high gas densities have to be employed for recording of low-noise signals. However, as pointed out above, with increasing gas densities ternary and perhaps higher order contributions do usually appear which may be difficult to separate from the the desired purely binary ones. Thus, it could have been possible that the measurement was affected by ternary and possibly higher order contributions, to an unknown extent. Theory is capable of calculating the binary spectra. Calculations of ternary spectra have not yet been attempted. The measurement ([9], [29]) was undertaken in the expressed desire to provide accurate knowledge of absorption data of dense hydrogen gas at wavelengths around 5μm where traces of other contributions could possibly be discovered in an analysis of the Voyager spectra ([12], [8]). However, at that time no definite conclusion could be drawn wether the measurement was deficient or the theory.

In the meantime, new quantum-chemical calculations of the dipole surfaces have been made with a greater selection of spherical tensor components

[33]. It is therefore interesting to reconsider the comparison of the latest theory and the existing measurements. In the previous calculation [9] only the $\lambda_1\lambda_2\Lambda L$ = 0001, 0221, 0223, 2021, 2023, 2211, 2233 dipole components were used, along with the lumped together 0443+0445 and 4043+4045 components, as described in [63]. In the present calculation the latter dipole components are now appropriately separated. Besides, components where one of the λ_1, λ_2 equals 2 and the other 4 are now also available [33].

In figure 5.1 the rototranslational collision-induced absorption spectrum at 300K is shown. The spectrum is given in a semi-logarithmic plot so that regions of high and low absorption are rendered with constant relative precession. In this figure an *ab initio* calculation (solid curve), based on the new dipole and potential energy surface, is compared with two measurements ([9], [29]). Over the whole range of the frequencies shown the measured and the calculated spectrum agree very well with each other. The quadrupole-induced dipole components, $\lambda_1\lambda_2\Lambda L$ = 0223, 2023 are the most important components of the spectrum. Near the rotational lines these give the dominating contributions. Near the $S_0(0)$ and $S_0(1)$ lines, these quadrupole-induced intensities are nearly identical with the total intensity and differ from it only at high frequencies, where the quadrupole interacting with the anisotropy of the polarizability ($\lambda_1\lambda_2\Lambda L$ = 2233) and some other components ($\lambda_1\lambda_2\Lambda L$ = 0221, 2021, 0443, 4043, 0445, 4045) add significantly to the total absorption. The structures are numerous because many rotational states are populated.

In contrast to the earlier calculation [9] the calculation based on the

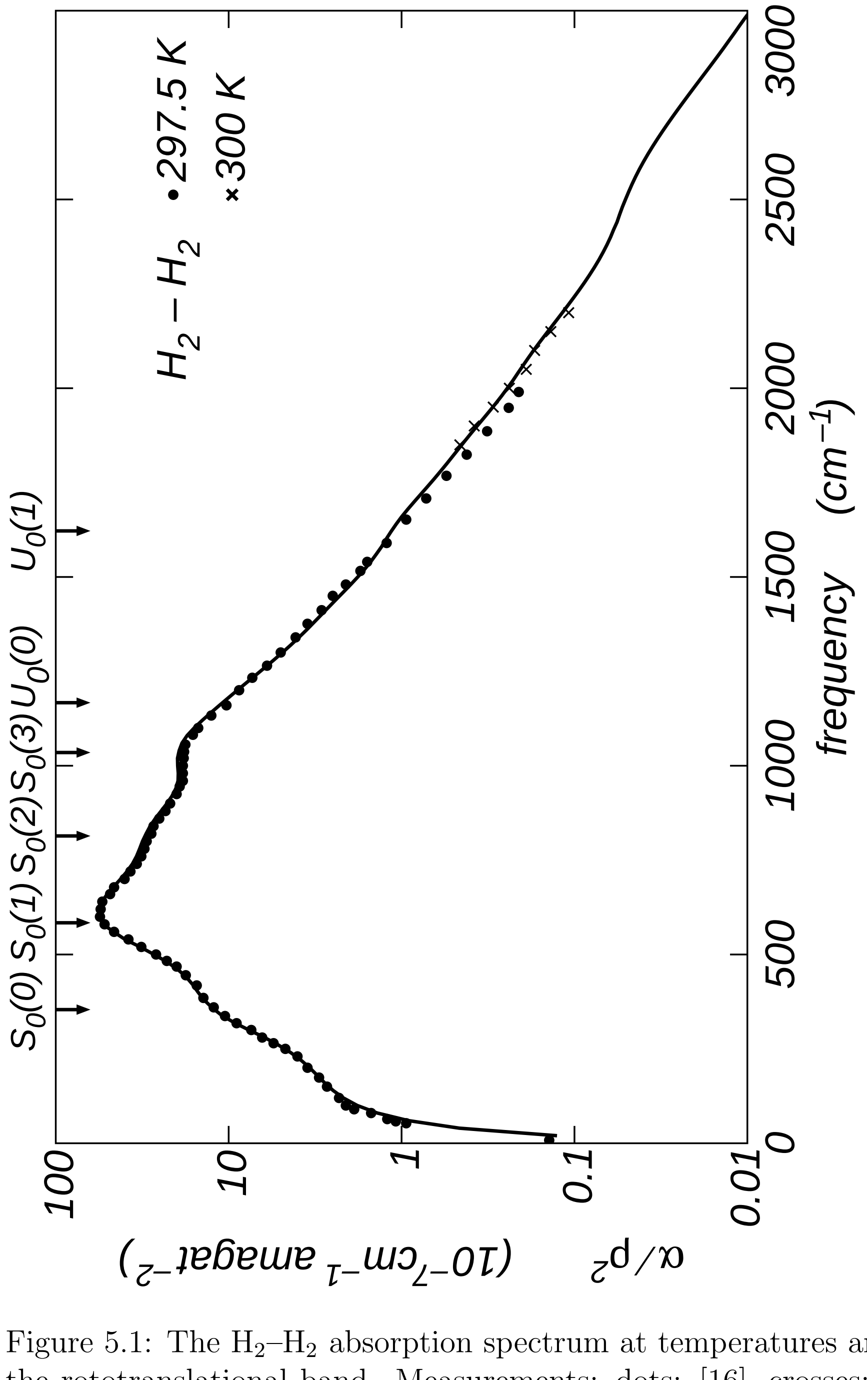

Figure 5.1: The H_2–H_2 absorption spectrum at temperatures around 300K in the rototranslational band. Measurements: dots: [16], crosses: [29]; calculation: solid curve

new dipole surface reproduces the measurements in the far blue wing closely, whereas the comparison of the earlier calculation with the measurements yielded that the calculation gave too much intensity in the far blue wing [9]. In the far blue wing several of the small dipole components contribute significantly to the absorption. The $\lambda_1\lambda_2\Lambda$L = 0443, 0445, 4043 and 4045 dipole components are nearly insignificant near the centers of the diffuse S lines but in the far wing they contribute substantially to the absorption. This is obvious in figure 5.2 which shows the calculation of the same spectrum but without these dipole components (lower curve). For comparison the calculation from figure 5.1 (upper curve) is shown. At the lower frequencies the two curves are nearly identical. However, in the far blue wing there is a substantial difference.

It should be remarked here that in previous calculations in the group it was found that the spectra based on those new dipole components that were also available in the earlier calculations, i. e. the $\lambda_1\lambda_2\Lambda L$ = 0001, 0221, 0223, 2021, 2023, 2233 dipole components, were nearly identical with the ones based on the old dipole surface. However, in the present calculation the $\lambda_1\lambda_2\Lambda$L = 0443+0445 and 4043+4045 dipole components are now appropriately separated. The new dipole surface can explain the measured spectra of the rototranslational spectrum of H_2–H_2 at the temperature of 300K.

It should be mentioned here that the other fifteen dipole components have negligible contribution to the calculated spectrum. Also the $\lambda_1\lambda_2\Lambda$L = 0001 dipole component has negligible contribution to the rototranslational spectrum at the temperature of 300K. If one calculates the spectrum based

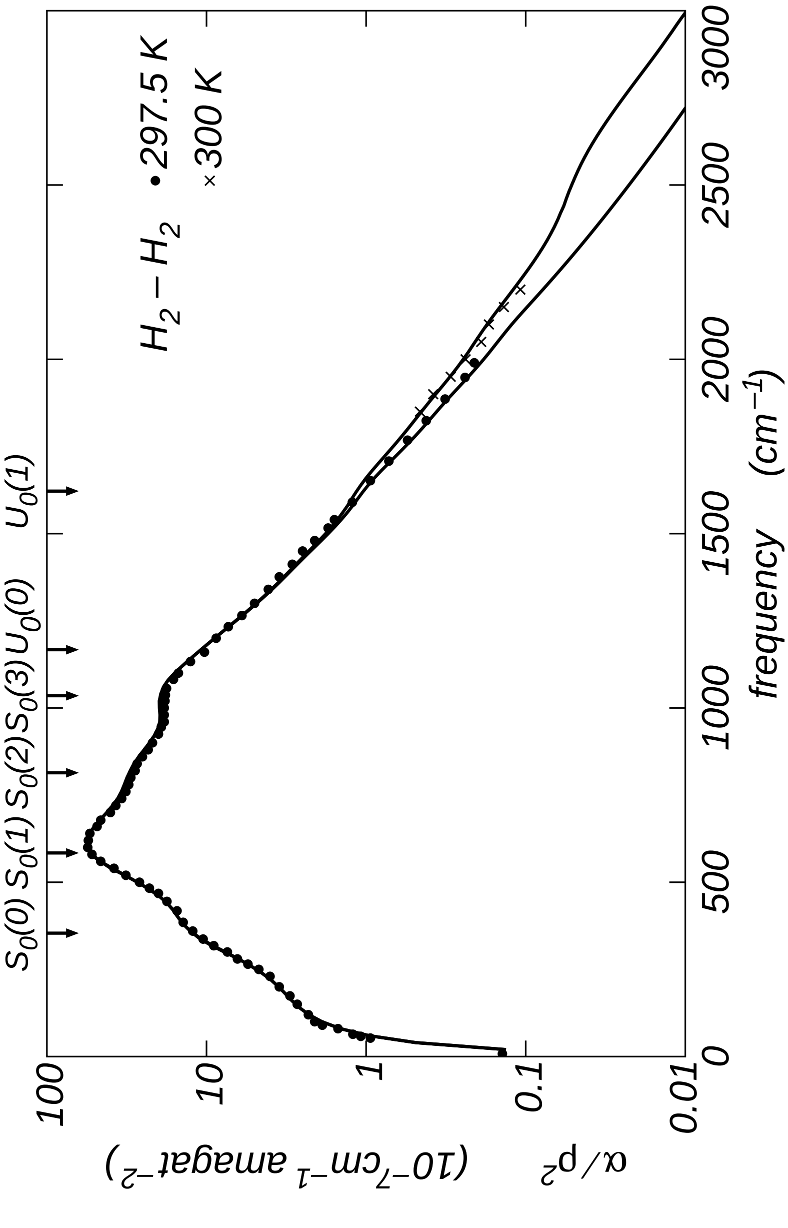

Figure 5.2: The H_2–H_2 absorption spectrum at 300K (upper curve). The lower curve corresponds to a calculation in which the $\lambda_1\lambda_2\Lambda L$ = 0443, 0445, 4043 and 4045 dipole components were omited.

only on the $\lambda_1\lambda_2\Lambda L$ = 0221, 0223, 2021, 2023, 2233, 0443, 0445, 4043 and 4045 dipole components and compares it with the calculation in which all dipole components where included the relative difference amounts to less than 1%, which is remarkable.

The far wing is also noticeably shaped by the repulsive part of the potential energy. The isotropic potential approximation was applied since close-coupled calculations require prohibitive computer time. As the figure shows, the isotropic potential approximation is in quite good agreement with the measurement at that temperature and in the frequency range considered here. *Ab initio* calculations that account for the anisotropy of the intermolecular potential where not yet undertaken at the temperature of 300K. In [9] a close-coupled calculation at the temperature of 77K was undertaken and quite striking differences were observed between the isotropic and the anisotropic calculation. However, since in calculations that take into account the anisotropy the Hamilton operator is not diagonalizable these calculations require much more computer time. The close-coupled calculation [9] required several months of computer time. Since at the temperature of 300K many more excited states have a significant population probability many more transitions can take place which makes the computations even more time consuming. The good agreement between the calculation based on the isotropic potential approximation and the measurements suggests that the anisotropy does not have much influence on the spectra at higher temperatures. Nevertheless it would be desirable to compare IPA calculations with calculations that take into account the anisotropy of the intermolecular potential at higher temperatures, but for this one will probably have to wait until more computer power is available.

As mentioned above, as the frequencies approach zero, absorption falls of to zero for several reasons. One of them is stimulated emission. The rapid increase of absorption with frequency increasing from zero and the first broad peak correspond to translational absorption. The next two peaks near 354 and 585 cm^{-1} are the collision-induced $S_0(0)$ and $S_0(1)$ lines of H_2. The remaining two broad peaks are double rotational transitions of the type S(0)+S(1) and S(1)+S(1), combined with a change of the translational state of the pair by absorption of a single photon, truly a supramolecular feature.

5.1 Dependence of the calculated spectrum on the intermolecular potential energy surface

In order to model the radiative processes in the atmospheres of cool-white dwarf stars, for which collision-induced absorption by supramolecular complexes of hydrogen up to temperatures of at least 7000K is important, besides knowledge of the dipole surface one needs accurate knowledge of the potential energy surface of H_2–H_2. These surfaces come from quantum-chemical calculations with the H_2 bonds stretched or compressed far from equilibrium length. Since no measurements of the collision-induced absorption for these high temperatures exist, one has to undertake *ab initio* calculations which take into account the high vibrational excitation of H_2–H_2. Up to now no potential was available that accounts for these high vibrational levels, since for the lower temperatures considered in previous *ab initio* calculations they could be ignored, due to their low population probability. They also do not have much influence at the temperature of 300K. However, for the temperatures envisioned they have to be taken into account. For these purposes K. L. C. Hunt and X. Li at Michigan State University [33] have provided such data of pairs of highly rotovibrating hydrogen molecules. Nevertheless, before one proceeds to higher temperatures it is important to test the new intermolecular potential energy surface. Therefore the rototranslational spectrum of H_2–H_2 at the temperature of 300K was calculated with two different potential energy surfaces, and the two results where compared (see figure 5.3). The Schaefer-Koehler potential, which does not take into account the vibration of the H_2 molecules, i.e. corresponds to the rigid rotor approximation, is further described in [1], and is only applicable for the ground state of H_2–H_2. It is used by linking cirme.for with the potential function vaoo.for. On the other hand, the isotropic potential provided by Li and Hunt [33] is used by linking cirme.for with the Fortran program V000rvib.FOR. Besides the vibrational ground state it is furthermore applicable for highly vibrating H_2–H_2 supramolecules such as those encountered at temperatures of several thousand kelvin. Nevertheless, at low temperatures the two potential energy surfaces should give similar results since nearly no vibrations occur at these temperatures.

As the comparison between the two differently calculated spectra (figure 5.3) shows the agreement is quite good over the complete range of frequencies considered. The solid curve corresponds to the calculation with the potential

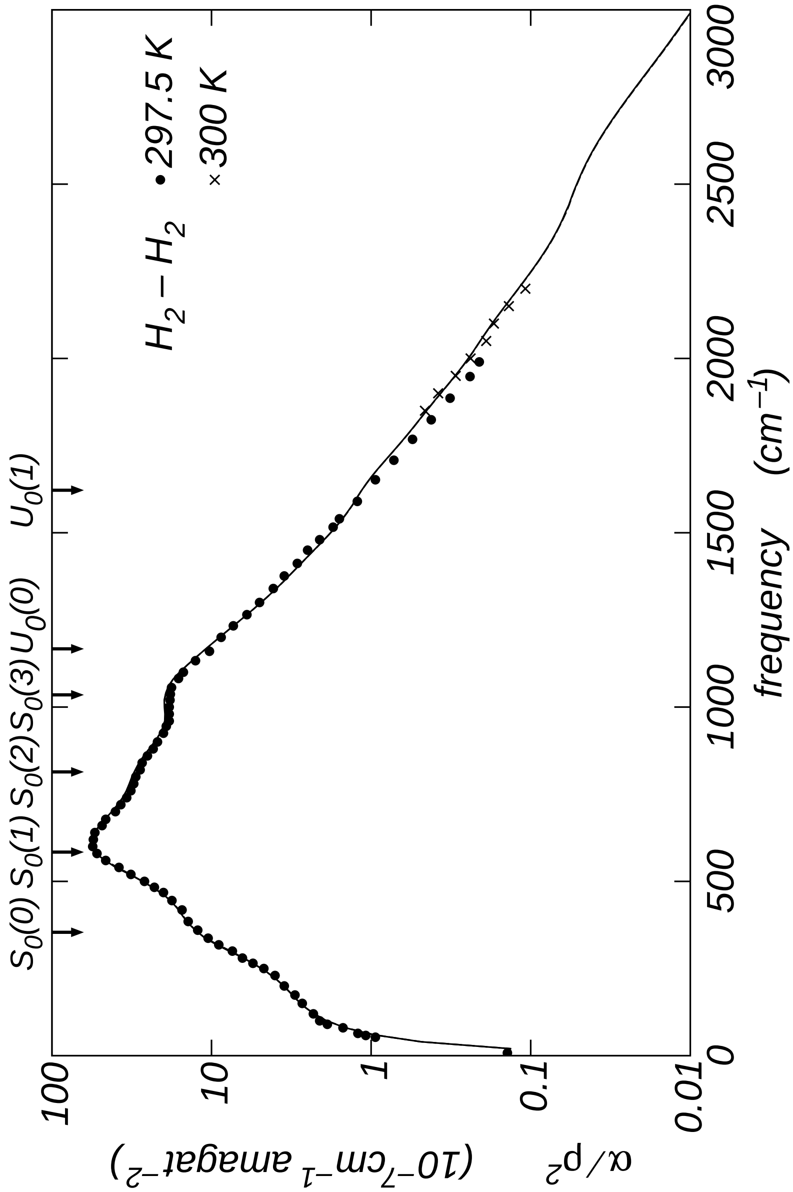

Figure 5.3: The H_2-H_2 absorption spectrum at 300K, calculated using the Hunt potential (solid curve), and using the Schaefer-Koehler potential (dashed curve)

accounting for the vibrational excitation, the dashed one to the calculation for which the Schaefer-Koehler potential was used. The two curves are nearly indistinguishable from one another. The difference between the two curves is less than what can be distinguished with the accuracy of the plot. This is remarkable, since all previous *ab initio* calculations of collision-induced absorption by dense hydrogen gas were based on the Schaefer-Koehler potential. It shows furthermore that as theory suggests the vibrational excitation can be neglected even at the temperature of 300K. What is even more this comparison shows that the new potential energy surface is capable of reproducing the existing measurements. Thus it can be considered tested and one can safely proceed to the higher temperatures which are of great interest for astrophysical applications.

5.2 Temperature dependence of the calculated spectrum

It should be pointed out at this point that as mentioned above collision-induced absorption spectra show a strong dependence on temperature. To further demonstrate this dependence the rototranslational spectrum of H_2–H_2 has been calculated at the temperatures of 275K and 325K and was compared to the calculation at 300K (see figure 5.4). At frequencies below about 600cm^{-1} the calculations for the three temperatures give quite similar results. This can easy be understood by consideration of the Boltzmann factor in the equation (3.2.1) for the absorption coefficient. At low frequencies the temperature dependence of the argument of the exponential function is negligible since it is small due to the small frequencies. However, as excitation energies hν become comparable to the thermal energy k_BT the temperature dependence becomes quite striking. At the higher frequencies it can be seen that the collision-induced absorption intensities become greater with increasing temperature (see figure 5.4) which again can be understood by consideration of the Boltzmann factor in equation (3.2.1).

While at temperatures around 300K temperature control should not be too difficult in measurements, since these temperatures are fairly close to room temperature, it is fair to expect measurements at different temperatures to be likely to be affected by temperature gradients. As can be seen in figure 5.4 the temperature has a great influence on the absorption intensities. This is a point one should keep in mind when attempting to do measurements of collision-induced absorption at temperatures far from room temperature.

5.3 The fundamental band of hydrogen

As a further test of the new method the collision-induced absorption of dense hydrogen gas was investigated in the fundamental band. *Ab initio* calculations of the absorption were compared with measurements at the temperature of 300K (see figure 5.5). As for the rototranslational band the agreement between fundamental theory and experiment is remarkable.

For the rototranslational band of H_2–H_2 it was seen that the collision-induced absorption spectrum is essentially composed of a of number dipole components labeled $\lambda_1\lambda_2\Lambda L$ = 0221, 2021, 0223, 2023, 2233, 0443, 4043, 0445

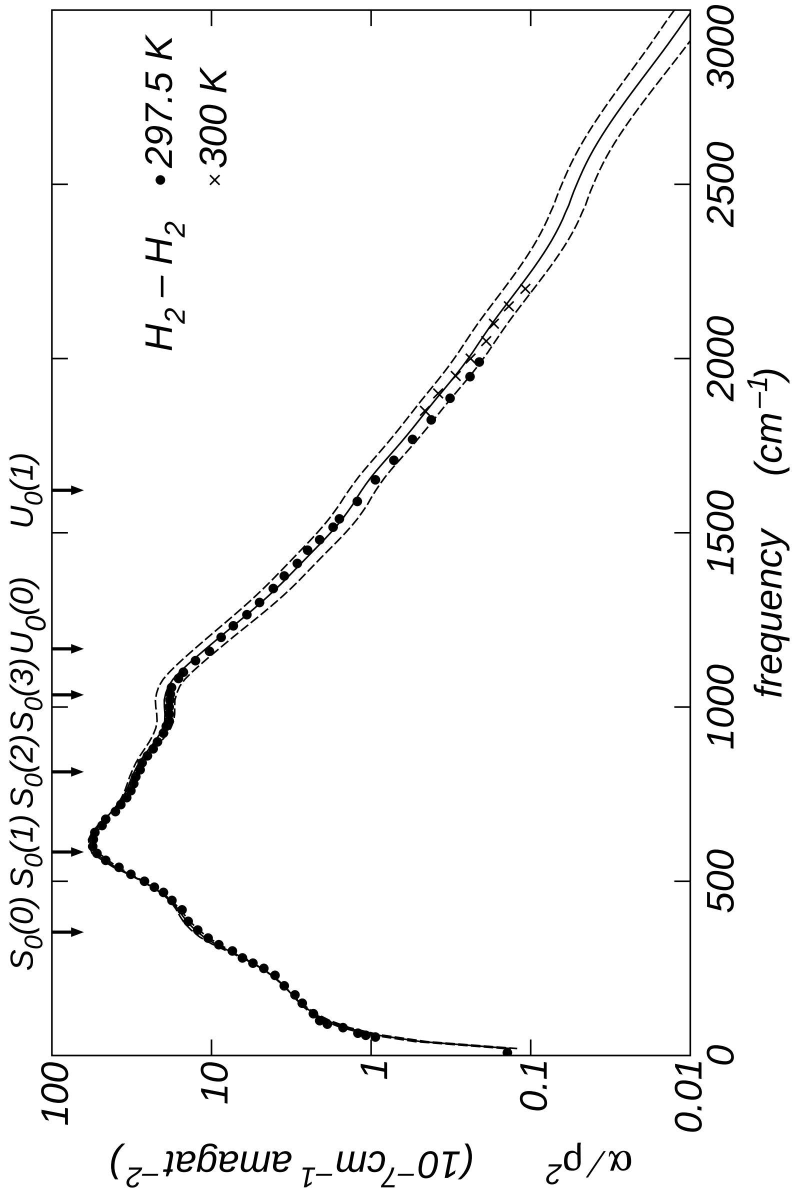

Figure 5.4: The calculated H_2–H_2 absorption spectrum at 300K (solid curve), at 275K (lower dashed curve) and at 325K (upper dashed curve)

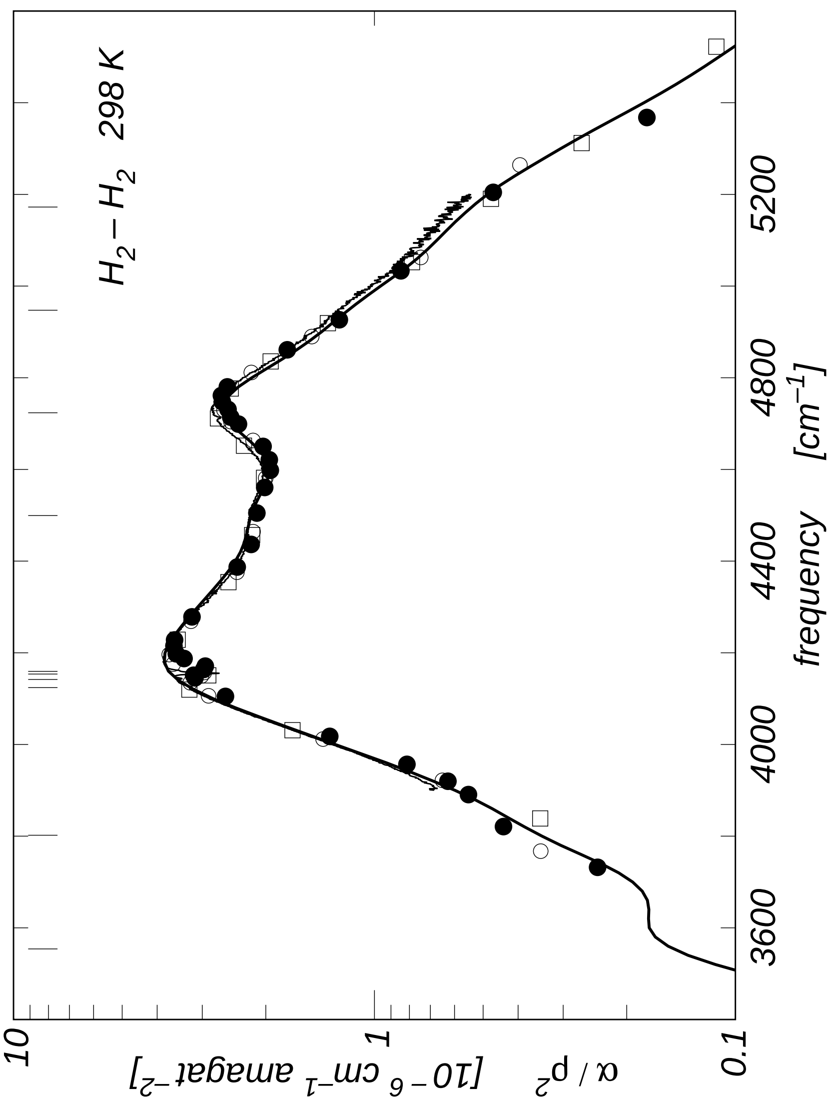

Figure 5.5: Comparison between the calculated (heavy solid curve) H_2 absorption spectrum at 300K in the region of the fundamental band and the measured spectrum (squares: [64], big dots: [26], circles: [50])

and 4045. For the fundamental band also the $\lambda_1\lambda_2\Lambda L = 0001$ component, completely negligible in the rototranslational spectrum, has significant contribution to the absorption, arising from overlap induction. It occurs because a vibrating H_2 molecule differs from a non-vibrating one.

Astrophysicists want to determine the species which are present in planetary atmospheres as accurate as possible. Since in general one has to do this remotely an important way of determining the abundant species is to subtract the calculated absorption of the known species, hydrogen and helium, from the measured absorption. The remaining absorption intensity corresponds to other species and gives one a hint of the amount of other species present in planetary atmospheres. Whereas regions of great absorption of molecular hydrogen have been known accurately for quite a while the same cannot be said about regions of weak absorption. Therefore, the region of weak absorption by collisional hydrogen complexes in between the rototranslational and fundamental band was further investigated. In figure 5.6 the calculated absorption of this region is magnified so that astrophysicists and other specialists may find information about this important absorption region.

5.4 The first and second overtone of hydrogen

At the temperature of 300K there are furthermore measurements reported of the collision-induced absorption by H_2 in the first and second overtone region. As a further test of the new method *ab initio* calculations of the absorption were undertaken for these absorption regions and compared with

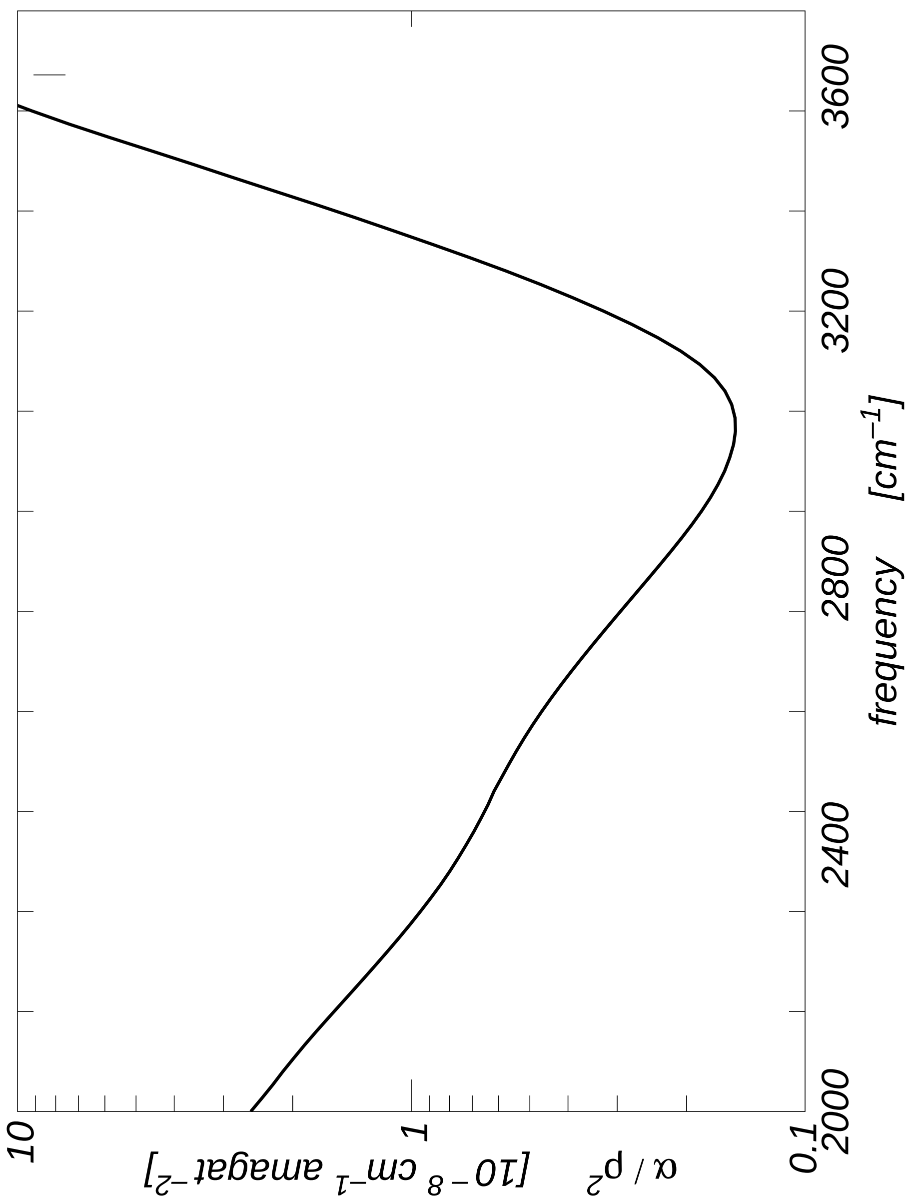

Figure 5.6: The calculated absorption in the region between the rototranslational and fundamental band of dense hydrogen gas at the temperature of 300K

the measurements (see figures 5.7, 5.8). Again close agreement between calculated and measured spectra is observed (see figures 5.7, 5.8), which demonstrates that the new method is capable of reproducing the existing measurements closely.

5.5 Proceeding to higher temperatures

In figure 5.9 the complete collision-induced absorption spectrum of hydrogen at the temperature of 300K from 0 to 20000cm^{-1} is shown. For better clarity of the plot the measurements are obmitted in this plot. As outlined above astrophysical applications require the knowledge of the collision-induced absorption by molecular hydrogen pairs up to temperatures of several thousand kelvin. Extensive comparison between the fundamental theory and existing measurements at temperatures of 300K has yielded excellent agreement. With the new dipole and potential energy surfaces [33] it is now possible to proceed to higher temperatures where there are no measurements for comparison with the theory. These *ab initio* calculations of the absorption at higher temperatures have been undertaken, beginning at temperatures of 300K and successively proceeding to higher temperatures [33]. As an example for such calculations that cannot be compared with measurements since there are no measurements available in this work the collision-induced absorption spectra of collisional hydrogen complexes at temperatures of 600K (see figure 5.10), 1000K (see figure 5.11) and 2000K (see figure 5.12) are shown, again from 0 to 20000cm^{-1}. Since there are no measurements one has to rely on the cal-

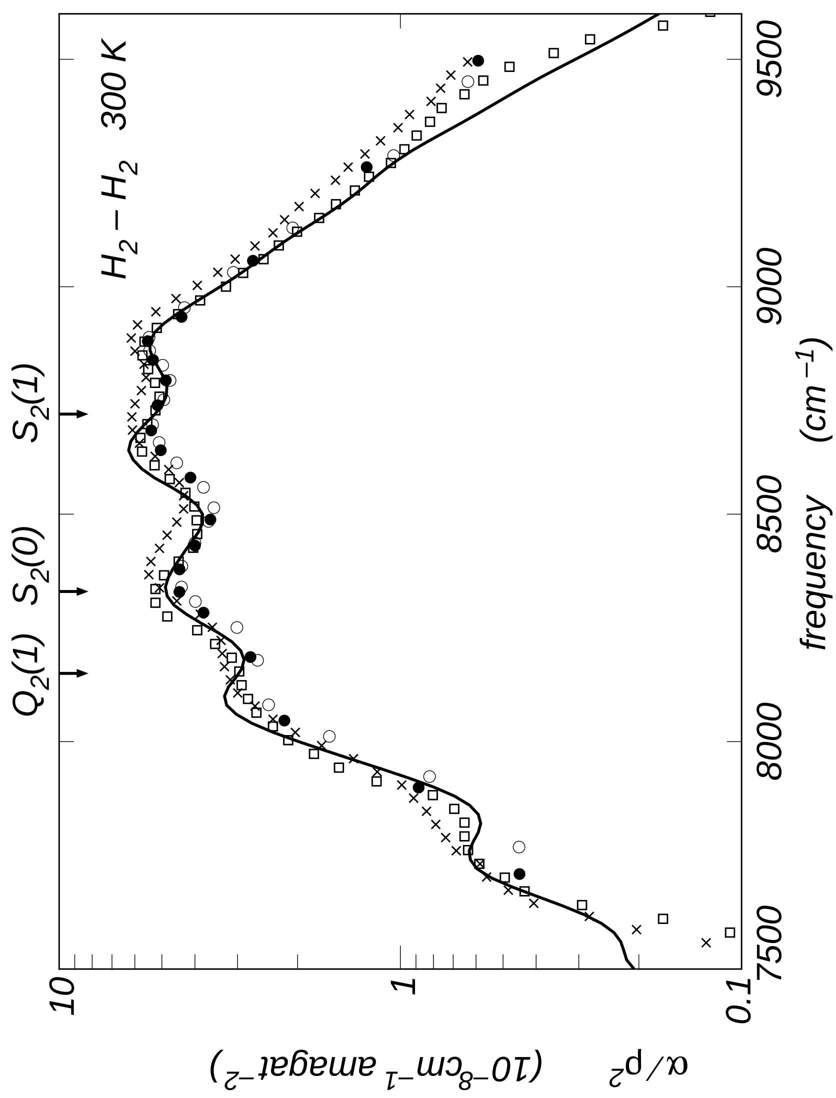

Figure 5.7: Comparison between the calculated (heavy solid curve) H_2 absorption spectrum at 300K in the region of the first overtone and the measured spectrum (squares: [20]), crosses: [28]), dots: [27]

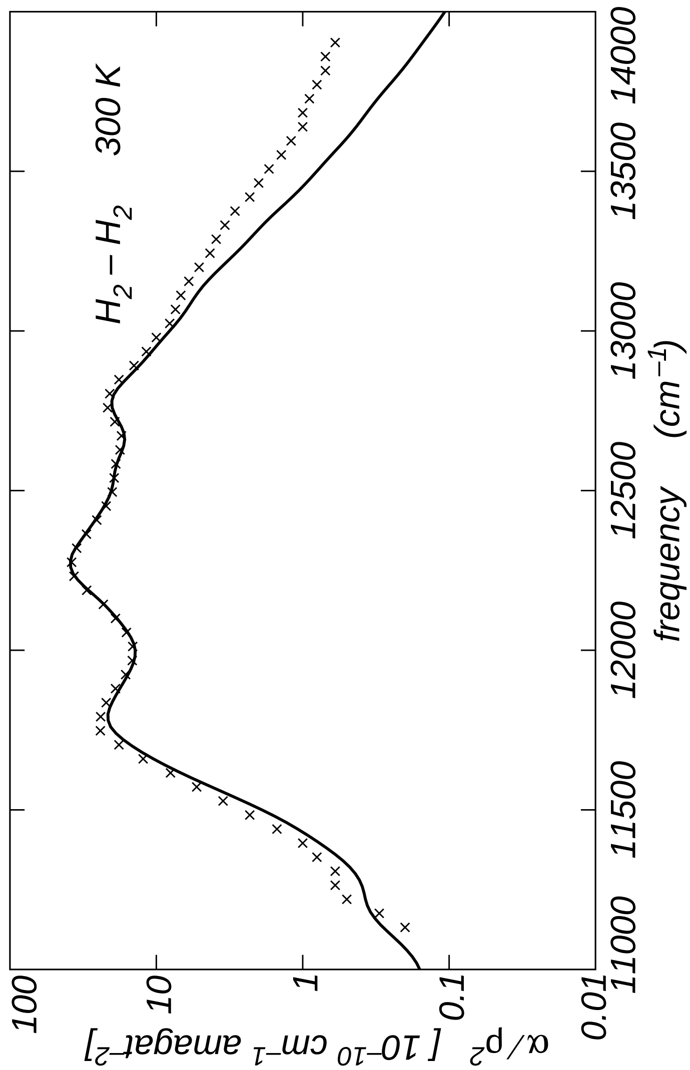

Figure 5.8: Comparison between the calculated (heavy solid curve) H_2 absorption spectrum at 300K in the region of the second overtone and the measured spectrum (crosses: [57])

culated absorption spectra, supported by excellent agreement between theory and measurements at lower temperatures.

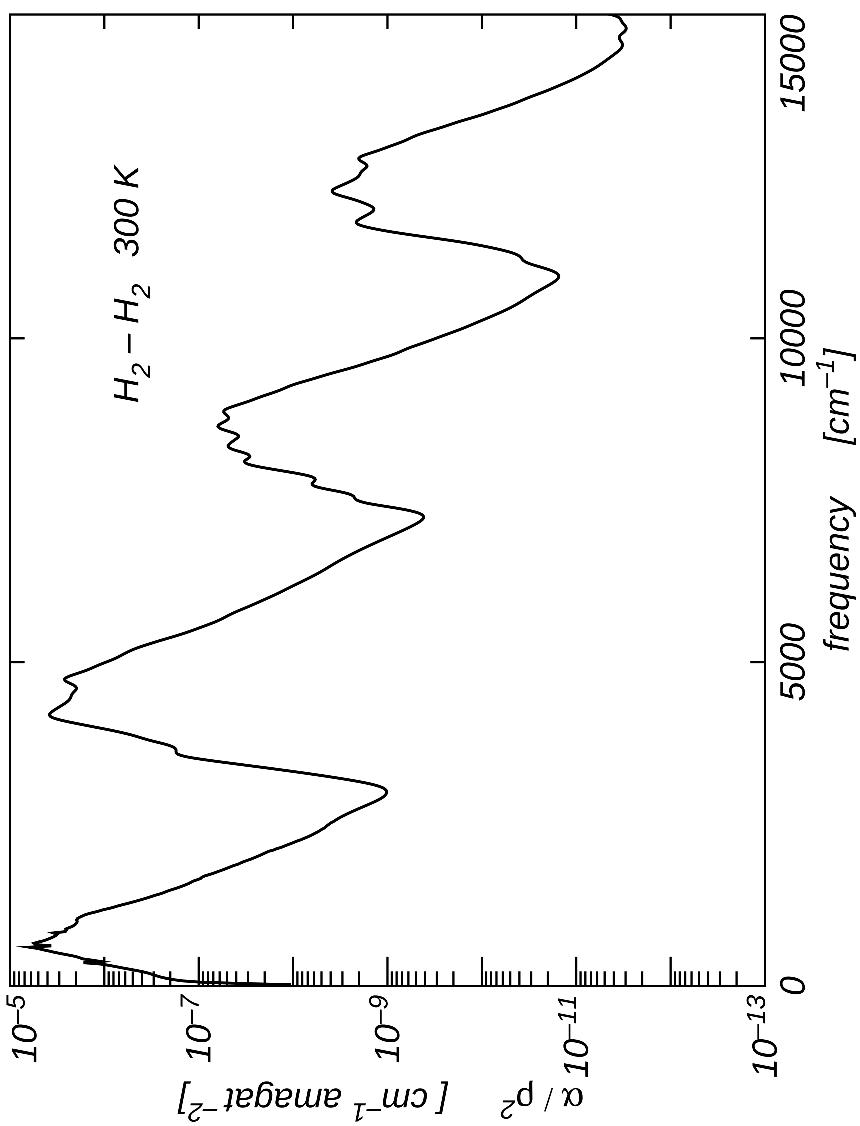

Figure 5.9: The calculated collision-induced absorption spectrum of dense hydrogen gas at the temperature of 300K

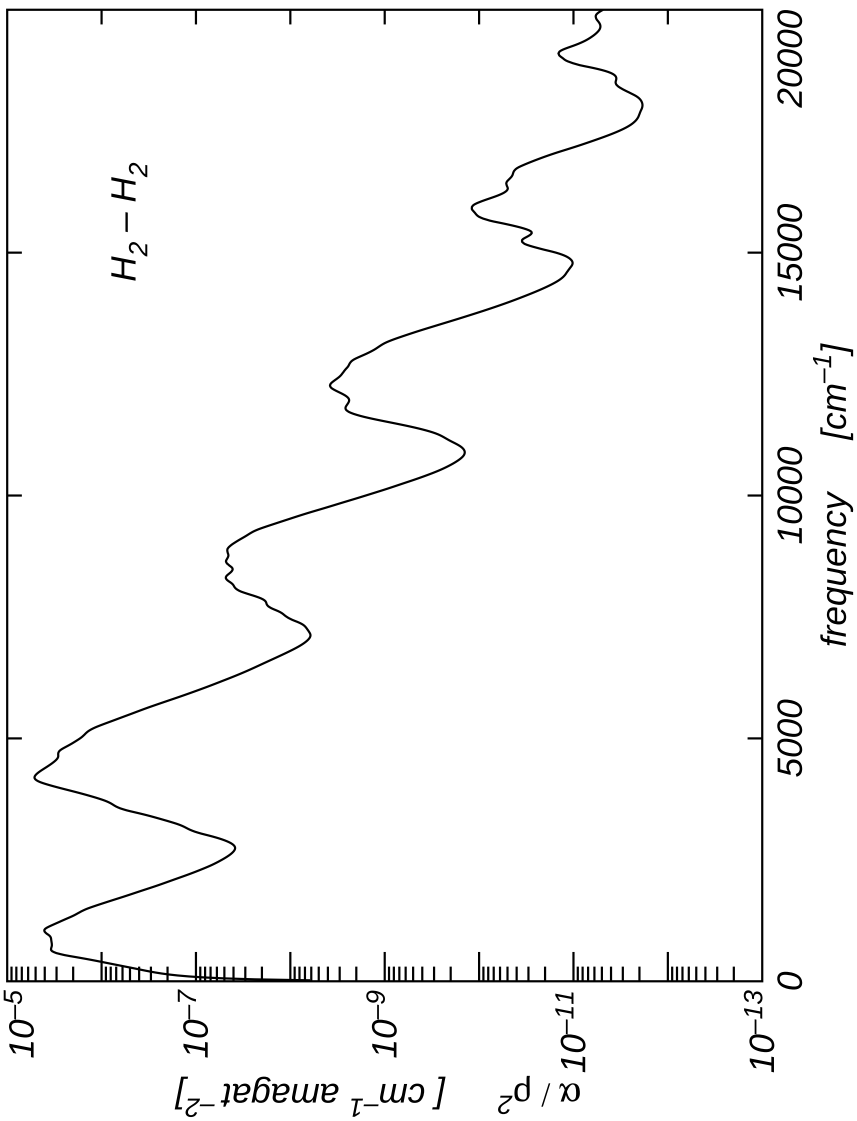

Figure 5.10: The calculated collision-induced absorption spectrum of dense hydrogen gas at the temperature of 600K

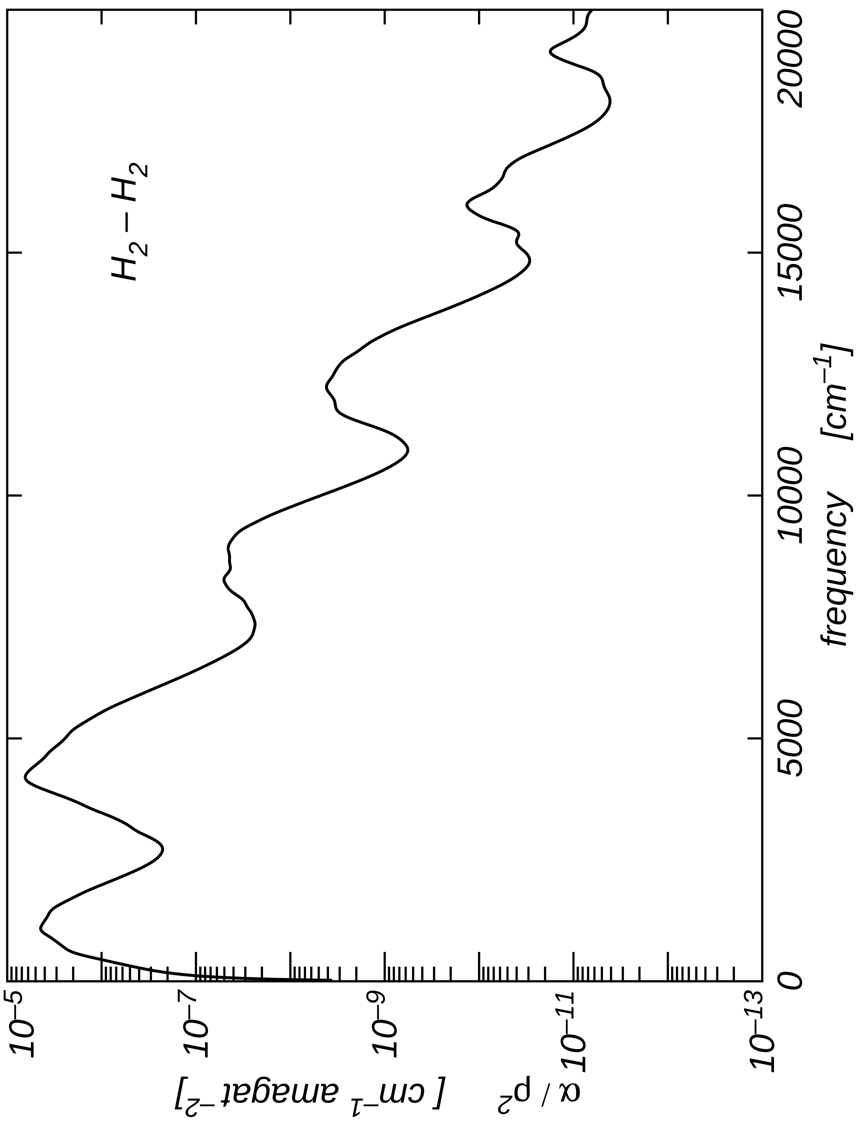

Figure 5.11: The calculated collision-induced absorption spectrum of dense hydrogen gas at the temperature of 1000K

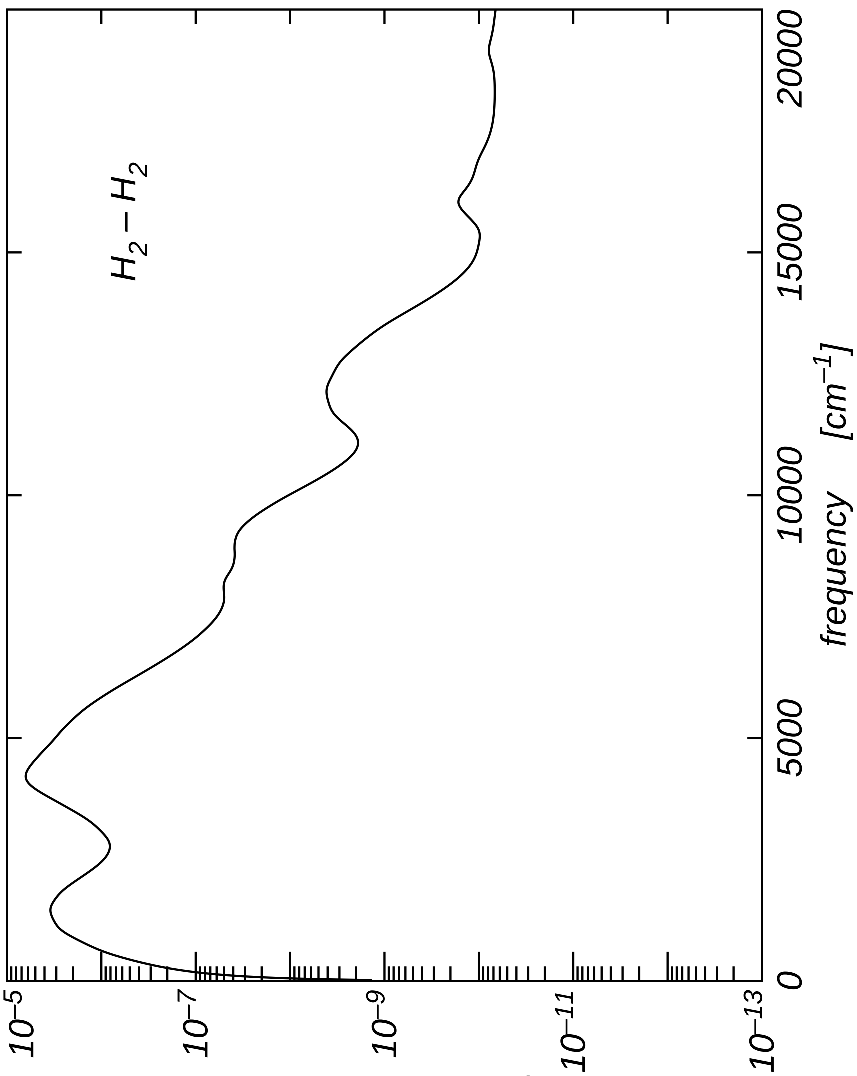

Figure 5.12: The calculated collision-induced absorption spectrum of dense hydrogen gas at the temperature of 2000K

Appendix

In the following the physical constants and units which are important for this work are listed. Numbers in parantheses represent the uncertainties of the constants.

1 Debye = 0.3934267 atomic units of dipole strength = 3.335611×10^{-30}C×m [13]

speed of light in vacuum:

c = 299 792 458 m×s $^{-1}$ [25]

Planck constant:

h = 6.626 068 96(33)×10^{-34} J×s [25]

Planck constant, reduced:

$\hbar$ = h/2π = 1.054 571 628(53)×10^{-34} J×s [25]

electron charge magnitude:

e = 1.602 176 487(40)×10^{-19} C [25]

electron mass:

m_e= 9.109 382 15(45)×10^{-31} kg [25]

proton mass:

m_p= 1.672 621 637(83)×10^{-27} kg [25]

unified atomic mass unit (u):

(mass ^{12}C atom)/12 = (1 g) / (N_A mol) = 1.660 538 782(83)$\times 10^{-27}$ kg [25]

permittivity of free space:

ϵ_0 = 8.854 187 817...$\times 10^{-12}$ F$\times$m^{-1} [25]

Avogadro constant:

N_A = 6.022 141 79(30)$\times 10^{23}$ mol^{-1} [25]

Boltzmann constant:

k_B= 1.380 6504(24)$\times 10^{-23}$ J$\times$K^{-1} [25]

the irrational number π:

$\pi \approx$ 3.141 592 653 589 793 238 [25]

conversion from inches to meters:

1 in = 0.0254 m [25]

conversion from electron volts to Joule:

1 eV = 1.602 176 487(40)$\times 10^{-19}$J [25]

k_BT at 300 K = [38.681 685(68)]$^{-1}$ eV [25]

Index

Bibliography

[1] Z. Phys. D. 13, 217, 1989.

[2] U. G. Jorgensen A. Borysow and Y. Fu. *High Temperature (1000 - 7000K) collsion-induced absorption spectra of H_2 pairs from first principles with applications to dense stellar atmospheres.* J. Quant. Spectroscopy and Rad. Transfer, 68, 235-255, 2001.

[3] J. N. Bradley. *Shock Waves in Chemistry and Physics.* (London: Methuen), 1962.

[4] L. M. Branscomb. *Atomic and Molecular Processes, edited by D. R. Bates.* (New York: Academic Press), pp. 100-140, 1962.

[5] F. R. Britton and M. F. Crawford. *Theory of collision-induced absorption in hydrogen and deuterium.* Can. J. Phys., 36:761, 1958.

[6] J. P. Colpa. *Induced absorption in the infrared.* In A. van Itterbeck, ed., Physics of High Pressure and the Condensed Phase, Ch. 12, p. 490, North Holland, Amsterdam, 1965.

[7] J. P. Colpa and J. A. A. Ketelaar. *The pressure-induced rotational absorption spectrum of hydrogen.* I. Molec. Phys., 1:14, 1958.

[8] A. Marten J. P. Baluteau D. Gautier and G. Bachet. Can. J. Phys. 61, 1455, 1983.

[9] Jean-Pierre Bouanich Magnus Gustafsson Lothar Frommhold Denise Bailly and Claude Brodbeck. *Collision-induced absorption in the rototranslational band of dense hydrogen gas.* Journal of Chemical Physics, 119, 23, 2003.

[10] P. L. DeVries and T. F. George. Molec. Phys. 36, 151, 1978.

[11] P. L. DeVries and T. F. George. Molec. Phys. 36, 151, 1978.

[12] B. Conrath M. Flasar V. Kunde P. Lowman W. McGuire J. Pearl J. Pirraglia R. Samuelson D. Gautier et al. R. Hanel. Science 204, 972, 1979.

[13] L. Frommhold. *Collision-Induced Absorption in Gases.* Cambridge University Press, Cambridge, New York, 1993 and 2006.

[14] Lothar Frommhold. *Collision-Induced Spectroscopy.* University of Texas.

[15] R. Fuchs. Z. Phys., 130, 69, 1951.

[16] E. R. Cohen P. Dore G. Bachet and G. Birnbaum. Can. J. Phys. 61, 591, 1983.

[17] M. Rigby E. B. Smith G. C. Maitland and W. A. Wakeham. *in Collision- and Interaction-Induced Spectroscopy.* Intermolecular Forces (Clarendom Press, Oxford, 1981), 1989.

[18] H. Griem. *Principles of Plasma Spectroscopy*. New York: Cambridge University Press, 1977.

[19] Magnus Gustafsson. *Collision-induced absorption and anisotropy of the intermolecular potential*. Dissertation, Supervisor: Lothar Frommhold, Physics Department, University of Texas at Austin, 2002.

[20] M. F. Crawford J. C. F. MacDonald H. L. Welsh and D. A. Chisholm. *Induced Infrared Absorptions of H2, N2, and O2 in the First Overtone Regions*. McLennan Laboratory, University of Toronto, Toronto, Canada Phys. Rev. 83, 1264 - 1264 (1951), 1951.

[21] Dominik Hammer and Lothar Frommhold. *Topical review Sonoluminescence: how bubbles glow*. Journal of Modern Optics, vol. 48, No. 2, 239-277, 2001.

[22] B. M. S. Hansen. *Old and blue white dwarf stars as a detectable source of microlensing events*. Nature, 394, 860-862, 1998.

[23] W. F. J. Hare and H. L. Welsh. *Pressure-induced infrared absorption of hydrogen and hydrogen-foreign gas mixtures in the range 1500-5000 atmospheres*. Can. J. Phys., Vol. 36, 1958.

[24] G. Herzberg. *Spectroscopic evidence of molecular hydrogen in the atmospheres of uranus and neptune*. Astrophys. J., 115:337, 1952.

[25] http://pdg.lbl.gov. 2009.

[26] J. L. Hunt. *Ph. D. thesis.* University of Toronto, 1959.

[27] J. L. Hunt and H. L. Welsh. Can. J. Phys. 42, 873, 1964.

[28] A. Watanabe J. L. Hunt and H. L. Welsh. Can. J. Phys. 49, 860, 1971.

[29] C. Brodbeck P. Drossart J. P. Bouanich and E. Lellouch. J. Quant. Spectroscopy and Rad. Transfer 42, 141, 1989.

[30] P. S. Julienne. Phys. Review A 26, 3299, 1982.

[31] J. Camm J. Keck and B. Kivel. *J. chem. Phys., 28, 723.* 1958.

[32] J. Camm J. Kivel B. Keck and T. Wentin Jr. *Ann. Phys. (New York) , 7, 1.* 1959.

[33] Xiaping Li, Fei Wang Martin Abel Katherine L. C. Hunt, and Lothar Frommhold. *Collision-induced absorption by Molecular Hydrogen Pairs at Thousands of Kelvin.* International Journal of Spectroscopy, xxx, 2009.

[34] W. Lochte-Holtgreven and H. Maecker. Z. Phys., 38, 258, 1951.

[35] H. L. Welsh M. F. Crawford and J. L. Locke. *Infrared absorption of oxygen and nitrogen induced by intermolecular forces.* Phys. Rev., 75:1607, 1949.

[36] L. Frommhold M. Gustafsson. *Spectra of two- and three body van der Waals Complexes.* Physics Department, University of Texas.

[37] L. Frommhold M. Gustafsson and W. Meyer. J. Chem. Phys. 113, 3631, 2000.

[38] G. T. McConville. *A consistent spherical potential function for para-hydrogen.* J. Chem. Phys., 74:2201, 1981.

[39] D. A. McQuarrie. *Statistical Mechanics.* Harper and Row, New York, 1976.

[40] W. Meyer and L. Frommhold. *in Collision- and Interaction-Induced Spectroscopy.* edited by G. C. Tabisz and M. N. Neumann (Kluwer, Dordrecht, 1995).

[41] W. Meyer and L. Frommhold. *Collision-induced rototranslational spectra of* $H_2 - He$ *from an accurate ab initio potential surface.* Phys. Review A, 34, 2771-2779, 1986.

[42] F. H. Mies. *in Theoretical Chemistry: Advances and Perspectives.* edited by D. Henderson (Academic Press, New York, 1981), Vol. 6B, pp. 127-198.

[43] M. Mizushima. *A theory of pressure absorption.* Phys. Rev., 76:1268, Erratum: ibid. 77:149, 1950, 1949.

[44] M. Mizushima. *On the infrared absorption of the hydrogen molecule.* Phys. Rev., 77:150, 1950.

[45] J. Mould and J. Liebert. *Infrared photometry and atmospheric composition of cool white dwarfs.* Astrophys. J., 226, L29-33, 1978.

[46] D. Saumon P. Bergeron and F. Wesemael. *New model of atmospheres for very cool white dwarfs with mixed H/He and pure He compositions.* Astrophys. J., 443, 764-779, 1995.

[47] S. K. Leggett P. Bergeron and M. T. Ruiz. *Photometric and spectroscopic analysis of cool white dwarfs with trigonometric parallax.* Astrophys. J. Supp., 133, 413-449, 2001.

[48] J. D. Poll and J. L. Hunt. Can. J. Phys. 54, 461, 1976.

[49] J. D. Poll and J. van Kranendonk. Can. J. Phys. 39, 189, 1961.

[50] G. Varghese S. P. Reddy and R. D. G. Prasad. Phys. Rev. A 15, 975, 1977.

[51] D. Saumon and S. B. Jacobson. *Pure hydrogen model atmospheres for very cool white dwarfs.* Astrophys. J., 511, L107-110, 1999.

[52] R. H. Tipping and J. D. Poll. *in Molecular Spectroscopy: Modern Research.* vol. 3, edited by K. N. Rao (Academic Press, New York, 1985), Chap. 7, pp. 421-446.

[53] L. M. Trafton. *The thermal opacity in the major planets.* Astrophys. J., 140, 1340, 1964.

[54] L. M. Trafton. *Planetary Atmospheres: The role of collsion-induced absorption.* in [58], pages 177-193, 1998.

[55] A. Unsoeld. *Physik der Sternatmosphaeren.* Berlin: Springer, 1955.

[56] J. van Kranendonk. *Intermolecular spectroscopy.* Physica, 73:156, 1974.

[57] J.-P. Bouanich Nguyen van Thanh Y. Fu A. Borysow C. Brodbeck. *Collision-induced absorption by H2 pairs in the second overtone band at 298 and 77.5K: Comparison between experimental and theoretical results.* Journal of Chemical Physics, 10, 4750, 1999.

[58] A. A. Vigasin and editors Z. Slanina. *Molecular Complexes in Earth' s, Planetary, Cometary and Interstellar Atmospheres.* World Sci., Singapore, 1998.

[59] K. Szalewicz W. Kolos and H. J. Monkhorst. J. Chem. Phys. 84, 3278, 1986.

[60] A. Borysow W. Meyer and L. Frommhold. *Absorption spectra of $H_2 - H_2$ pairs in the fundamental band.* Phys. Review A, 40, 6931-6949, 1989.

[61] A. Borysow W. Meyer and L. Frommhold. *Absorption spectra of $H_2 - H_2$ pairs in the fundamental band.* Phys. Rev. A, 40:6931, 1989.

[62] A. Borysow W. Meyer and L. Frommhold. *Collsion-induced first overtone band of gaseous hydrogen from first principles.* Phys. Review A, 47, 4065-4077, 1993.

[63] L. Frommhold W. Meyer and G. Birnbaum. *Rototranslational absorption spectra of $H_2 - H_2$ pairs in the far infrared.* Phys. Review A, 39, 2434-2448, 1989.

[64] A. Watanabe. *Ph. D. thesis.* University of Toronto, 1964.

[65] H. L. Welsh. *Pressure induced absorption spectra of hydrogen.* A. D. Buckingham and D. A. Ramsay, editors, MTP Internat. Review of Science - Physical Chemistry, Series one, Vol. 3: Spectroscopy, chapter 3, pages 33-71, Butterworths, London, 1972.

[66] Y. B. Zel' Dovich and Y. P. Raizer. *Physics of Shock Waves and High Temperature Hydrodynamic Phenomena.* Vol. 1 (New York: Academic Press), 1966.

Vita

Martin Andreas Abel was born in Fulda, Germany, on August 28, 1985, the son of Roswitha Waltraud and Werner Gregor Abel. He graduated from the Wigbertgymnasium in Huenfeld, Germany, with the university-entrance diploma. In 2005 he started his higher education in the natural science and mathematics program at the University of Wuerzburg, Germany. He received his prediploma in physics in 2007 and the prediploma in mathematics in 2008 from the University of Wuerzburg, Germany. In August 2008 he entered the Graduate School of the University of Texas at Austin and since then he was a graduate student there.

Permanent address: Am Langen Garten 1, Eiterfeld/ Arzell, 36132,
Germany

This thesis was typeset with LaTeX[†] by Martin Andreas Abel.

[†]LaTeX is a document preparation system developed by Leslie Lamport as a special version of Donald Knuth's TeX Program.